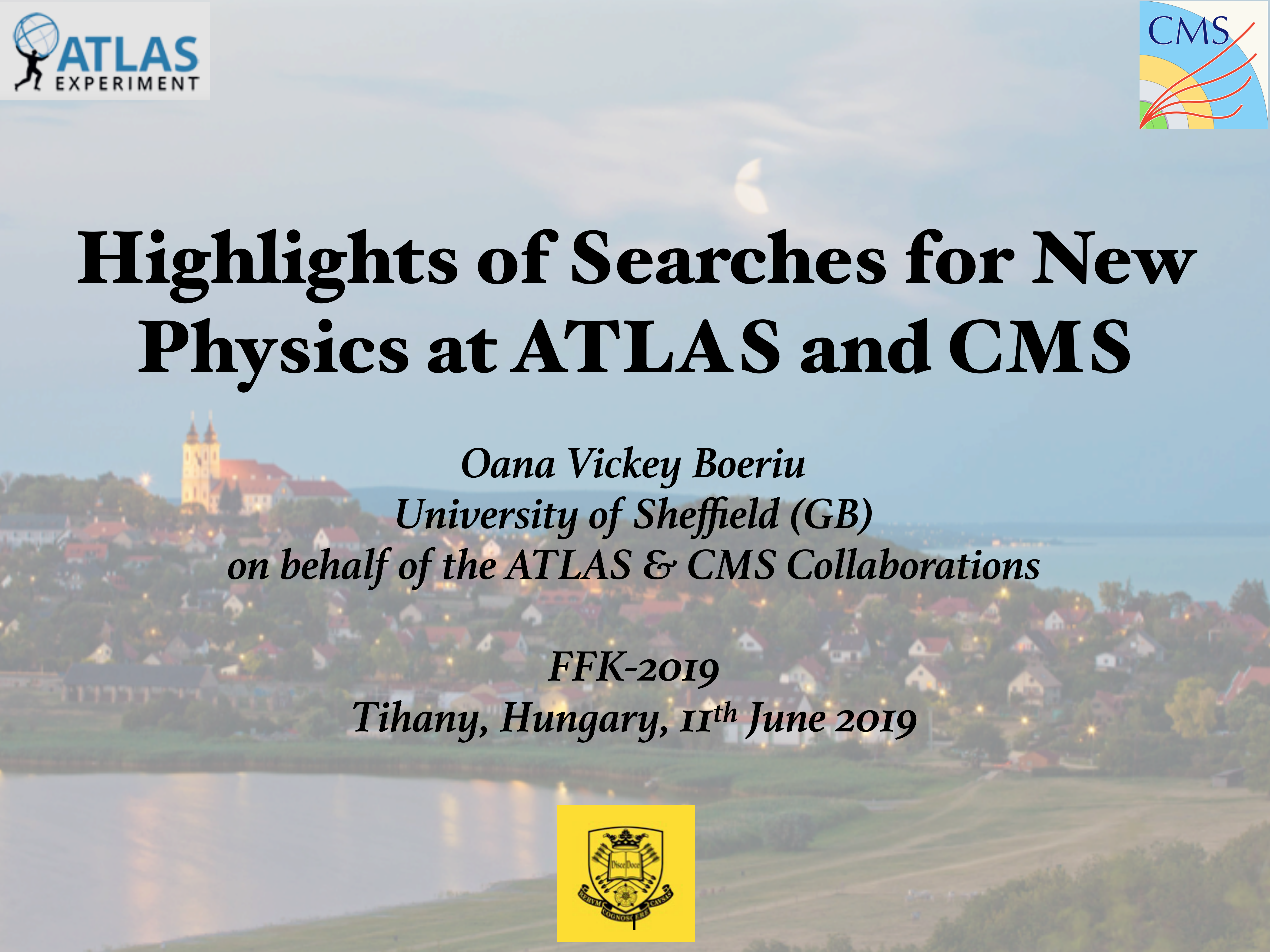

Highlights of Searches for New Physics at ATLAS and CMS

Oana Vickey Boeriu
University of Sheffield (GB)
on behalf of the ATLAS & CMS Collaborations

FFK-2019
Tihany, Hungary, 11th June 2019

Outlook

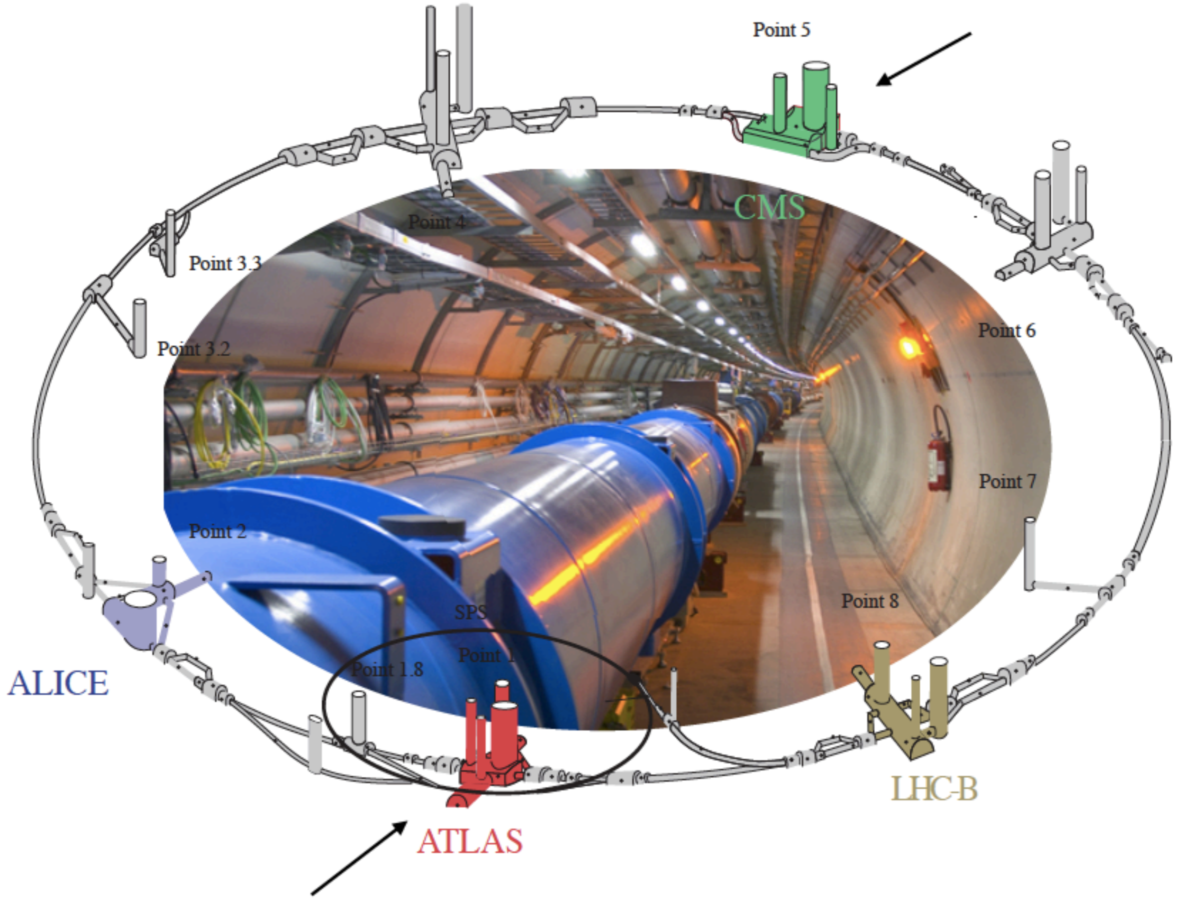

- Introduction
  - LHC Performance during Run 2
  - ATLAS and CMS Detectors
- ***Results presented in this talk***:
  - Search for high-mass di-lepton, di-jet and di-boson resonances
  - Search for heavy charged boson $W' \rightarrow l\nu$
  - Multilepton searches
  - Search for heavy neutral leptons from W's
  - Search for a right-handed gauge boson
  - Search for compressed mass spectra
  - Search for staus and disappearing tracks
  - Anomalous quartic gauge couplings search

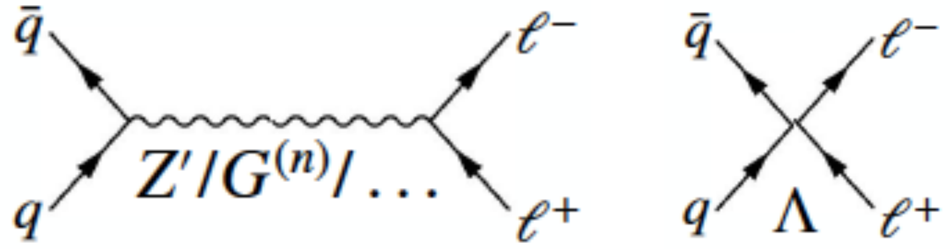

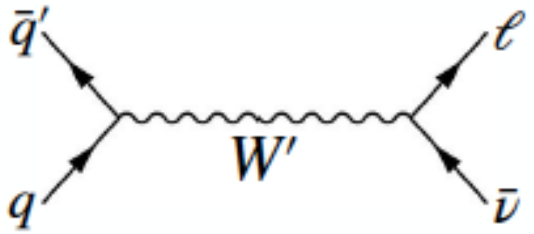

Why look for new physics ?

Many questions still unanswered

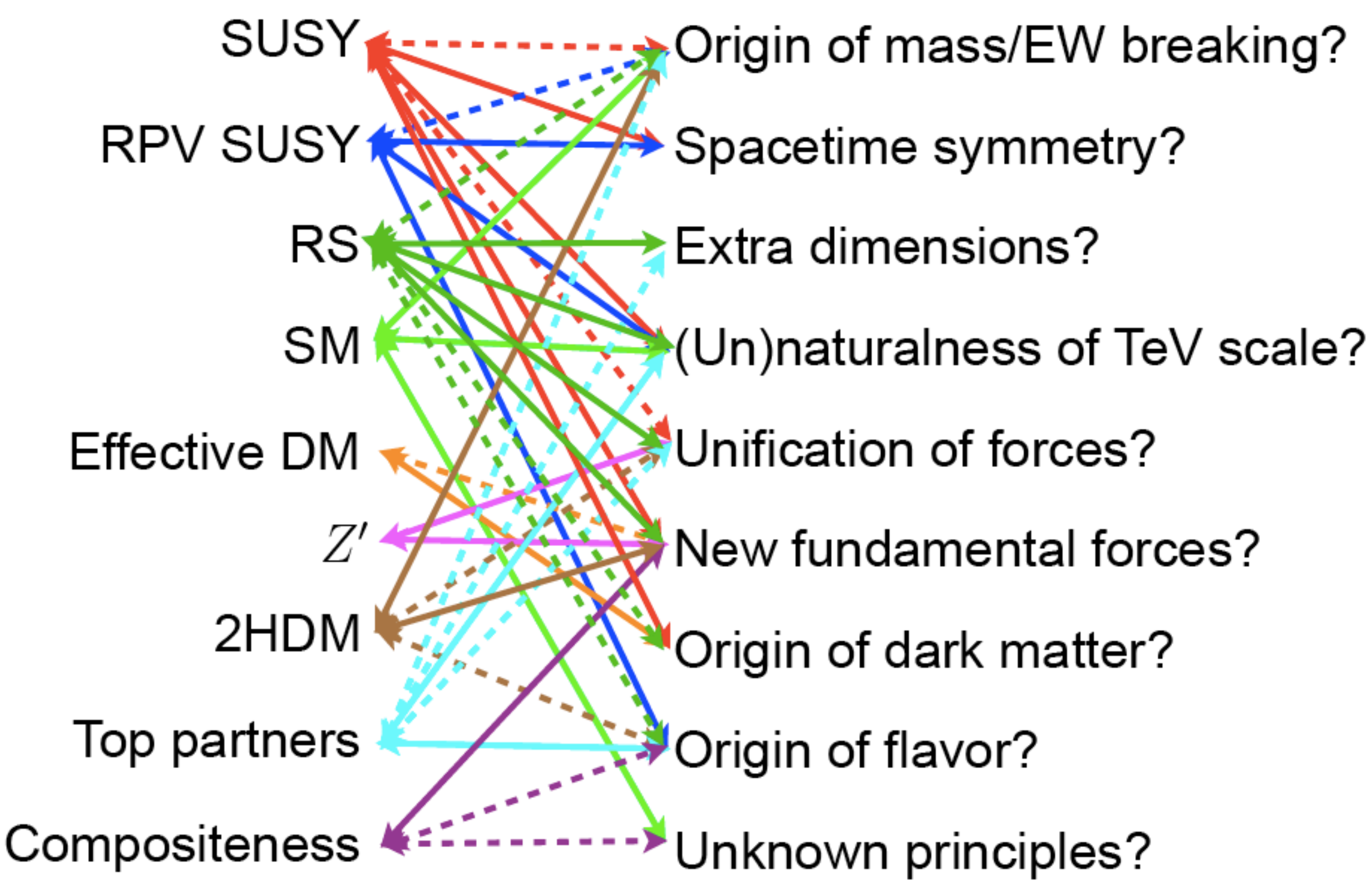

SUSY
RPV SUSY
RS
SM
Effective DM
Z'
2HDM
Top partners
Compositeness

Origin of mass/EW breaking?
Spacetime symmetry?
Extra dimensions?
(Un)naturalness of TeV scale?
Unification of forces?
New fundamental forces?
Origin of dark matter?
Origin of flavor?
Unknown principles?

- The search for new heavy particles important part of the LHC physics program and has been the focus of an intense effort to uncover BSM physics in a broad range of final states.

- **Resonances** are the classic collider methodology in searches for new particles
- Approach: 'Look for an **unexpected peak** on a smooth background'
- One decay channel can be used to search for a wide range of models

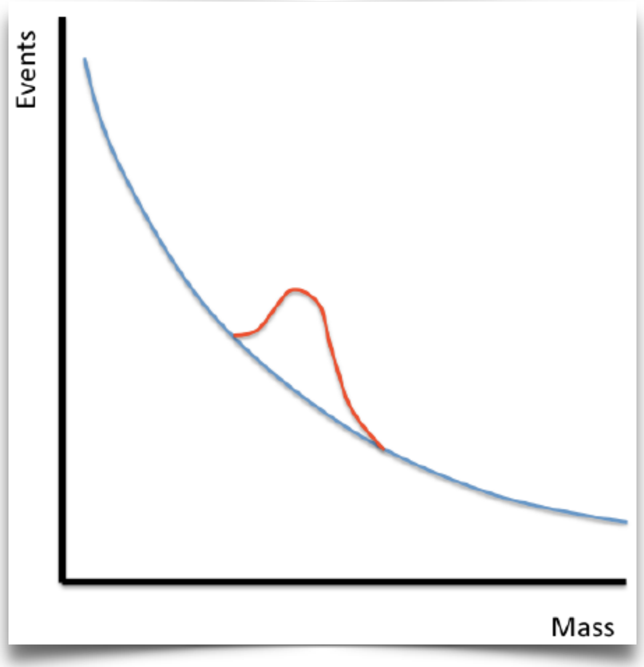

- Reconstruct 4-vectors of the decay products
- Combine them and plot the **invariant mass**

LHC Performance in Run 2

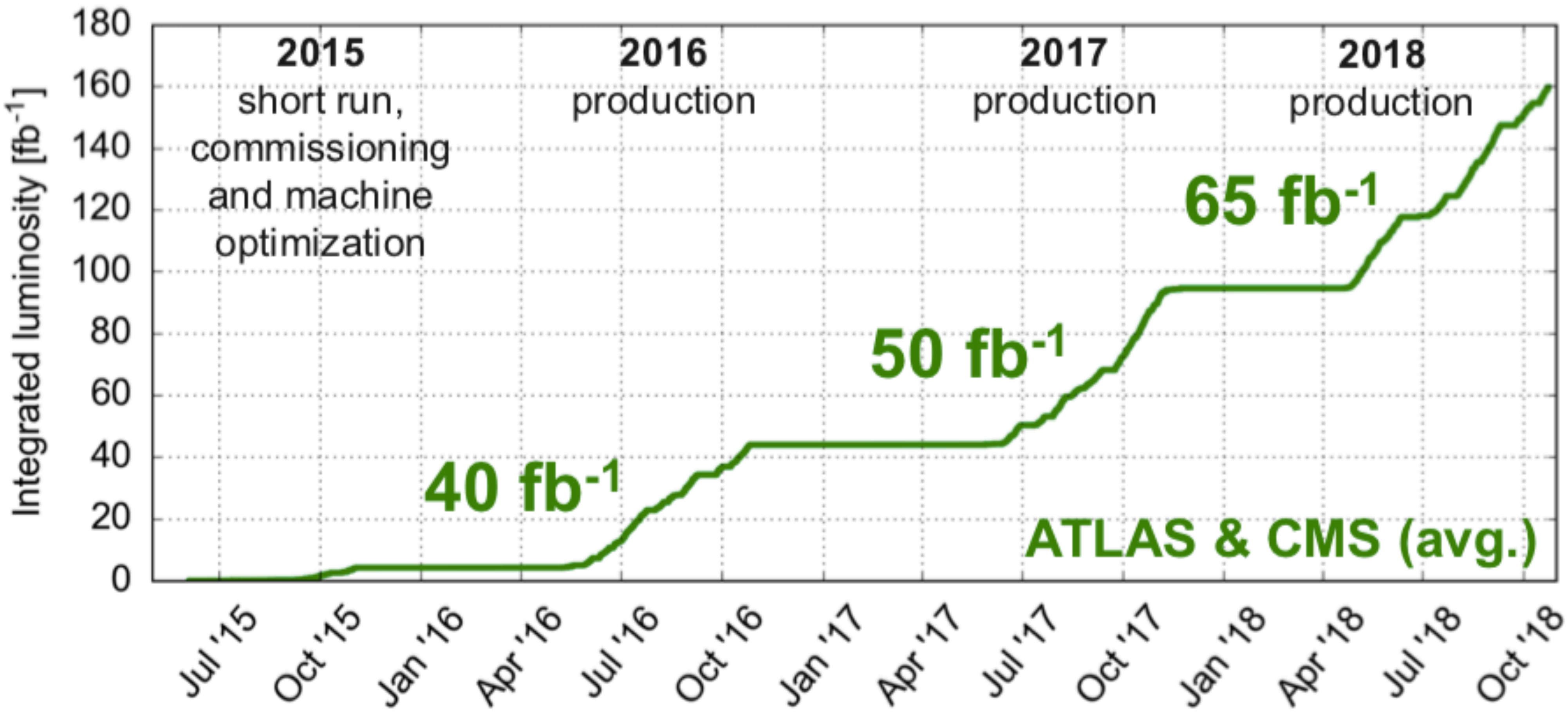

- ***LHC performed beyond expectations during Run 2 (2015-2018):***
  - ***Demonstrated reliable operation with 6.5 TeV beams***
  - ***Exploited 25 ns bunch spacing to operate with > 2500 bunches***
  - ***Reached design luminosity $L_{IP1/5} = 10^{34}$ cm^{-2}s^{-1} and doubled it!***
  - ***Delivered more than 160 fb^{-1} to ATLAS and CMS***

The ATLAS Detector in Run 2

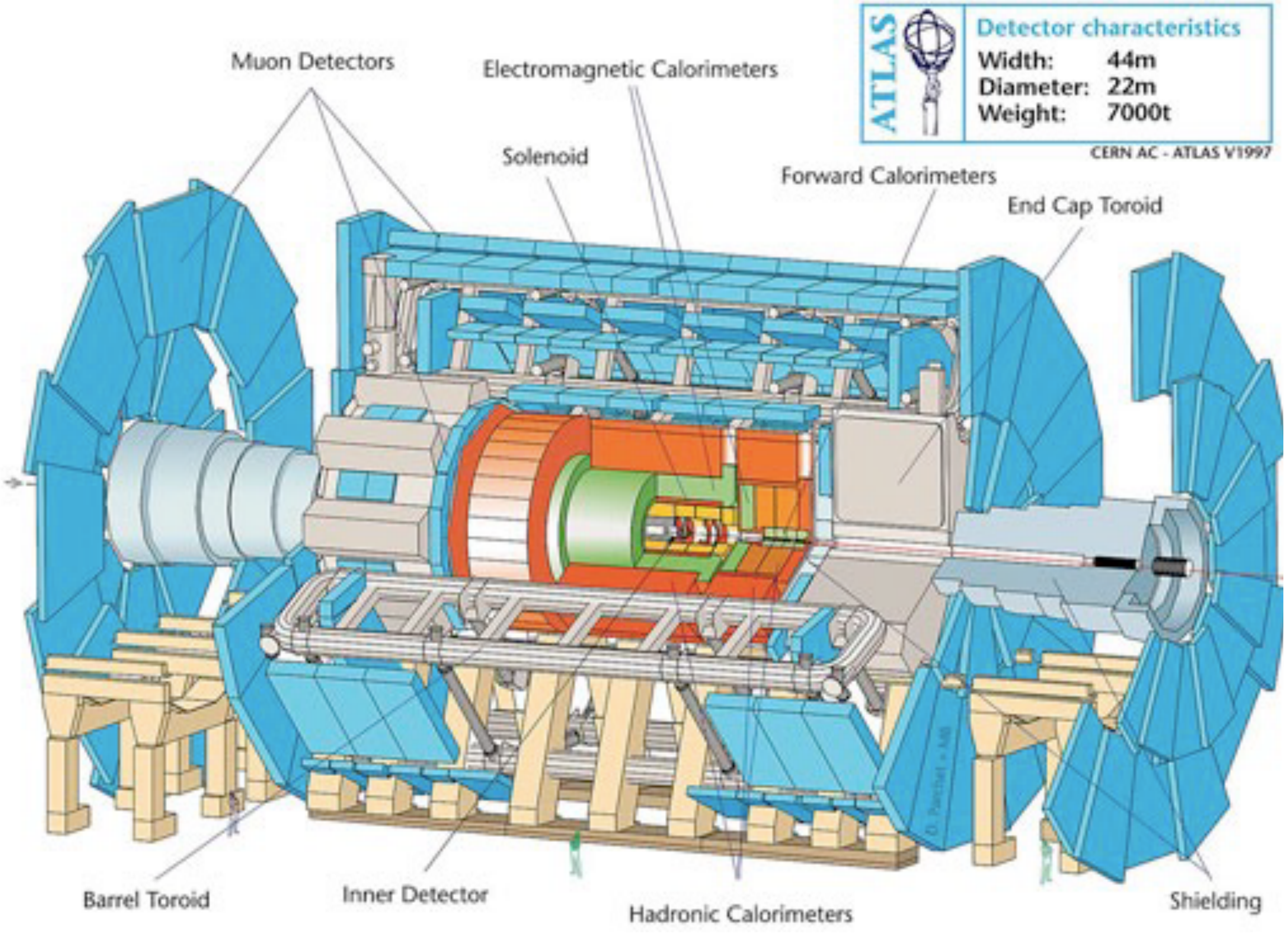

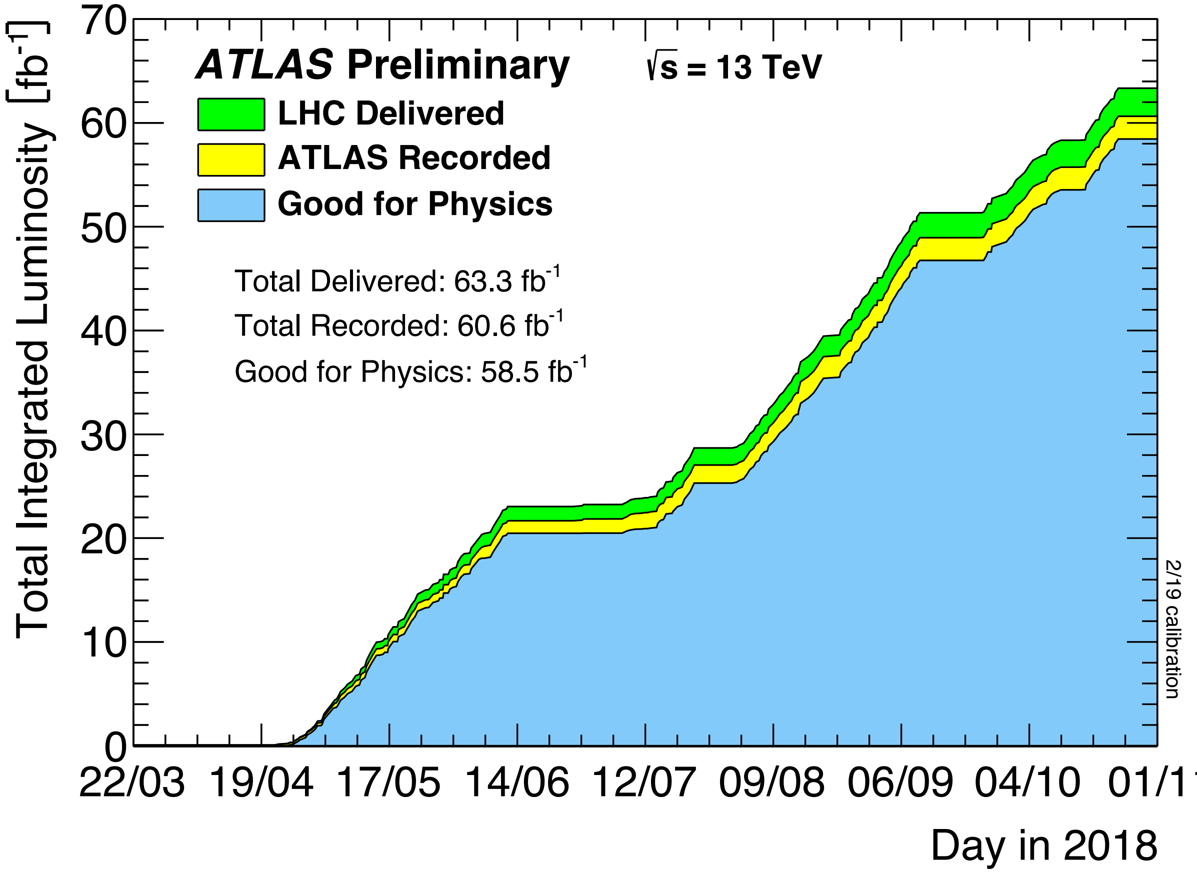

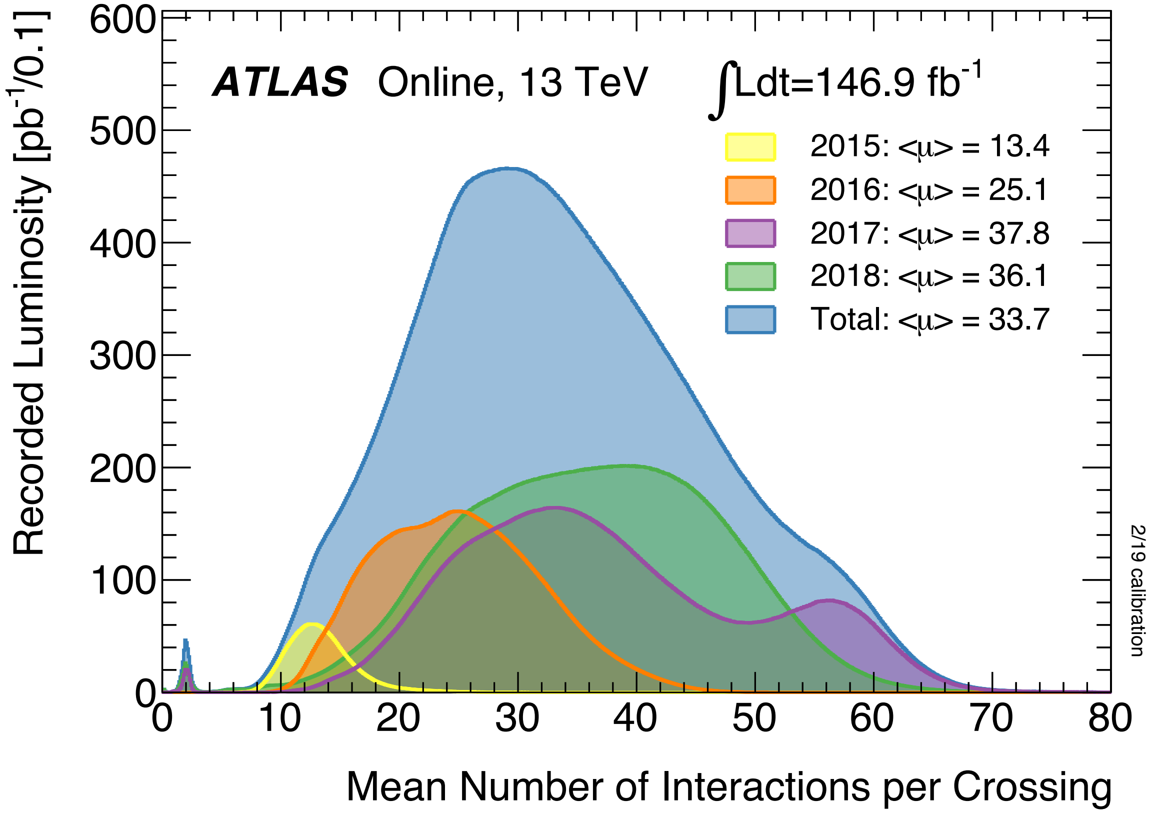

- ~ 94% recording efficiency
- ~ 95% validation efficiency
- Subdetectors efficiency 95-100%
- Trigger efficiency ~100%

- ***Good for Physics*** criteria require all reconstructed physics objects to be of good data quality.

The CMS Detector in Run 2

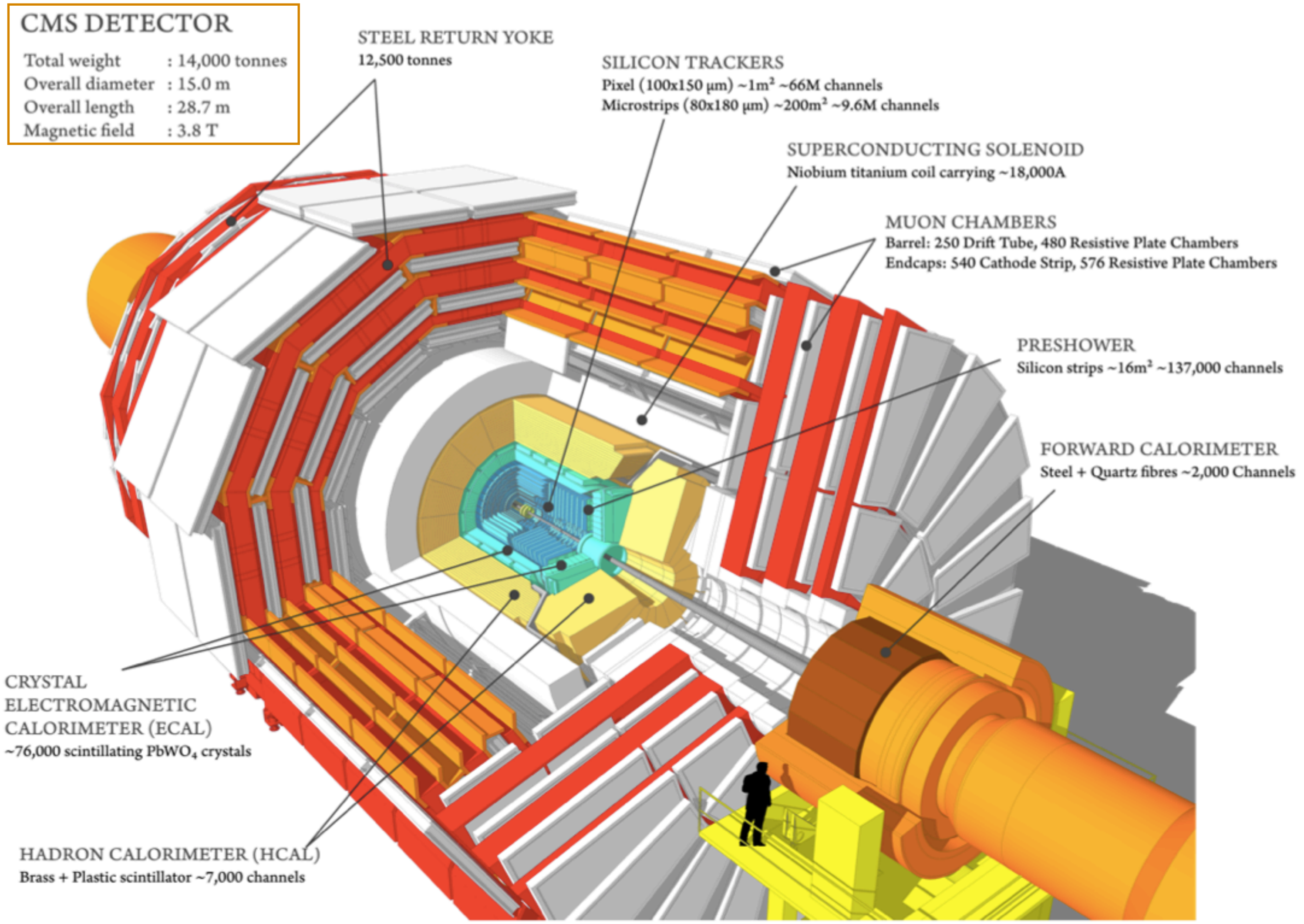

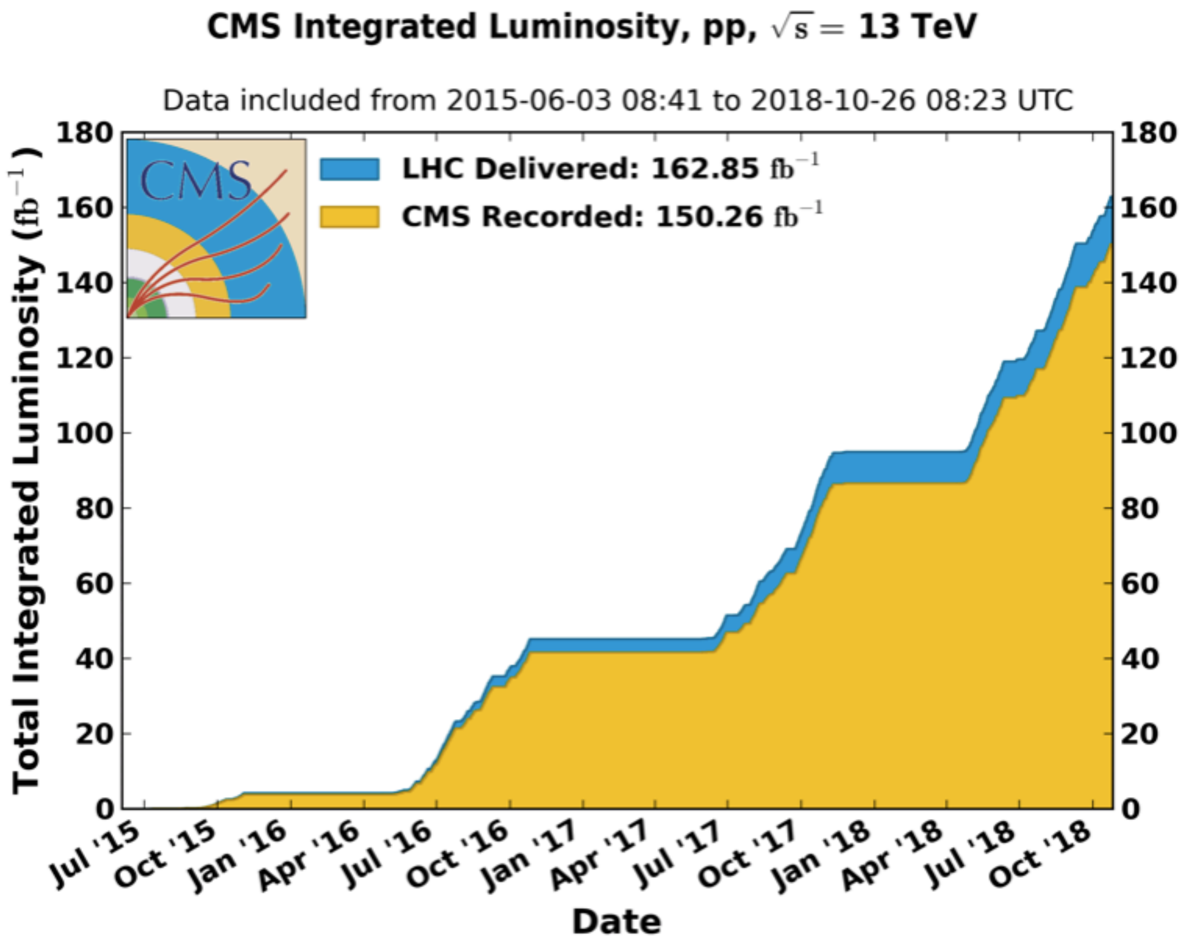
CMS Integrated Luminosity, pp, $\sqrt{s} = 13$ TeV

Data included from 2015-06-03 08:41 to 2018-10-26 08:23 UTC

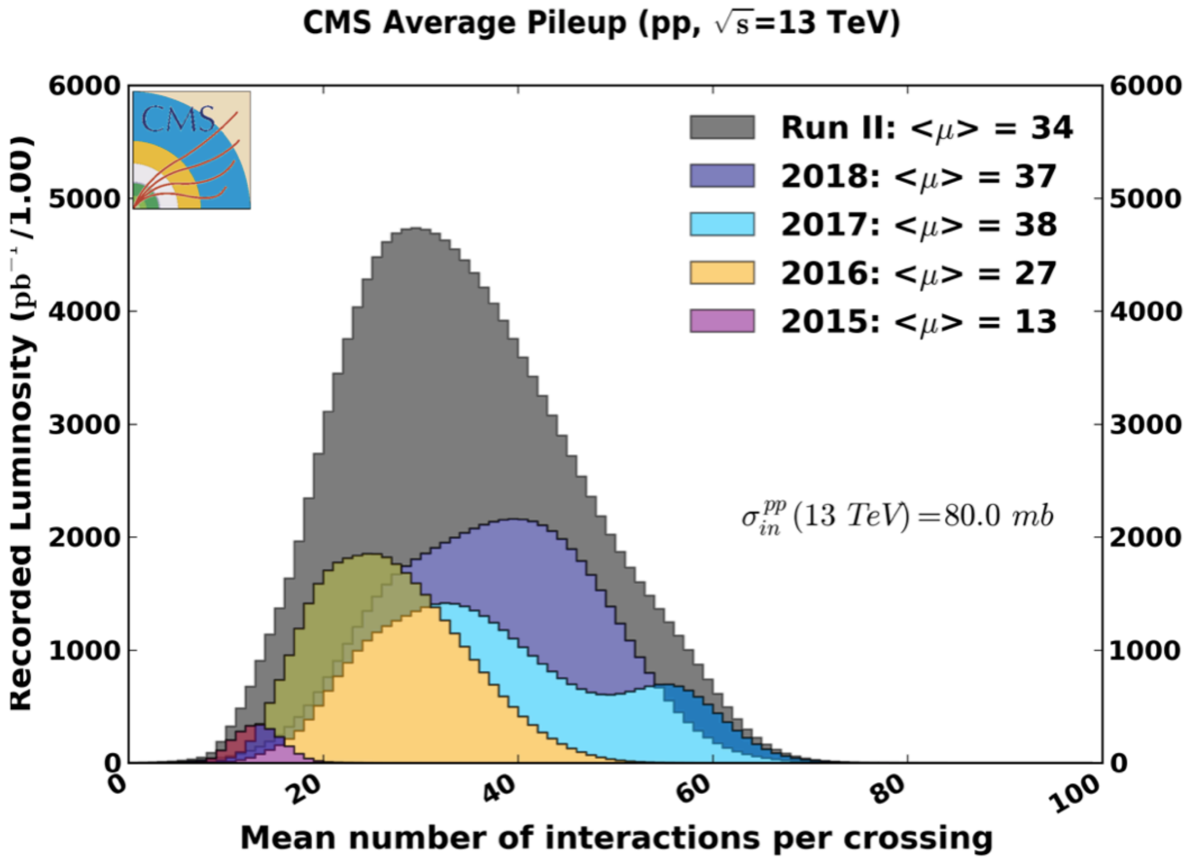
CMS Average Pileup (pp, $\sqrt{s}$=13 TeV)

- ~ 94% recording efficiency
- ~ 95% validation efficiency

Search Results

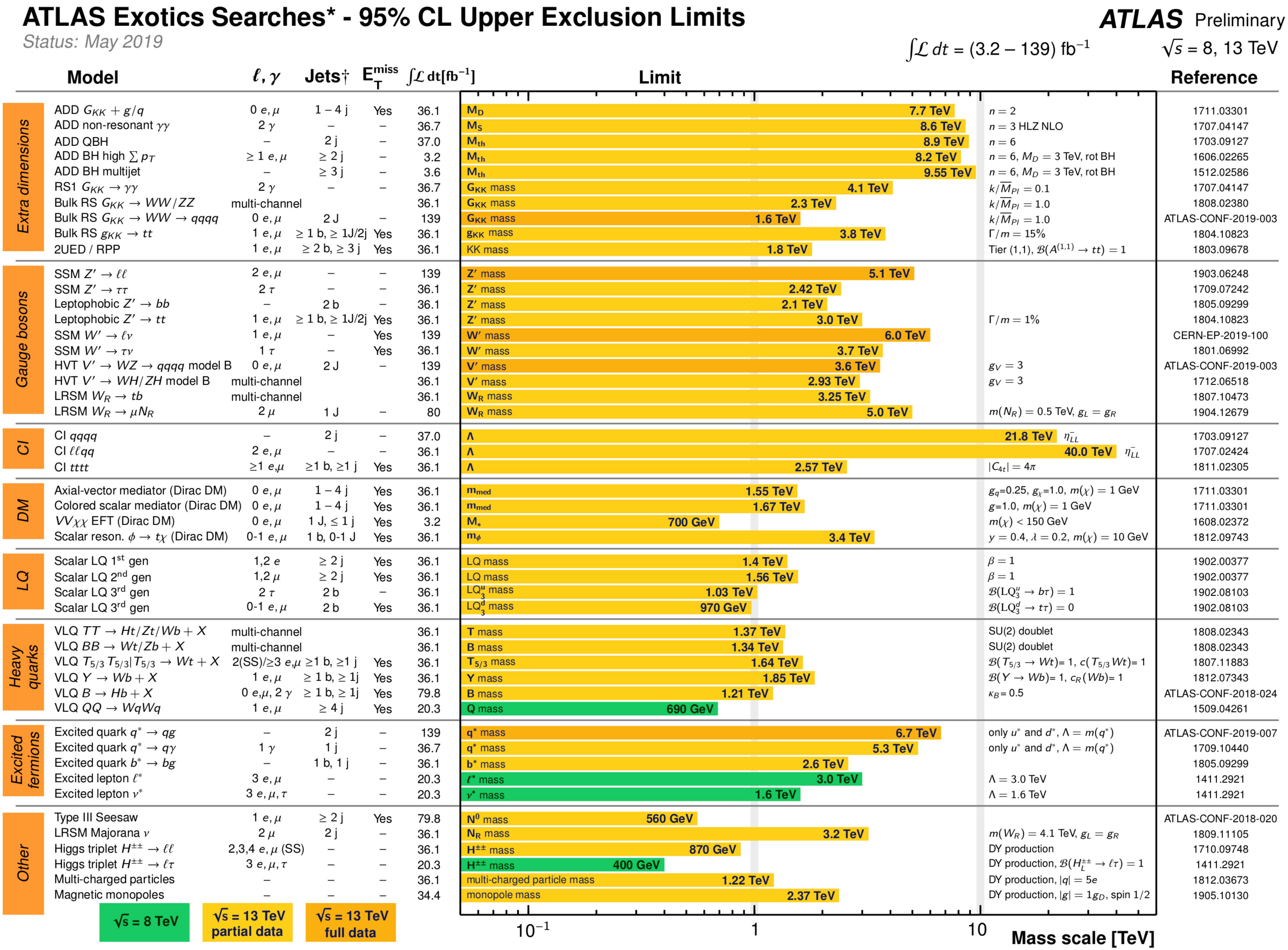

ATLAS Exotics Searches* - 95% CL Upper Exclusion Limits

Status: May 2019

ATLAS Preliminary

$\int \mathcal{L}\, dt = (3.2 - 139)\ \mathrm{fb}^{-1}$

$\sqrt{s} = 8,\ 13$ TeV

	Model	ℓ, γ	Jets†	E_T^{miss}	$\int\mathcal{L}\, dt[\mathrm{fb}^{-1}]$	Limit		Reference
Extra dimensions	ADD $G_{KK} + g/q$	$0\ e, \mu$	$1-4$ j	Yes	36.1	M_D 7.7 TeV	$n = 2$	1711.03301
	ADD non-resonant $\gamma\gamma$	$2\ \gamma$	–	–	36.7	M_S 8.6 TeV	$n = 3$ HLZ NLO	1707.04147
	ADD QBH	–	2 j	–	37.0	M_{th} 8.9 TeV	$n = 6$	1703.09127
	ADD BH high $\sum p_T$	$\geq 1\ e, \mu$	≥ 2 j	–	3.2	M_{th} 8.2 TeV	$n = 6$, $M_D = 3$ TeV, rot BH	1606.02265
	ADD BH multijet	–	≥ 3 j	–	3.6	M_{th} 9.55 TeV	$n = 6$, $M_D = 3$ TeV, rot BH	1512.02586
	RS1 $G_{KK} \to \gamma\gamma$	$2\ \gamma$	–	–	36.7	G_{KK} mass 4.1 TeV	$k/\overline{M}_{Pl} = 0.1$	1707.04147
	Bulk RS $G_{KK} \to WW/ZZ$	multi-channel			36.1	G_{KK} mass 2.3 TeV	$k/\overline{M}_{Pl} = 1.0$	1808.02380
	Bulk RS $G_{KK} \to WW \to qqqq$	$0\ e, \mu$	2 J	–	139	G_{KK} mass 1.6 TeV	$k/\overline{M}_{Pl} = 1.0$	ATLAS-CONF-2019-003
	Bulk RS $g_{KK} \to tt$	$1\ e, \mu$	≥ 1 b, ≥ 1J/2j	Yes	36.1	g_{KK} mass 3.8 TeV	$\Gamma/m = 15\%$	1804.10823
	2UED / RPP	$1\ e, \mu$	≥ 2 b, ≥ 3 j	Yes	36.1	KK mass 1.8 TeV	Tier (1,1), $\mathcal{B}(A^{(1,1)} \to tt) = 1$	1803.09678
Gauge bosons	SSM $Z' \to \ell\ell$	$2\ e, \mu$	–	–	139	Z' mass 5.1 TeV		1903.06248
	SSM $Z' \to \tau\tau$	$2\ \tau$	–	–	36.1	Z' mass 2.42 TeV		1709.07242
	Leptophobic $Z' \to bb$	–	2 b	–	36.1	Z' mass 2.1 TeV		1805.09299
	Leptophobic $Z' \to tt$	$1\ e, \mu$	≥ 1 b, ≥ 1J/2j	Yes	36.1	Z' mass 3.0 TeV	$\Gamma/m = 1\%$	1804.10823
	SSM $W' \to \ell\nu$	$1\ e, \mu$	–	Yes	139	W' mass 6.0 TeV		CERN-EP-2019-100
	SSM $W' \to \tau\nu$	$1\ \tau$	–	Yes	36.1	W' mass 3.7 TeV		1801.06992
	HVT $V' \to WZ \to qqqq$ model B	$0\ e, \mu$	2 J	–	139	V' mass 3.6 TeV	$g_V = 3$	ATLAS-CONF-2019-003
	HVT $V' \to WH/ZH$ model B	multi-channel			36.1	V' mass 2.93 TeV	$g_V = 3$	1712.06518
	LRSM $W_R \to tb$	multi-channel			36.1	W_R mass 3.25 TeV		1807.10473
	LRSM $W_R \to \mu N_R$	$2\ \mu$	1 J	–	80	W_R mass 5.0 TeV	$m(N_R) = 0.5$ TeV, $g_L = g_R$	1904.12679
CI	CI $qqqq$	–	2 j	–	37.0	Λ 21.8 TeV η_{LL}^{-}		1703.09127
	CI $\ell\ell qq$	$2\ e, \mu$	–	–	36.1	Λ 40.0 TeV η_{LL}^{-}		1707.02424
	CI $tttt$	$\geq 1\ e,\mu$	≥ 1 b, ≥ 1 j	Yes	36.1	Λ 2.57 TeV	$\lvert C_{4t} \rvert = 4\pi$	1811.02305
DM	Axial-vector mediator (Dirac DM)	$0\ e, \mu$	$1-4$ j	Yes	36.1	m_{med} 1.55 TeV	g_q=0.25, g_χ=1.0, $m(\chi) = 1$ GeV	1711.03301
	Colored scalar mediator (Dirac DM)	$0\ e, \mu$	$1-4$ j	Yes	36.1	m_{med} 1.67 TeV	g=1.0, $m(\chi) = 1$ GeV	1711.03301
	$VV\chi\chi$ EFT (Dirac DM)	$0\ e, \mu$	1 J, ≤ 1 j	Yes	3.2	M_* 700 GeV	$m(\chi) < 150$ GeV	1608.02372
	Scalar reson. $\phi \to t\chi$ (Dirac DM)	0-1 e, μ	1 b, 0-1 J	Yes	36.1	m_ϕ 3.4 TeV	$y = 0.4$, $\lambda = 0.2$, $m(\chi) = 10$ GeV	1812.09743
LQ	Scalar LQ 1st gen	1,2 e	≥ 2 j	Yes	36.1	LQ mass 1.4 TeV	$\beta = 1$	1902.00377
	Scalar LQ 2nd gen	1,2 μ	≥ 2 j	Yes	36.1	LQ mass 1.56 TeV	$\beta = 1$	1902.00377
	Scalar LQ 3rd gen	$2\ \tau$	2 b	–	36.1	LQ_3^u mass 1.03 TeV	$\mathcal{B}(\mathrm{LQ}_3^u \to b\tau) = 1$	1902.08103
	Scalar LQ 3rd gen	0-1 e, μ	2 b	Yes	36.1	LQ_3^d mass 970 GeV	$\mathcal{B}(\mathrm{LQ}_3^d \to t\tau) = 0$	1902.08103
Heavy quarks	VLQ $TT \to Ht/Zt/Wb + X$	multi-channel			36.1	T mass 1.37 TeV	SU(2) doublet	1808.02343
	VLQ $BB \to Wt/Zb + X$	multi-channel			36.1	B mass 1.34 TeV	SU(2) doublet	1808.02343
	VLQ $T_{5/3}T_{5/3}\vert T_{5/3} \to Wt + X$	2(SS)/$\geq$3 e,μ	≥ 1 b, ≥ 1 j	Yes	36.1	$T_{5/3}$ mass 1.64 TeV	$\mathcal{B}(T_{5/3} \to Wt)$= 1, $c(T_{5/3}Wt)$= 1	1807.11883
	VLQ $Y \to Wb + X$	$1\ e, \mu$	≥ 1 b, ≥ 1j	Yes	36.1	Y mass 1.85 TeV	$\mathcal{B}(Y \to Wb)$= 1, $c_R(Wb)$= 1	1812.07343
	VLQ $B \to Hb + X$	$0\ e,\mu$, $2\ \gamma$	≥ 1 b, ≥ 1j	Yes	79.8	B mass 1.21 TeV	κ_B= 0.5	ATLAS-CONF-2018-024
	VLQ $QQ \to WqWq$	$1\ e, \mu$	≥ 4 j	Yes	20.3	Q mass 690 GeV		1509.04261
Excited fermions	Excited quark $q^* \to qg$	–	2 j	–	139	q^* mass 6.7 TeV	only u^* and d^*, $\Lambda = m(q^*)$	ATLAS-CONF-2019-007
	Excited quark $q^* \to q\gamma$	$1\ \gamma$	1 j	–	36.7	q^* mass 5.3 TeV	only u^* and d^*, $\Lambda = m(q^*)$	1709.10440
	Excited quark $b^* \to bg$	–	1 b, 1 j	–	36.1	b^* mass 2.6 TeV		1805.09299
	Excited lepton ℓ^*	$3\ e, \mu$	–	–	20.3	ℓ^* mass 3.0 TeV	$\Lambda = 3.0$ TeV	1411.2921
	Excited lepton ν^*	$3\ e, \mu, \tau$	–	–	20.3	ν^* mass 1.6 TeV	$\Lambda = 1.6$ TeV	1411.2921
Other	Type III Seesaw	$1\ e, \mu$	≥ 2 j	Yes	79.8	N^0 mass 560 GeV		ATLAS-CONF-2018-020
	LRSM Majorana ν	$2\ \mu$	2 j	–	36.1	N_R mass 3.2 TeV	$m(W_R) = 4.1$ TeV, $g_L = g_R$	1809.11105
	Higgs triplet $H^{\pm\pm} \to \ell\ell$	2,3,4 e, μ (SS)	–	–	36.1	$H^{\pm\pm}$ mass 870 GeV	DY production	1710.09748
	Higgs triplet $H^{\pm\pm} \to \ell\tau$	$3\ e, \mu, \tau$	–	–	20.3	$H^{\pm\pm}$ mass 400 GeV	DY production, $\mathcal{B}(H_L^{\pm\pm} \to \ell\tau) = 1$	1411.2921
	Multi-charged particles	–	–	–	36.1	multi-charged particle mass 1.22 TeV	DY production, $\lvert q \rvert = 5e$	1812.03673
	Magnetic monopoles	–	–	–	34.4	monopole mass 2.37 TeV	DY production, $\lvert g \rvert = 1g_D$, spin 1/2	1905.10130

*Only a selection of the available mass limits on new states or phenomena is shown.

†Small-radius (large-radius) jets are denoted by the letter j (J).

ATLAS SUSY Searches* - 95% CL Lower Limits

March 2019

ATLAS Preliminary

$\sqrt{s}$ = 13 TeV

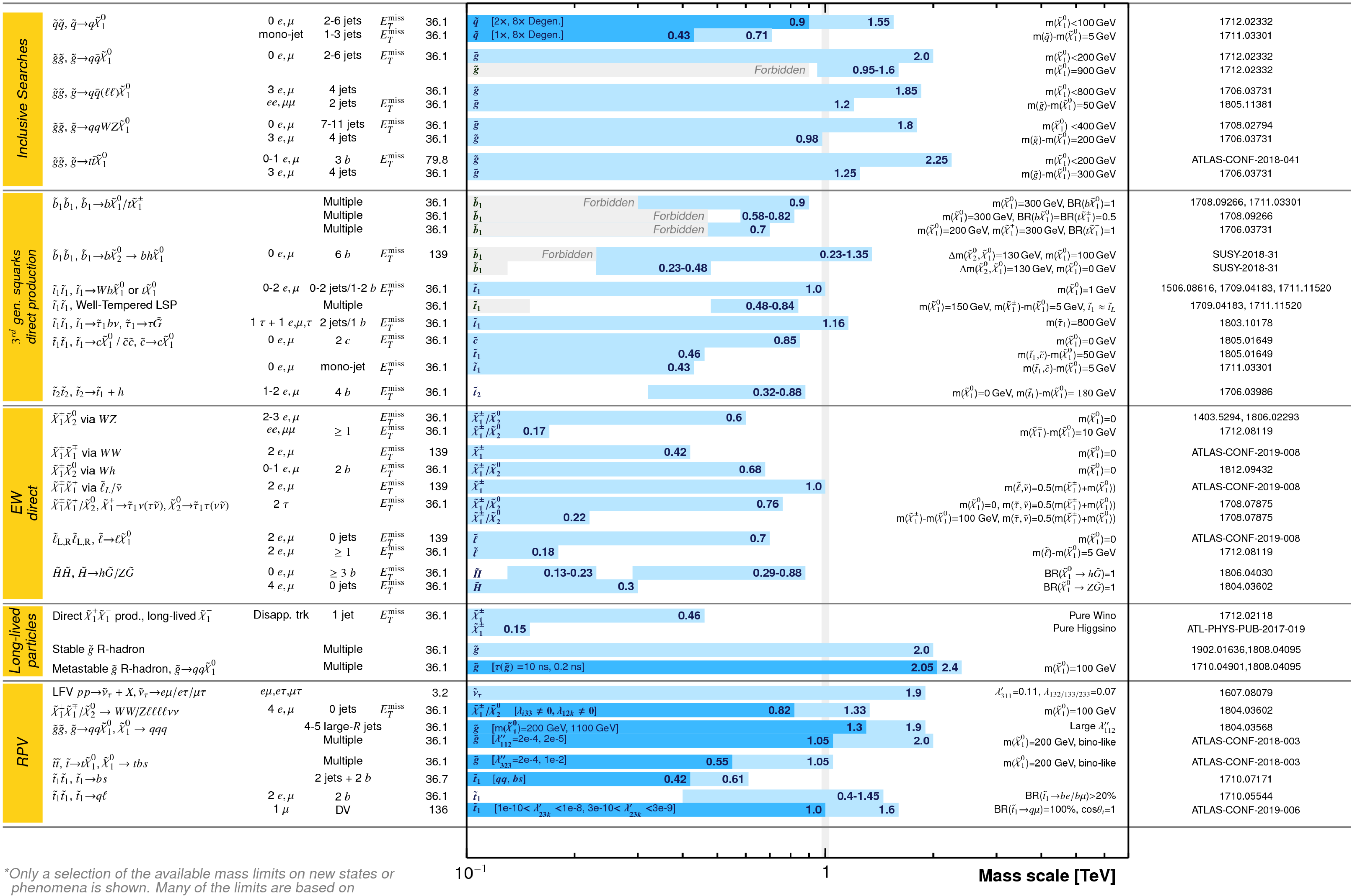

	Model	Signature			$\int \mathcal{L}\,dt$ [fb^{-1}]	Mass limit			Reference
Inclusive Searches	$\tilde{q}\tilde{q}$, $\tilde{q}\to q\tilde{\chi}^0_1$	0 e,μ	2-6 jets	E_T^{miss}	36.1	$\tilde{q}$	[2×, 8× Degen.] 0.9 1.55	m($\tilde{\chi}^0_1$)<100 GeV	1712.02332
		mono-jet	1-3 jets	E_T^{miss}	36.1	$\tilde{q}$	[1×, 8× Degen.] 0.43 0.71	m($\tilde{q}$)-m($\tilde{\chi}^0_1$)=5 GeV	1711.03301
	$\tilde{g}\tilde{g}$, $\tilde{g}\to q\bar{q}\tilde{\chi}^0_1$	0 e,μ	2-6 jets	E_T^{miss}	36.1	$\tilde{g}$	2.0	m($\tilde{\chi}^0_1$)<200 GeV	1712.02332
						$\tilde{g}$	Forbidden 0.95-1.6	m($\tilde{\chi}^0_1$)=900 GeV	1712.02332
	$\tilde{g}\tilde{g}$, $\tilde{g}\to q\bar{q}(\ell\ell)\tilde{\chi}^0_1$	3 e,μ	4 jets		36.1	$\tilde{g}$	1.85	m($\tilde{\chi}^0_1$)<800 GeV	1706.03731
		$ee,\mu\mu$	2 jets	E_T^{miss}	36.1	$\tilde{g}$	1.2	m($\tilde{g}$)-m($\tilde{\chi}^0_1$)=50 GeV	1805.11381
	$\tilde{g}\tilde{g}$, $\tilde{g}\to qqWZ\tilde{\chi}^0_1$	0 e,μ	7-11 jets	E_T^{miss}	36.1	$\tilde{g}$	1.8	m($\tilde{\chi}^0_1$) <400 GeV	1708.02794
		3 e,μ	4 jets		36.1	$\tilde{g}$	0.98	m($\tilde{g}$)-m($\tilde{\chi}^0_1$)=200 GeV	1706.03731
	$\tilde{g}\tilde{g}$, $\tilde{g}\to t\bar{t}\tilde{\chi}^0_1$	0-1 e,μ	3 b	E_T^{miss}	79.8	$\tilde{g}$	2.25	m($\tilde{\chi}^0_1$)<200 GeV	ATLAS-CONF-2018-041
		3 e,μ	4 jets		36.1	$\tilde{g}$	1.25	m($\tilde{g}$)-m($\tilde{\chi}^0_1$)=300 GeV	1706.03731
3^{rd} gen. squarks direct production	$\tilde{b}_1\tilde{b}_1$, $\tilde{b}_1\to b\tilde{\chi}^0_1/t\tilde{\chi}^\pm_1$		Multiple		36.1	$\tilde{b}_1$	Forbidden 0.9	m($\tilde{\chi}^0_1$)=300 GeV, BR($b\tilde{\chi}^0_1$)=1	1708.09266, 1711.03301
			Multiple		36.1	$\tilde{b}_1$	Forbidden 0.58-0.82	m($\tilde{\chi}^0_1$)=300 GeV, BR($b\tilde{\chi}^0_1$)=BR($t\tilde{\chi}^\pm_1$)=0.5	1708.09266
			Multiple		36.1	$\tilde{b}_1$	Forbidden 0.7	m($\tilde{\chi}^0_1$)=200 GeV, m($\tilde{\chi}^\pm_1$)=300 GeV, BR($t\tilde{\chi}^\pm_1$)=1	1706.03731
	$\tilde{b}_1\tilde{b}_1$, $\tilde{b}_1\to b\tilde{\chi}^0_2\to bh\tilde{\chi}^0_1$	0 e,μ	6 b	E_T^{miss}	139	$\tilde{b}_1$	Forbidden 0.23-1.35	Δm($\tilde{\chi}^0_2,\tilde{\chi}^0_1$)=130 GeV, m($\tilde{\chi}^0_1$)=100 GeV	SUSY-2018-31
						$\tilde{b}_1$	0.23-0.48	Δm($\tilde{\chi}^0_2,\tilde{\chi}^0_1$)=130 GeV, m($\tilde{\chi}^0_1$)=0 GeV	SUSY-2018-31
	$\tilde{t}_1\tilde{t}_1$, $\tilde{t}_1\to Wb\tilde{\chi}^0_1$ or $t\tilde{\chi}^0_1$	0-2 e,μ	0-2 jets/1-2 b	E_T^{miss}	36.1	$\tilde{t}_1$	1.0	m($\tilde{\chi}^0_1$)=1 GeV	1506.08616, 1709.04183, 1711.11520
	$\tilde{t}_1\tilde{t}_1$, Well-Tempered LSP		Multiple		36.1	$\tilde{t}_1$	0.48-0.84	m($\tilde{\chi}^0_1$)=150 GeV, m($\tilde{\chi}^\pm_1$)-m($\tilde{\chi}^0_1$)=5 GeV, $\tilde{t}_1\approx\tilde{t}_L$	1709.04183, 1711.11520
	$\tilde{t}_1\tilde{t}_1$, $\tilde{t}_1\to\tilde{\tau}_1 b\nu$, $\tilde{\tau}_1\to\tau\tilde{G}$	1 τ + 1 e,μ,τ	2 jets/1 b	E_T^{miss}	36.1	$\tilde{t}_1$	1.16	m($\tilde{\tau}_1$)=800 GeV	1803.10178
	$\tilde{t}_1\tilde{t}_1$, $\tilde{t}_1\to c\tilde{\chi}^0_1$ / $\tilde{c}\tilde{c}$, $\tilde{c}\to c\tilde{\chi}^0_1$	0 e,μ	2 c	E_T^{miss}	36.1	$\tilde{c}$	0.85	m($\tilde{\chi}^0_1$)=0 GeV	1805.01649
						$\tilde{t}_1$	0.46	m($\tilde{t}_1$,$\tilde{c}$)-m($\tilde{\chi}^0_1$)=50 GeV	1805.01649
		0 e,μ	mono-jet	E_T^{miss}	36.1	$\tilde{t}_1$	0.43	m($\tilde{t}_1$,$\tilde{c}$)-m($\tilde{\chi}^0_1$)=5 GeV	1711.03301
	$\tilde{t}_2\tilde{t}_2$, $\tilde{t}_2\to\tilde{t}_1+h$	1-2 e,μ	4 b	E_T^{miss}	36.1	$\tilde{t}_2$	0.32-0.88	m($\tilde{\chi}^0_1$)=0 GeV, m($\tilde{t}_1$)-m($\tilde{\chi}^0_1$)= 180 GeV	1706.03986
EW direct	$\tilde{\chi}^\pm_1\tilde{\chi}^0_2$ via WZ	2-3 e,μ		E_T^{miss}	36.1	$\tilde{\chi}^\pm_1/\tilde{\chi}^0_2$	0.6	m($\tilde{\chi}^0_1$)=0	1403.5294, 1806.02293
		$ee,\mu\mu$	≥ 1	E_T^{miss}	36.1	$\tilde{\chi}^\pm_1/\tilde{\chi}^0_2$	0.17	m($\tilde{\chi}^\pm_1$)-m($\tilde{\chi}^0_1$)=10 GeV	1712.08119
	$\tilde{\chi}^\pm_1\tilde{\chi}^\mp_1$ via WW	2 e,μ		E_T^{miss}	139	$\tilde{\chi}^\pm_1$	0.42	m($\tilde{\chi}^0_1$)=0	ATLAS-CONF-2019-008
	$\tilde{\chi}^\pm_1\tilde{\chi}^0_2$ via Wh	0-1 e,μ	2 b	E_T^{miss}	36.1	$\tilde{\chi}^\pm_1/\tilde{\chi}^0_2$	0.68	m($\tilde{\chi}^0_1$)=0	1812.09432
	$\tilde{\chi}^\pm_1\tilde{\chi}^\mp_1$ via $\tilde{\ell}_L/\tilde{\nu}$	2 e,μ		E_T^{miss}	139	$\tilde{\chi}^\pm_1$	1.0	m($\tilde{\ell}$,$\tilde{\nu}$)=0.5(m($\tilde{\chi}^\pm_1$)+m($\tilde{\chi}^0_1$))	ATLAS-CONF-2019-008
	$\tilde{\chi}^\pm_1\tilde{\chi}^\mp_1/\tilde{\chi}^0_2$, $\tilde{\chi}^+_1\to\tilde{\tau}_1\nu(\tau\tilde{\nu})$, $\tilde{\chi}^0_2\to\tilde{\tau}_1\tau(\nu\tilde{\nu})$	2 τ		E_T^{miss}	36.1	$\tilde{\chi}^\pm_1/\tilde{\chi}^0_2$	0.76	m($\tilde{\chi}^0_1$)=0, m($\tilde{\tau}$, $\tilde{\nu}$)=0.5(m($\tilde{\chi}^\pm_1$)+m($\tilde{\chi}^0_1$))	1708.07875
						$\tilde{\chi}^\pm_1/\tilde{\chi}^0_2$	0.22	m($\tilde{\chi}^\pm_1$)-m($\tilde{\chi}^0_1$)=100 GeV, m($\tilde{\tau}$, $\tilde{\nu}$)=0.5(m($\tilde{\chi}^\pm_1$)+m($\tilde{\chi}^0_1$))	1708.07875
	$\tilde{\ell}_{\mathrm{L,R}}\tilde{\ell}_{\mathrm{L,R}}$, $\tilde{\ell}\to\ell\tilde{\chi}^0_1$	2 e,μ	0 jets	E_T^{miss}	139	$\tilde{\ell}$	0.7	m($\tilde{\chi}^0_1$)=0	ATLAS-CONF-2019-008
		2 e,μ	≥ 1	E_T^{miss}	36.1	$\tilde{\ell}$	0.18	m($\tilde{\ell}$)-m($\tilde{\chi}^0_1$)=5 GeV	1712.08119
	$\tilde{H}\tilde{H}$, $\tilde{H}\to h\tilde{G}/Z\tilde{G}$	0 e,μ	≥ 3 b	E_T^{miss}	36.1	$\tilde{H}$	0.13-0.23 0.29-0.88	BR($\tilde{\chi}^0_1\to h\tilde{G}$)=1	1806.04030
		4 e,μ	0 jets	E_T^{miss}	36.1	$\tilde{H}$	0.3	BR($\tilde{\chi}^0_1\to Z\tilde{G}$)=1	1804.03602
Long-lived particles	Direct $\tilde{\chi}^+_1\tilde{\chi}^-_1$ prod., long-lived $\tilde{\chi}^\pm_1$	Disapp. trk	1 jet	E_T^{miss}	36.1	$\tilde{\chi}^\pm_1$	0.46	Pure Wino	1712.02118
						$\tilde{\chi}^\pm_1$	0.15	Pure Higgsino	ATL-PHYS-PUB-2017-019
	Stable $\tilde{g}$ R-hadron		Multiple		36.1	$\tilde{g}$	2.0		1902.01636,1808.04095
	Metastable $\tilde{g}$ R-hadron, $\tilde{g}\to qq\tilde{\chi}^0_1$		Multiple		36.1	$\tilde{g}$	[$\tau(\tilde{g})$ =10 ns, 0.2 ns] 2.05 2.4	m($\tilde{\chi}^0_1$)=100 GeV	1710.04901,1808.04095
RPV	LFV $pp\to\tilde{\nu}_\tau+X, \tilde{\nu}_\tau\to e\mu/e\tau/\mu\tau$	$e\mu$,$e\tau$,$\mu\tau$			3.2	$\tilde{\nu}_\tau$	1.9	λ'_{311}=0.11, $\lambda_{132/133/233}$=0.07	1607.08079
	$\tilde{\chi}^\pm_1\tilde{\chi}^\mp_1/\tilde{\chi}^0_2\to WW/Z\ell\ell\ell\ell\nu\nu$	4 e,μ	0 jets	E_T^{miss}	36.1	$\tilde{\chi}^\pm_1/\tilde{\chi}^0_2$	[$\lambda_{i33}\neq 0, \lambda_{12k}\neq 0$] 0.82 1.33	m($\tilde{\chi}^0_1$)=100 GeV	1804.03602
	$\tilde{g}\tilde{g}$, $\tilde{g}\to qq\tilde{\chi}^0_1$, $\tilde{\chi}^0_1\to qqq$		4-5 large-R jets		36.1	$\tilde{g}$	[m($\tilde{\chi}^0_1$)=200 GeV, 1100 GeV] 1.3 1.9	Large λ''_{112}	1804.03568
			Multiple		36.1	$\tilde{g}$	[λ''_{112}=2e-4, 2e-5] 1.05 2.0	m($\tilde{\chi}^0_1$)=200 GeV, bino-like	ATLAS-CONF-2018-003
	$\tilde{t}\tilde{t}$, $\tilde{t}\to t\tilde{\chi}^0_1$, $\tilde{\chi}^0_1\to tbs$		Multiple		36.1	$\tilde{g}$	[λ''_{323}=2e-4, 1e-2] 0.55 1.05	m($\tilde{\chi}^0_1$)=200 GeV, bino-like	ATLAS-CONF-2018-003
	$\tilde{t}_1\tilde{t}_1$, $\tilde{t}_1\to bs$		2 jets + 2 b		36.7	$\tilde{t}_1$	[qq, bs] 0.42 0.61		1710.07171
	$\tilde{t}_1\tilde{t}_1$, $\tilde{t}_1\to q\ell$	2 e,μ	2 b		36.1	$\tilde{t}_1$	0.4-1.45	BR($\tilde{t}_1\to be/b\mu$)>20%	1710.05544
		1 μ	DV		136	$\tilde{t}_1$	[1e-10< λ'_{23k} <1e-8, 3e-10< λ'_{23k} <3e-9] 1.0 1.6	BR($\tilde{t}_1\to q\mu$)=100%, cosθ_t=1	ATLAS-CONF-2019-006

*Only a selection of the available mass limits on new states or phenomena is shown. Many of the limits are based on simplified models, c.f. refs. for the assumptions made.

General Analysis Methodology

- All leptons (e, μ, τ) and jets are required to have a high transverse momentum (p_T) - usually above 20 GeV (some > 200/500 GeV), when neutrinos are present in the final states a large missing transverse energy (**$E_{T,miss}$**) amount (>200 GeV) is required.

- The signal processes are required to have large invariant mass of the final states leptons/jets (m_{ll},m_{jj}), or large transverse mass: $m_T = \sqrt{2p_T^{\ell}p_T^{\nu}(1-\cos\Delta\phi(\ell,\nu))}$

- Jets are reconstructed using the *anti-k_t algorithm* with different radius R (=0.4, 1)

- Some analyses use the ***particle-flow*** (*PF*) algorithm which reconstructs and identifies individual particles with information from the various elements of the ATLAS/CMS detectors.

- The main **backgrounds** (*BG*) to most analyses: Drell-Yan, top quarks, single-top, di-boson (WW,WZ,ZZ), QCD multijet, *W/Z* +jets, ttH, fake leptons from QCD.

- In general ***data-driven methods*** used for background estimation, different *parametrisation functions* and *3D fits* for modelling, and where this is not possible Monte Carlo simulation of specific processes is used.

- The background is reduced by applying ***kinematic criteria***, dividing the analysis in several *signal regions*, trigger/detector requirements.

arXiv:1903.06248

Search for high-mass di-lepton resonances at ATLAS

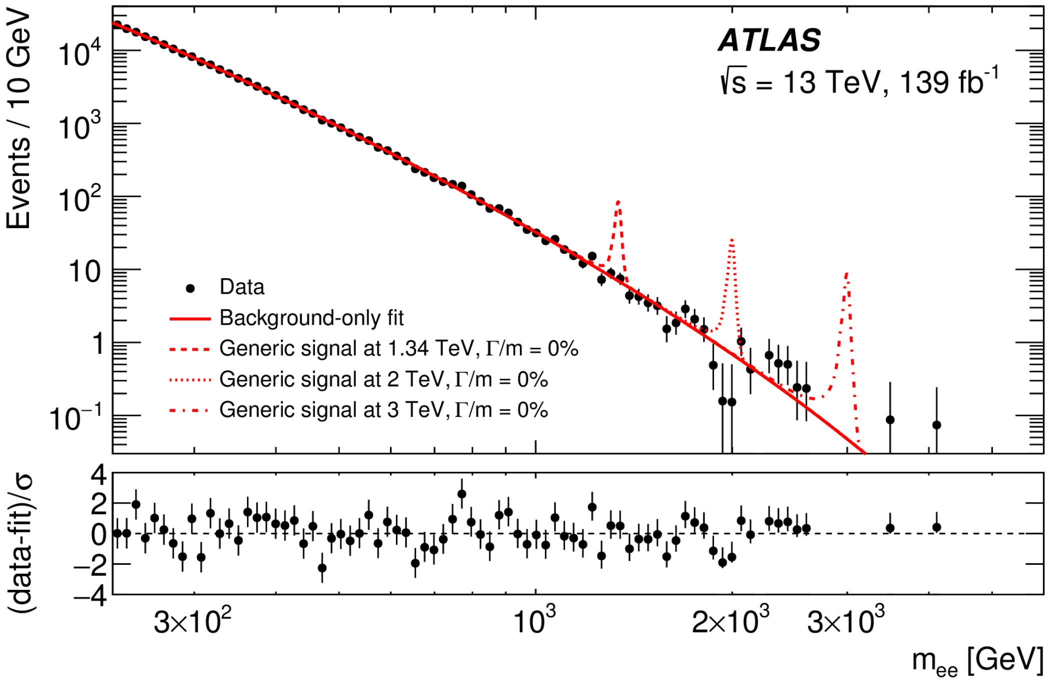

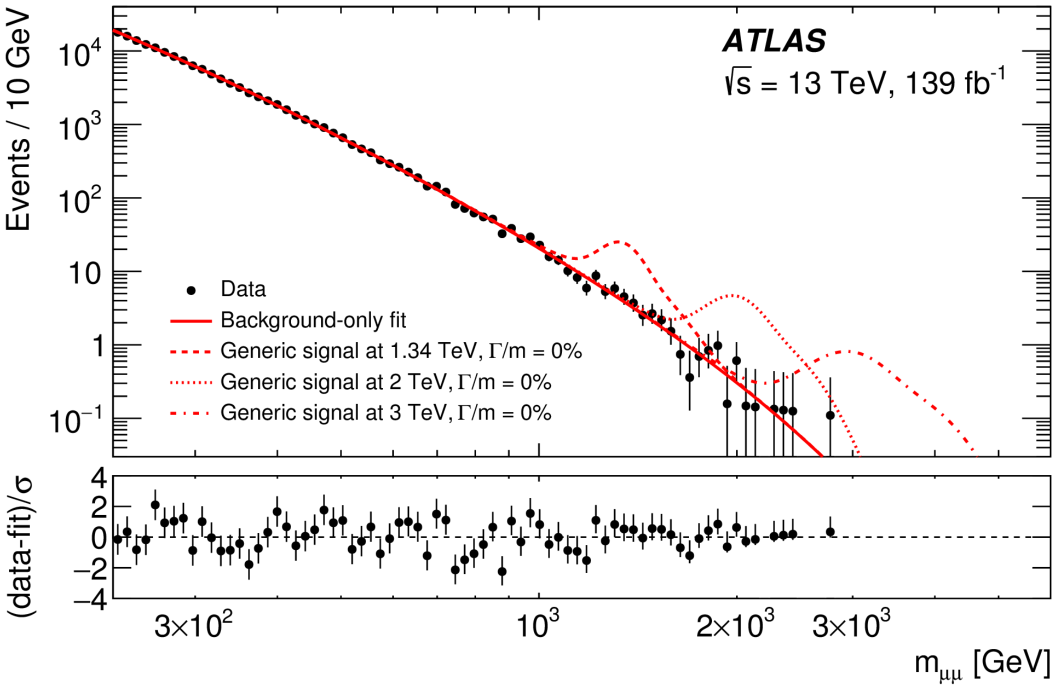

139 fb^{-1}

- Searching for resonances decaying **two e/μ** between ***250 GeV - 6 TeV*** predicted by MSSM (*spin-0 H*) / SSM (*spin-1 Z'*) / RS (*spin-2 G*) models

- No significant deviation from data-driven *BG*; limit set on a Z'_{SSM} at 95% CL > 5.1 TeV obs(exp) for combined e+μ

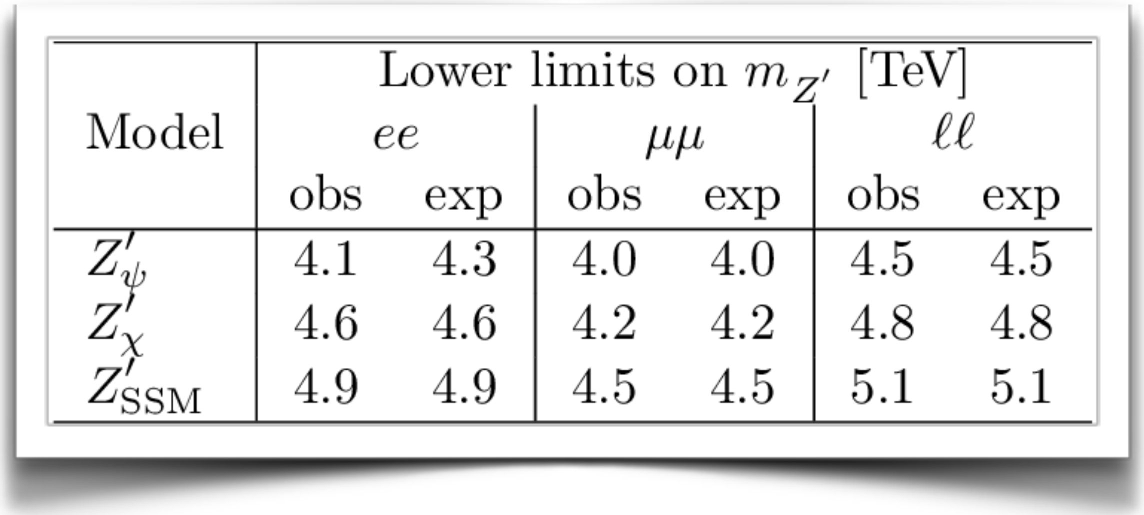

Model	Lower limits on $m_{Z'}$ [TeV]					
	ee		$\mu\mu$		$\ell\ell$	
	obs	exp	obs	exp	obs	exp
Z'_{ψ}	4.1	4.3	4.0	4.0	4.5	4.5
Z'_{χ}	4.6	4.6	4.2	4.2	4.8	4.8
Z'_{SSM}	4.9	4.9	4.5	4.5	5.1	5.1

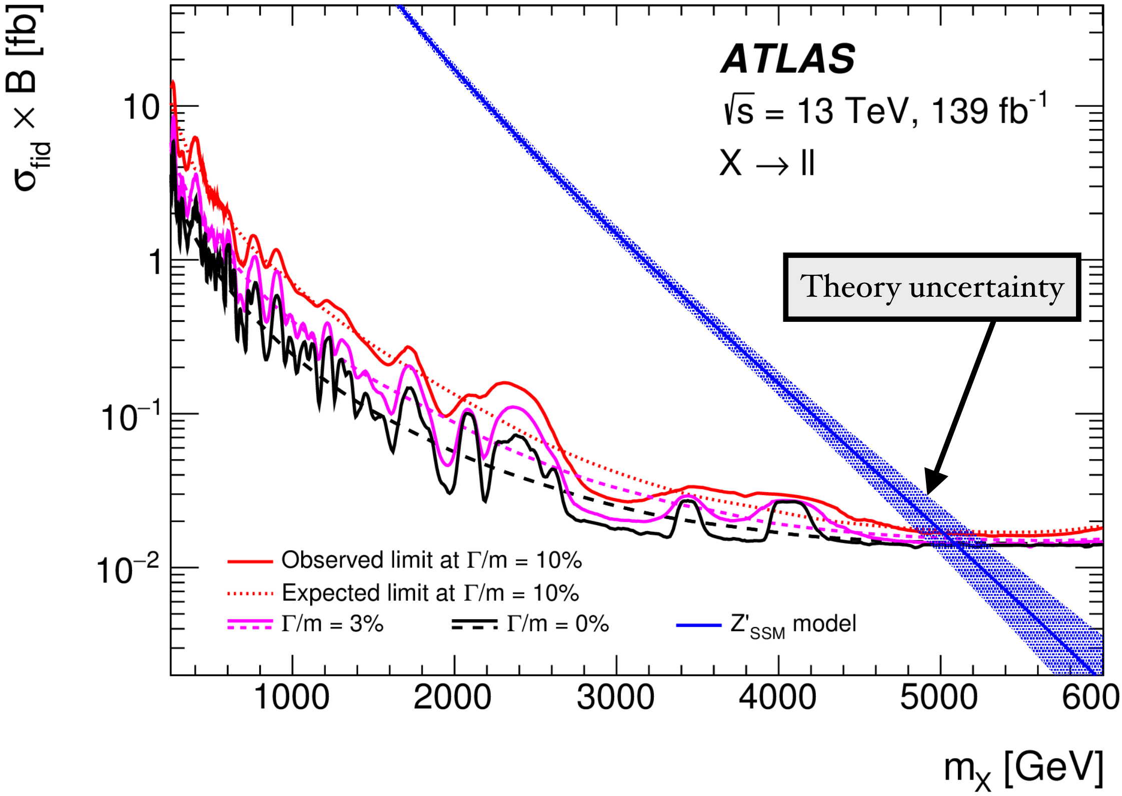

- CMS results for di-lepton resonances with 36 fb^{-1} can be found here

139 fb^{-1}

ATLAS-CONF-2019-007

Search for high-mass di-jet resonances at ATLAS

- Excited quarks (*q**) are predicted in models of compositeness and are a typical benchmark for *qg* resonances used in many di-jet searches.
- **QCD** *BG* - reduced by applying a kinematic requirement on the rapidity difference between the two leading jets: $|y^*| = \frac{1}{2}|y_1 - y_2| < 0.6$
- No significant deviation from *BG*, limit set on a *q* model* at 95% CL > 6.7 TeV (6.4 TeV) obs(exp).

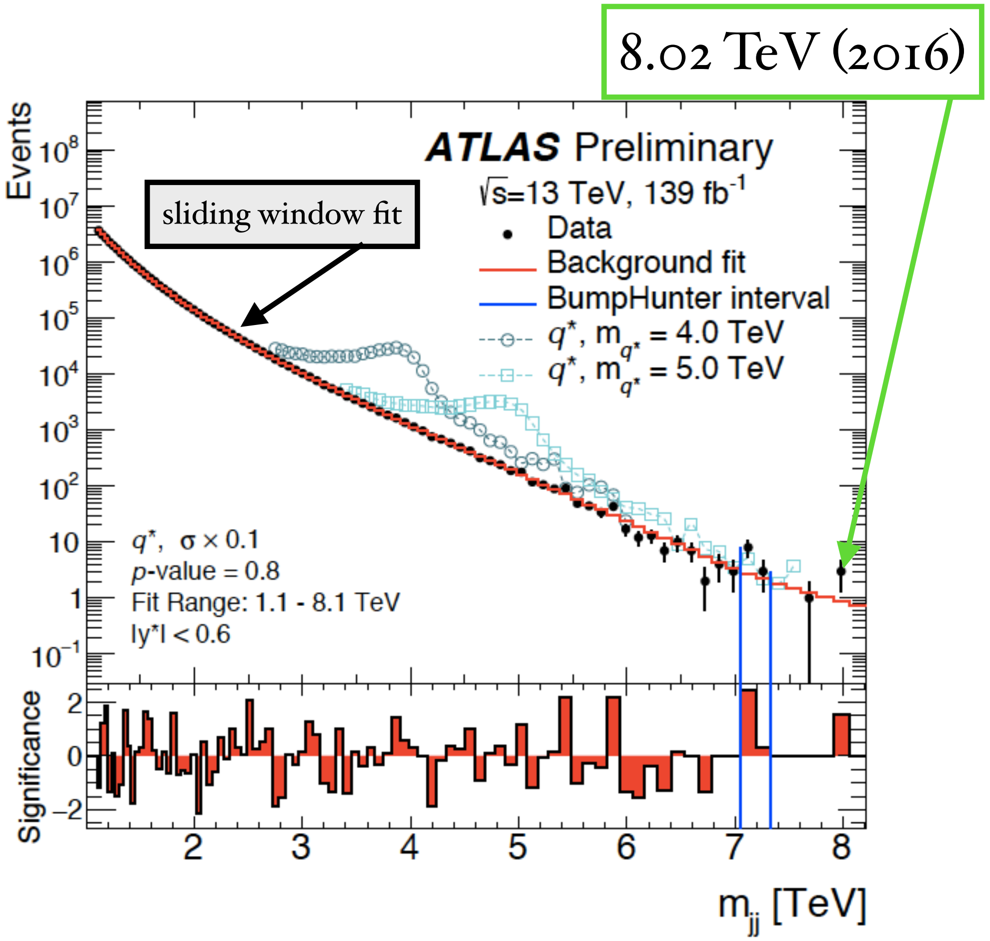

- CMS results for di-jet resonances with 80 fb^{-1} can be found here

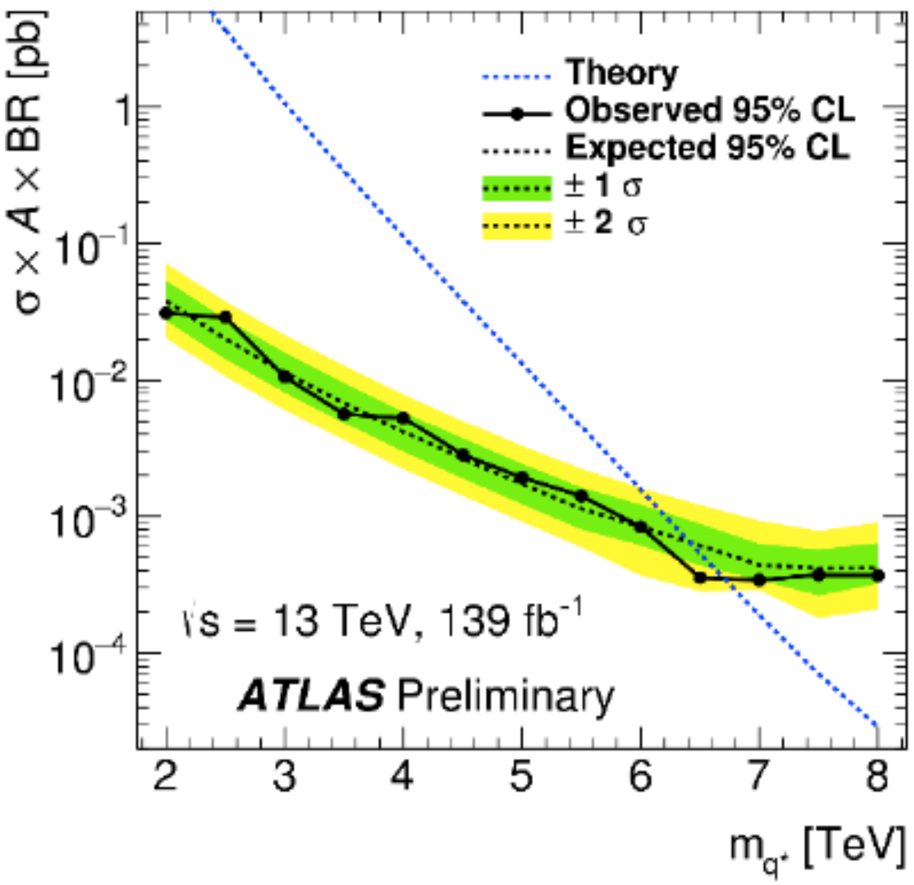

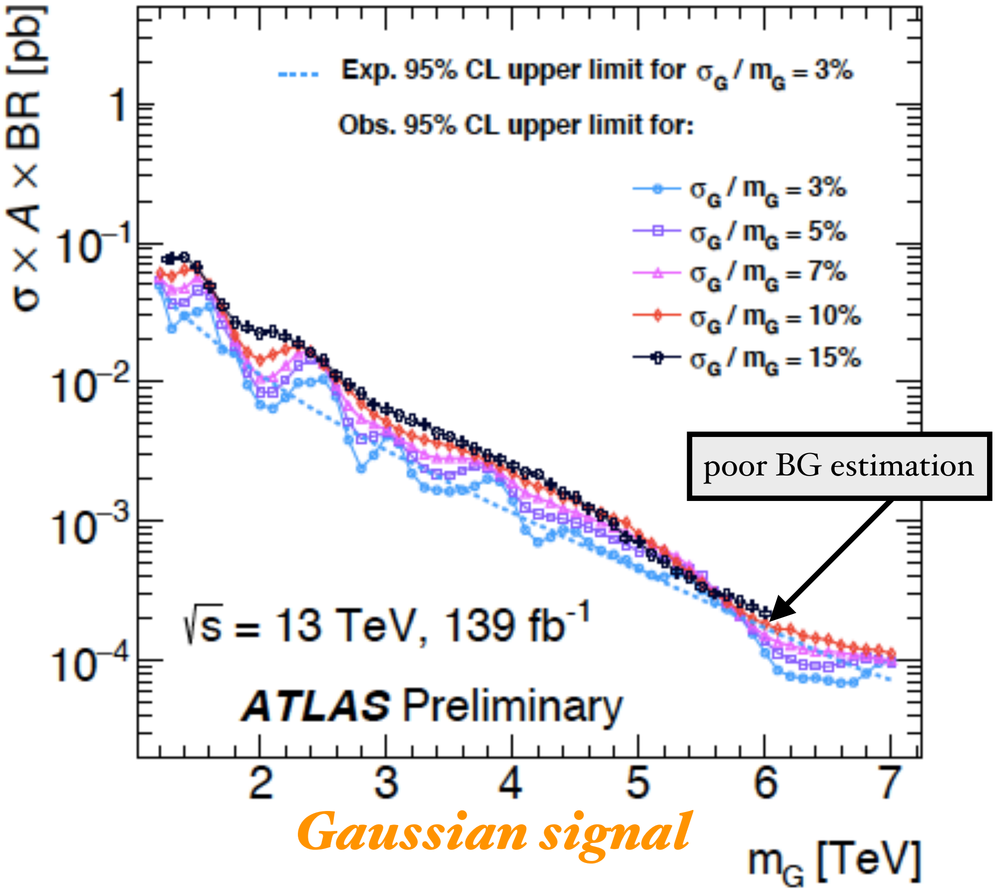

$77\ fb^{-1}$

CMS PAS B2G-18-002

Search for high-mass di-boson resonances at CMS

- ***Models:*** *Randall-Sundrum Warped Extra Dimensions* with a spin-2 bulk graviton (G_{bulk}) having an enhanced branching fraction to massive particles. *Heavy vector triplet (HVT) framework*, which serves as a generalisation of models predicting spin-1 resonances.

- **All-hadronic** final states coming from *1.2-5.5 TeV* resonances decays via *VV* (*V=W/Z*)

- No excess observed, upper limits in the cross section are between 27-0.2 fb for 1.2TeV< $m_{G_{bulk}}$ <5.2 TeV.
- *W'* and *Z'* with masses < 3.8 TeV and 3.5 TeV, resp. are excluded at 95% CL.

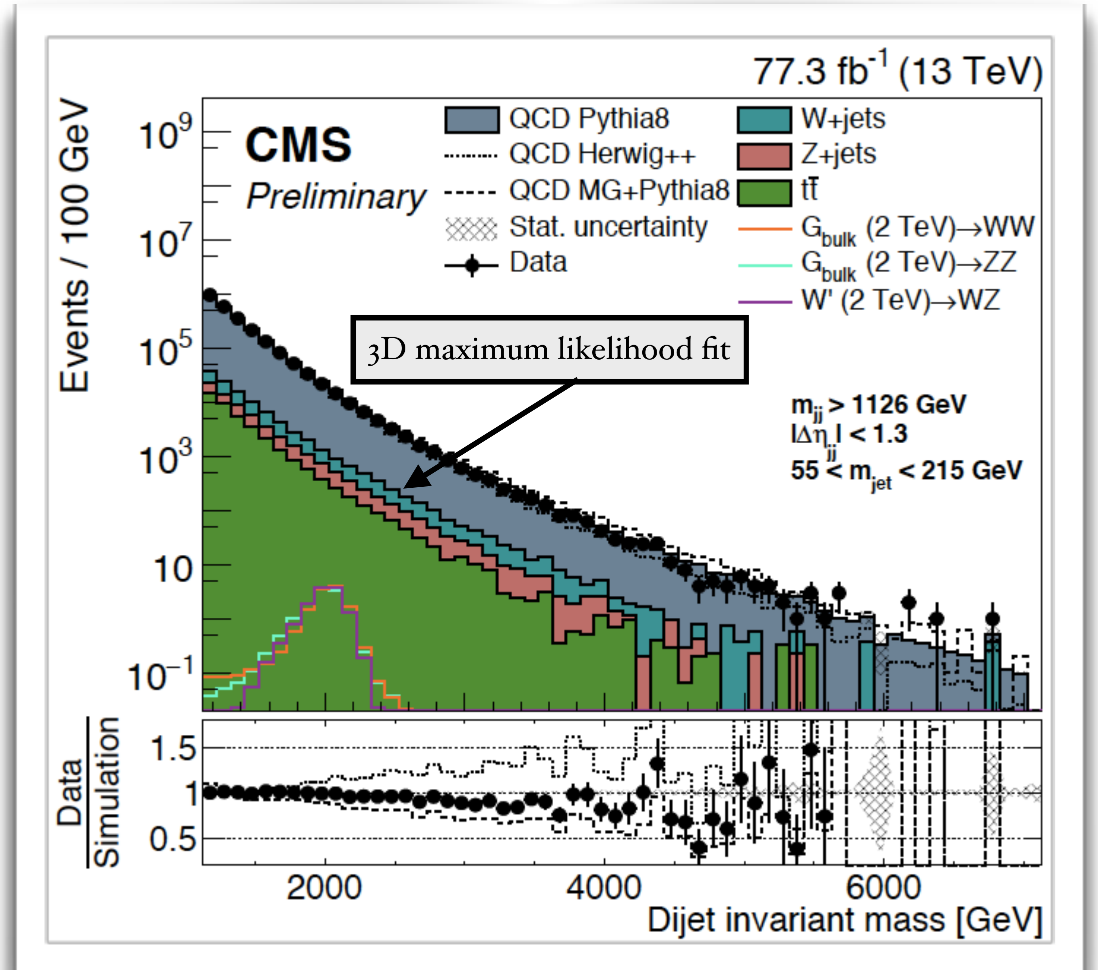
3D maximum likelihood fit

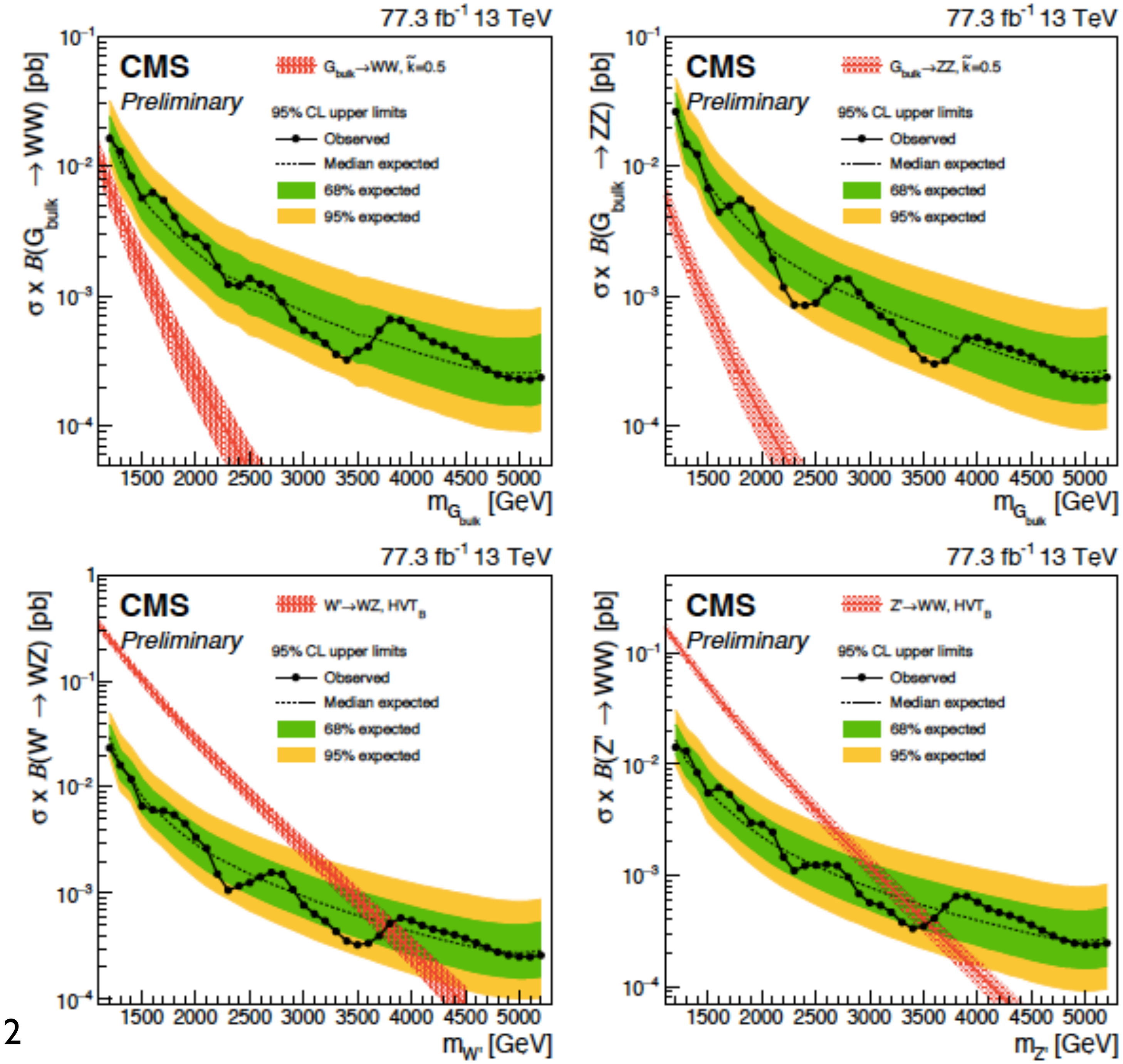

139 fb^{-1}

ATLAS-CONF-2019-003

Search for high-mass di-boson resonances at ATLAS

- Three specific benchmark models:
  - a spin-0 ***radion***
  - a spin-1 HVT Model (***W'/Z'***)
  - a spin-2 graviton ***G_{KK}***
- Narrow resonances (***m_{VV}> 1.3 TeV***) decaying into *WW*, *WZ* or *ZZ* boson pairs with m_{j1}>500GeV,m_{j2}>200GeV.
- The di-boson system reconstructed using pairs of *high p_T, large-radius jets*
- No excess, exclusion limits set at 95% CL for $m_{W'}$ > 3.6 TeV.

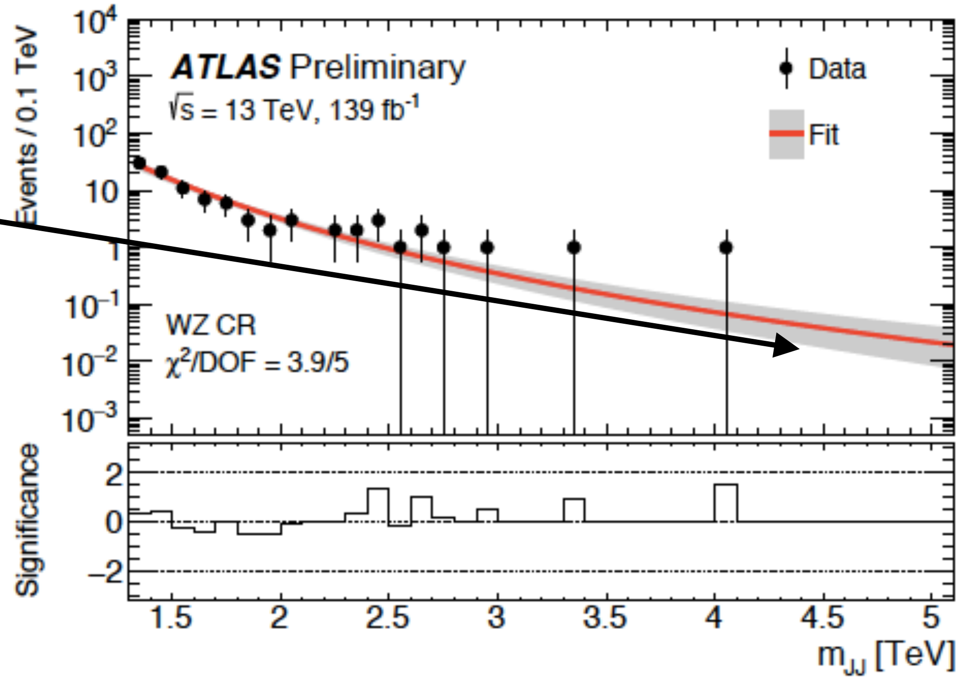

Uncertainty in the BG calculated from the maximum-likelihood function

Model	Signal Region	Excluded mass range [TeV]
Radion	*WW*	none
	ZZ	none
HVT model A, $g_V = 1$	*WW*	1.3–2.9
	WZ	1.3–3.4
HVT model B, $g_V = 3$	*WW*	1.3–3.1
	WZ	1.3–3.6
Bulk RS, $k/\overline{M}_{\rm Pl} = 1$	*WW*	1.3–1.6
	ZZ	none

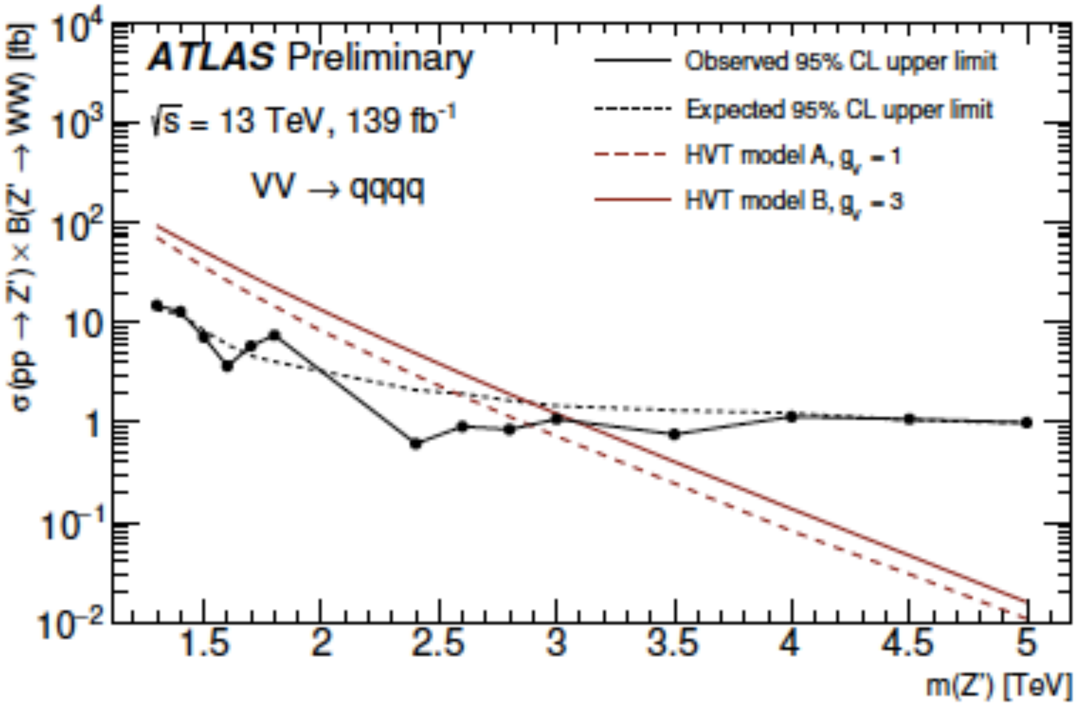

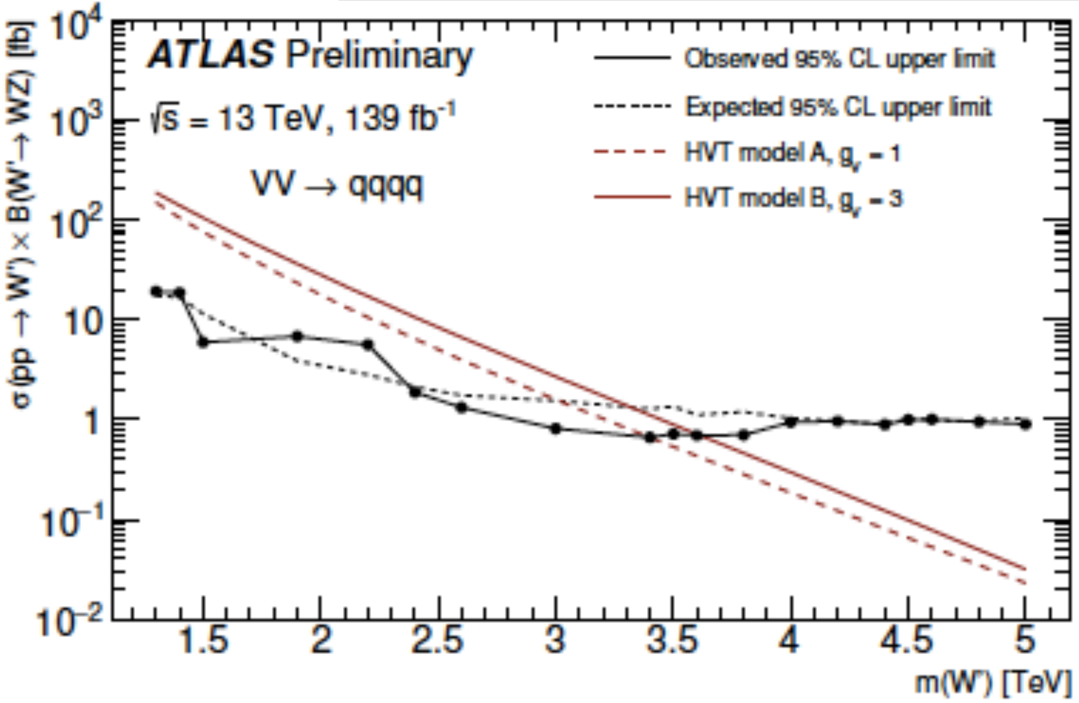

Multilepton search at CMS

CMS-PAS-EXO-19-002

$137\ \mathrm{fb}^{-1}$

- Exactly 3 (3L) or 4 and more (4L) high-p_T leptons
- *Type-III seesaw* pairs (***Σ******Σ***) of heavy fermions produce non-resonant tails in m_T or L_T+p_T^{miss} together with a light scalar or pseudoscalar boson with a pair of top quarks

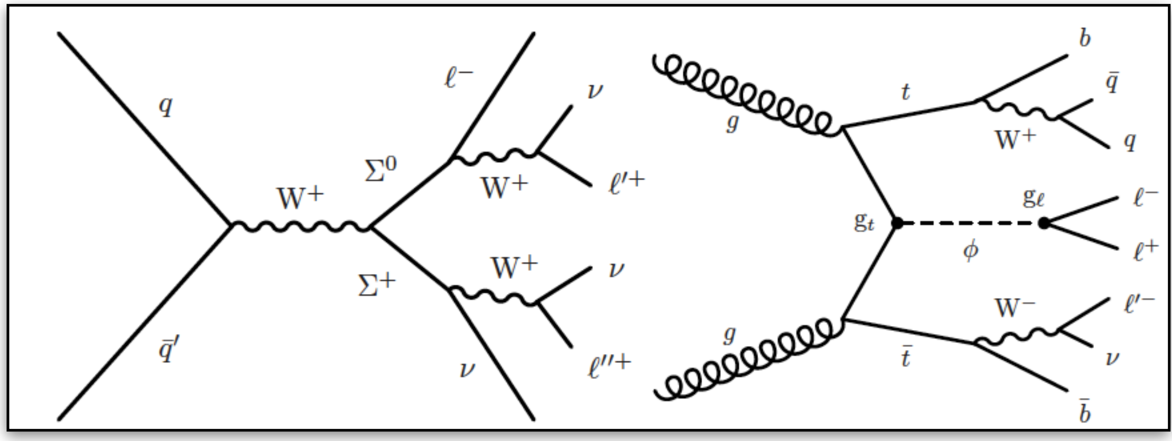

- *Light scalars/pseudoscalars (SUSY/DM)* may create resonant di-lepton mass spectra in multilepton events w/o b-quark jets
    - use of kinematic criteria for BG suppression: scalar sum of all lepton p_T + missing E_T
- No excess above the background, exclude ***heavy fermions*** below 880 GeV (930 GeV) obs(exp) for the lepton flavour democratic scenario. The branching ratio of ***new scalar (pseudoscalar) bosons*** to ee and $\mu\mu$ above 0.003 (0.03) and 0.04 (0.03) are excluded for masses between 15 − 75 GeV and 108 − 340 GeV, resp.

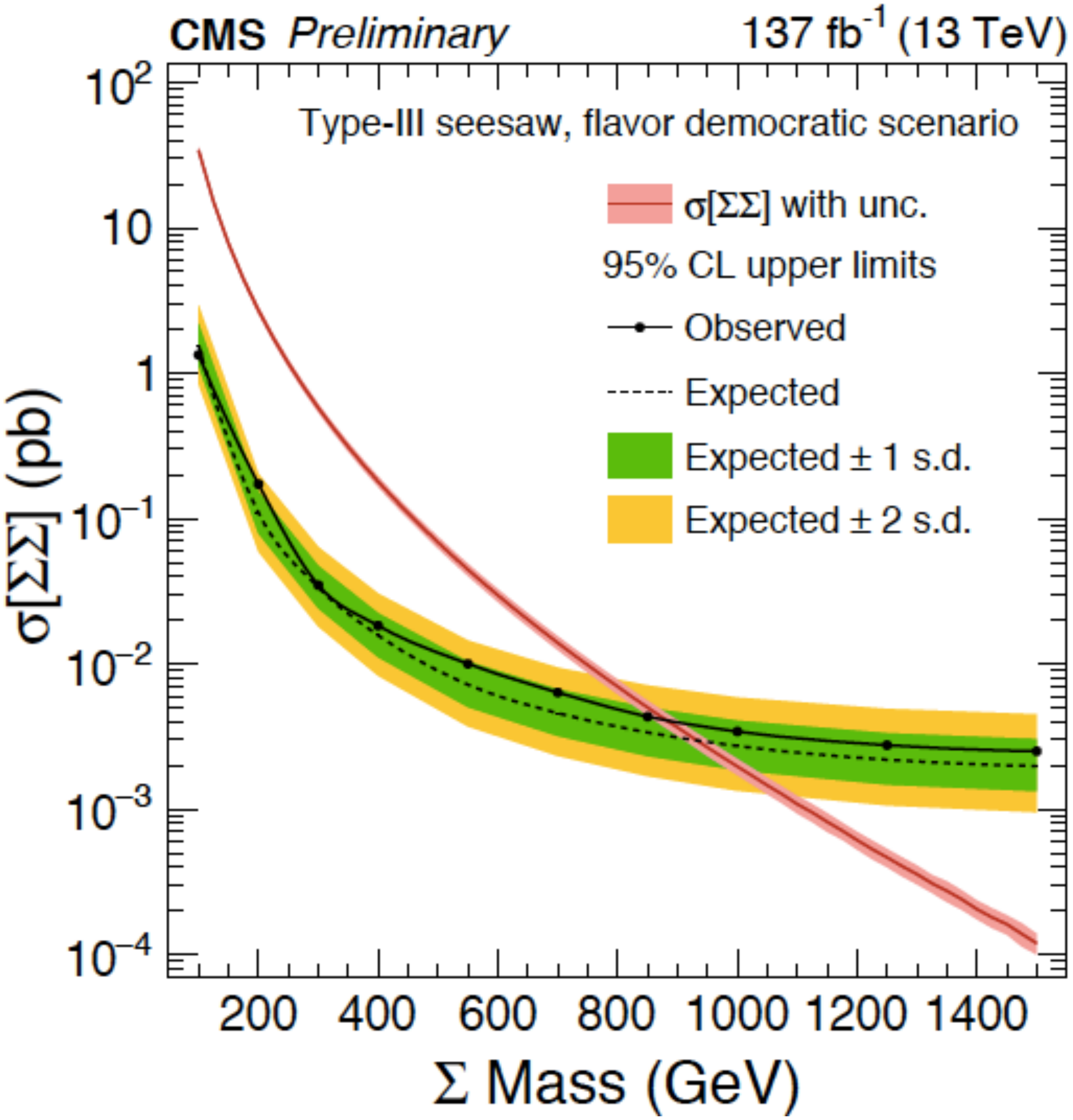

ATLAS-EXOT-2018-030

Search for heavy charged boson W′→lν at ATLAS

139 fb⁻¹

- Sequential Standard Model (***SSM***) predicts a *W'* with couplings to fermions identical to the W_{SM}
- No significant deviation from SM *BG*, limit on W'_{SSM} at 95% CL > 6.0 (5.8) TeV obs(exp) for combined e+μ result.
- Also provide σ(visible) => provide general constraints on all W′ models

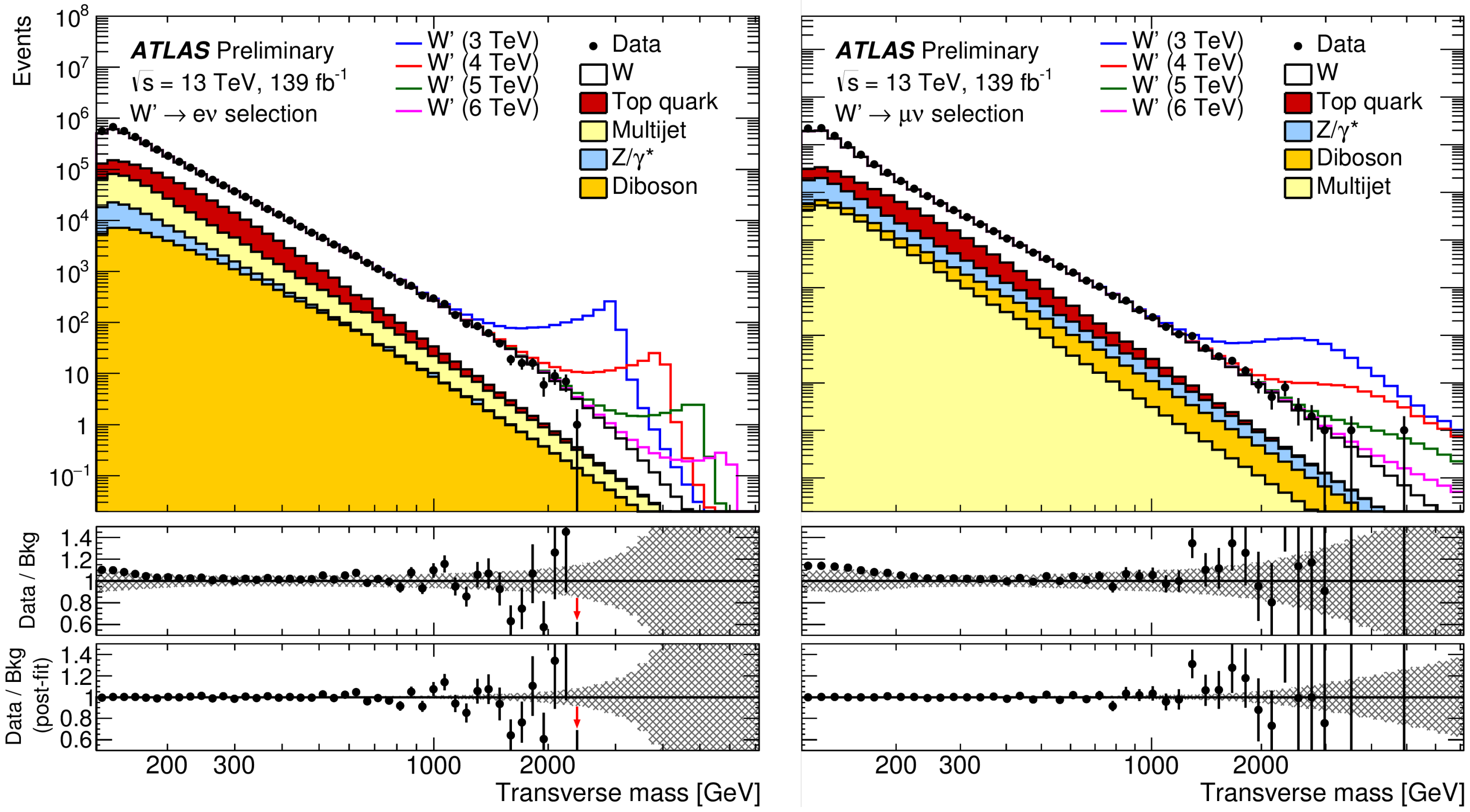

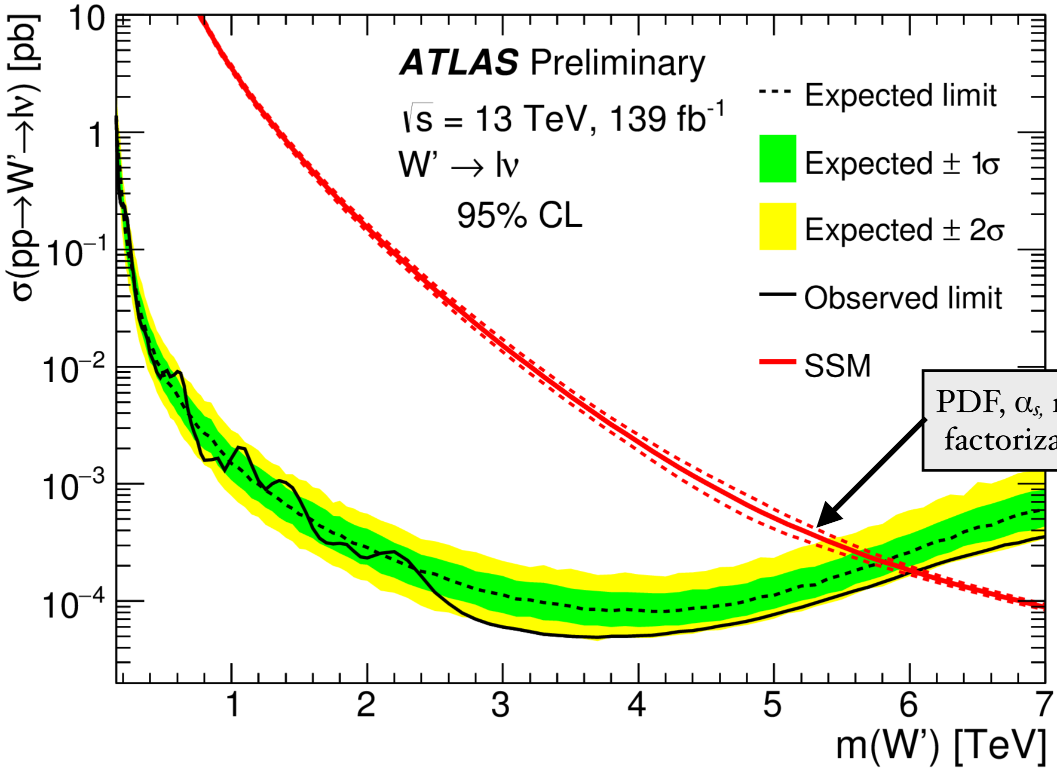

PDF, α_s, renormalization & factorization scale uncertainties

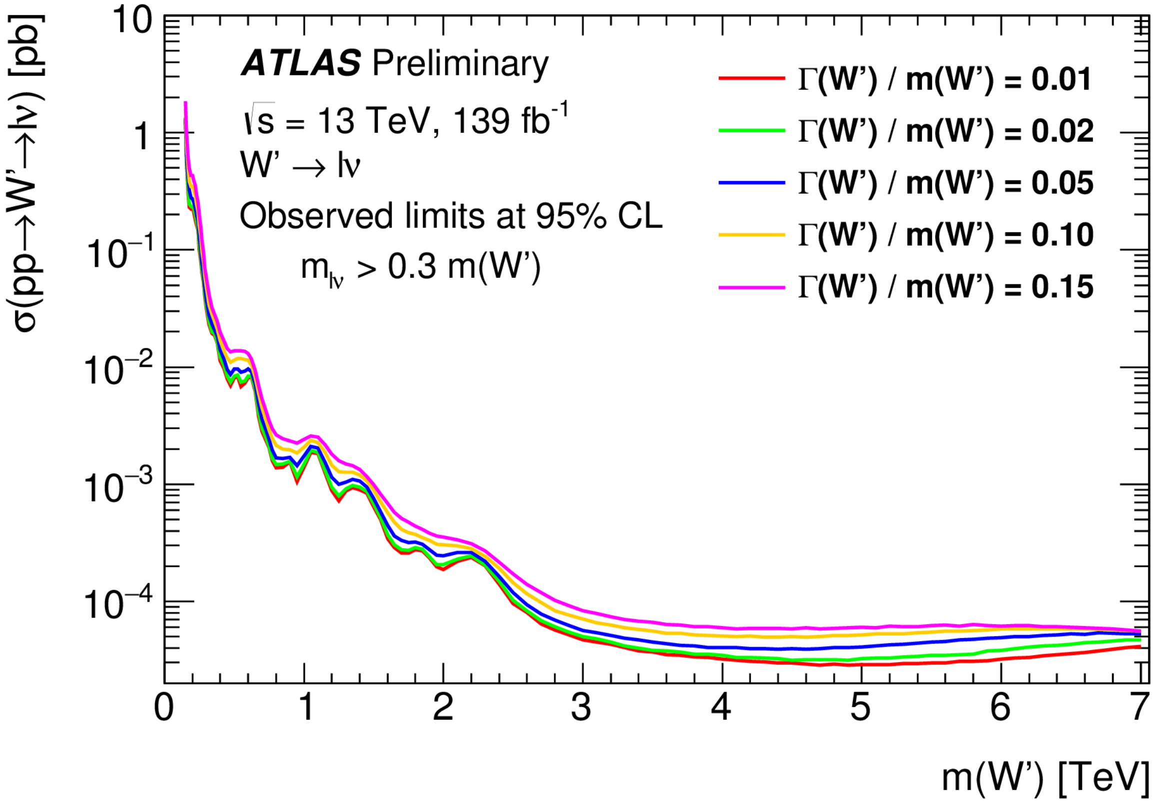

- The CMS results can be found here

33-36fb^{-1}

arXiv:1905.09787

Search for heavy neutral leptons from W bosons at ATLAS

- The problems of neutrino masses, matter–antimatter asymmetry and dark matter could be addressed by postulating right-handed neutrinos with Majorana masses below the EW scale.

- Search for heavy neutral leptons (*HNL*) produced through mixing with ν_e/ν_μ from *W*s decaying in both prompt ($\mu\mu e$ or $ee\mu$) and displaced ($\mu\mu$ or μe) signatures. Results are consistent with background expectations:
  - the *prompt signature* excludes coupling strengths above 4×10^{-5} in the mass range 10–50 GeV
  - the *displaced signature* excludes coupling strengths down to 2×10^{-6} (1.5×10^{-6}) in the mass range 4.5–10 GeV assuming lepton-number violation (conservation)

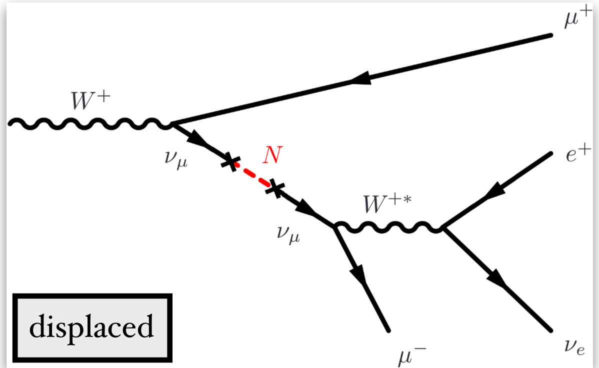

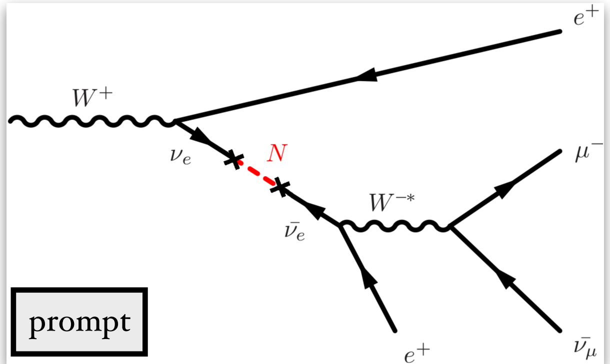

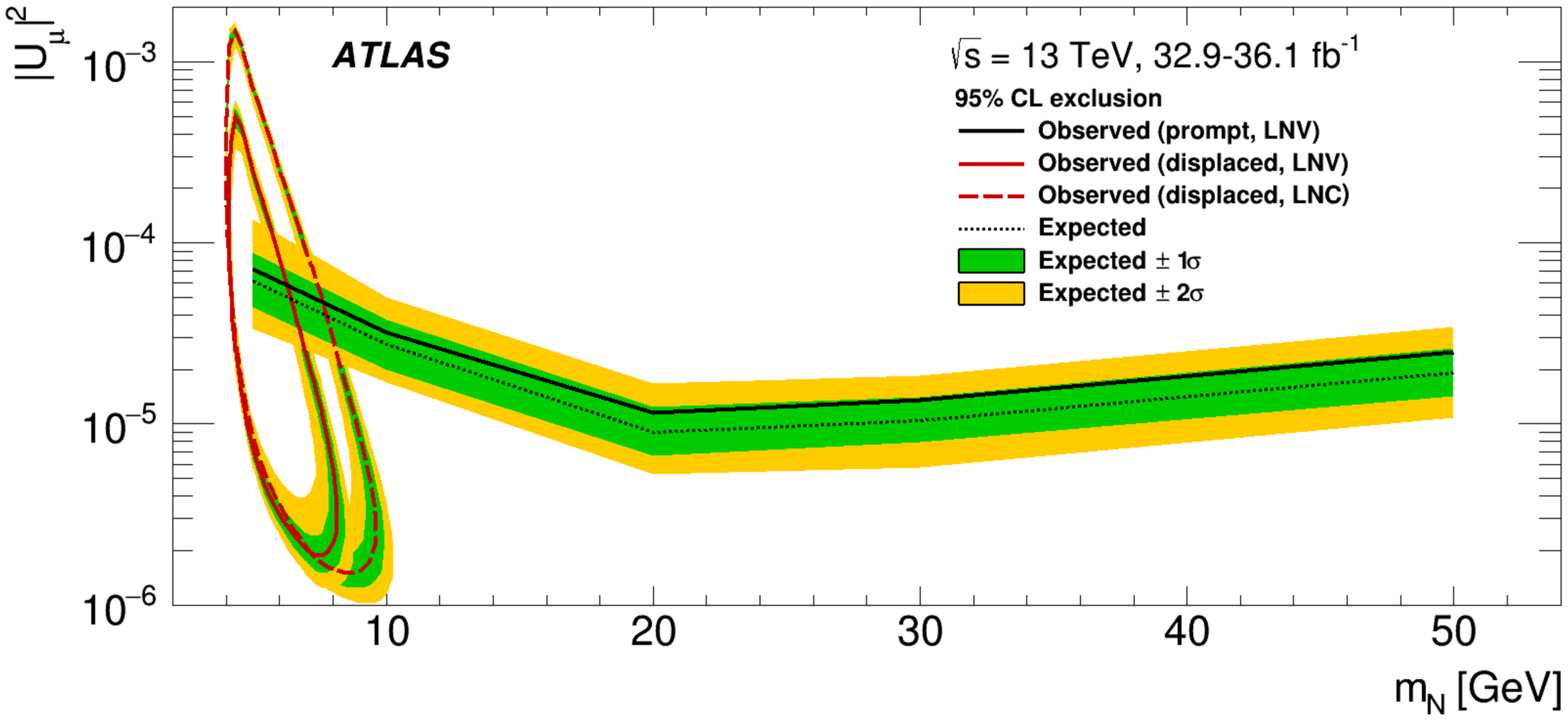

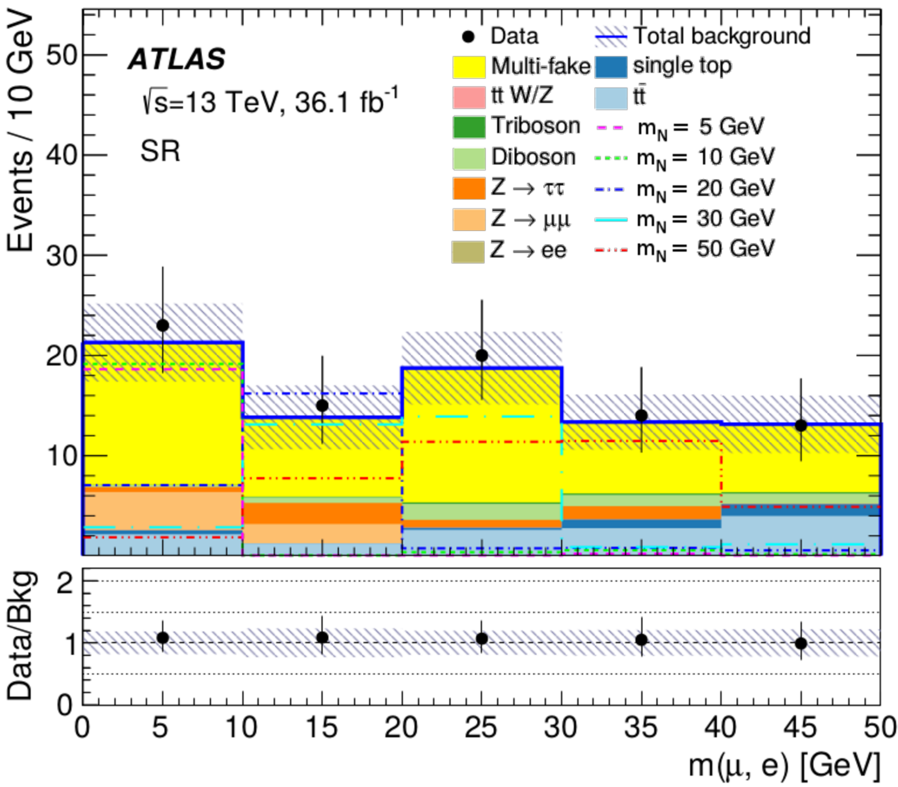

- The CMS results for *HNL* with 36 fb^{-1} here

80 fb^{-1}

arXiv:1904.12679

Search for a right-handed gauge boson $W_R \rightarrow N_R l$ at ATLAS

- In order to explain the *neutrino mass generation* look at the seesaw mechanism which can further be embedded into a *Left-Right Symmetric Model* which contains SM-singlet heavy neutrinos N_R, and a right-handed gauge boson W_R.
- Investigate the region where $m_{W_R} \gg m_{N_R}$ and N_R is produced with large p_T (highly boosted) and the decay products (l+jets) are very collimated
- Separate search in the e/μ channel and make use of large-radius jets containing electrons
- Lower limits are set in the W_R and N_R mass plane excluding m_{W_R} < 3.8–5 TeV for N_R in the mass range 0.1–1.8 TeV

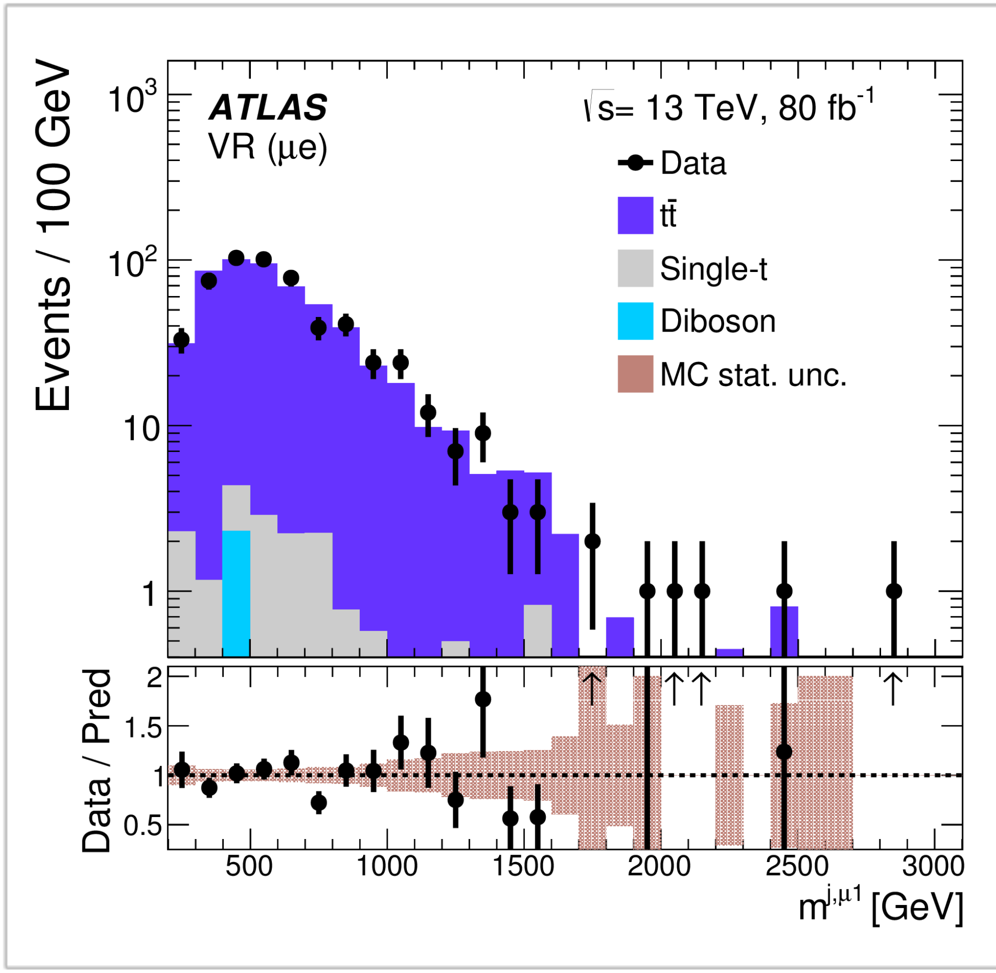

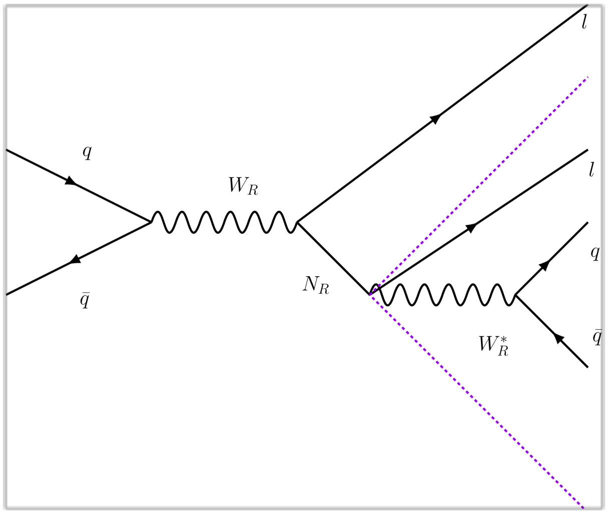

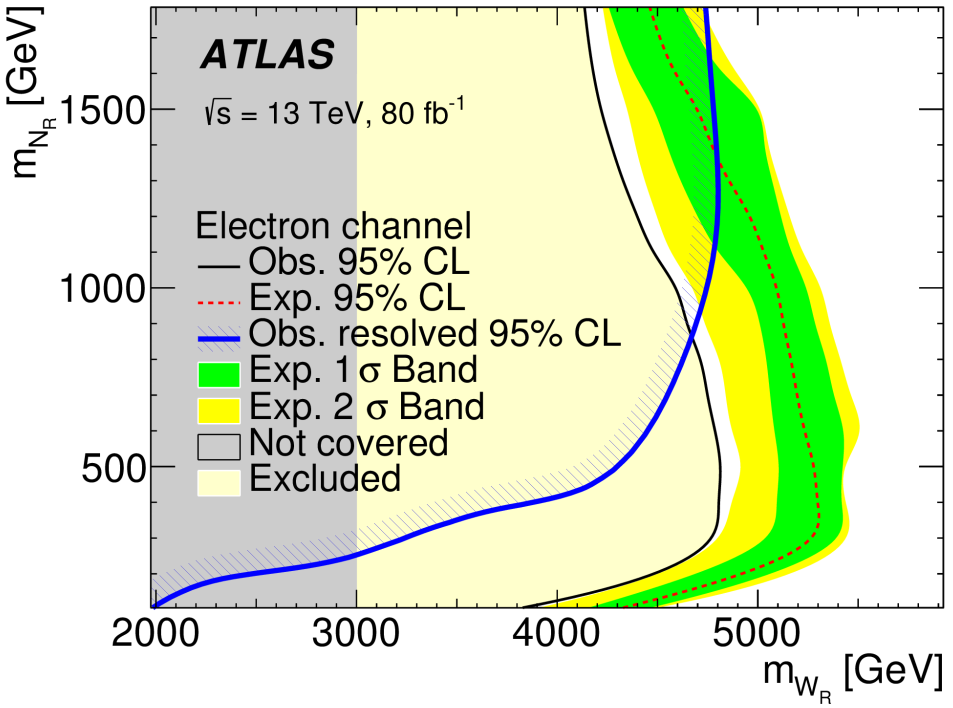

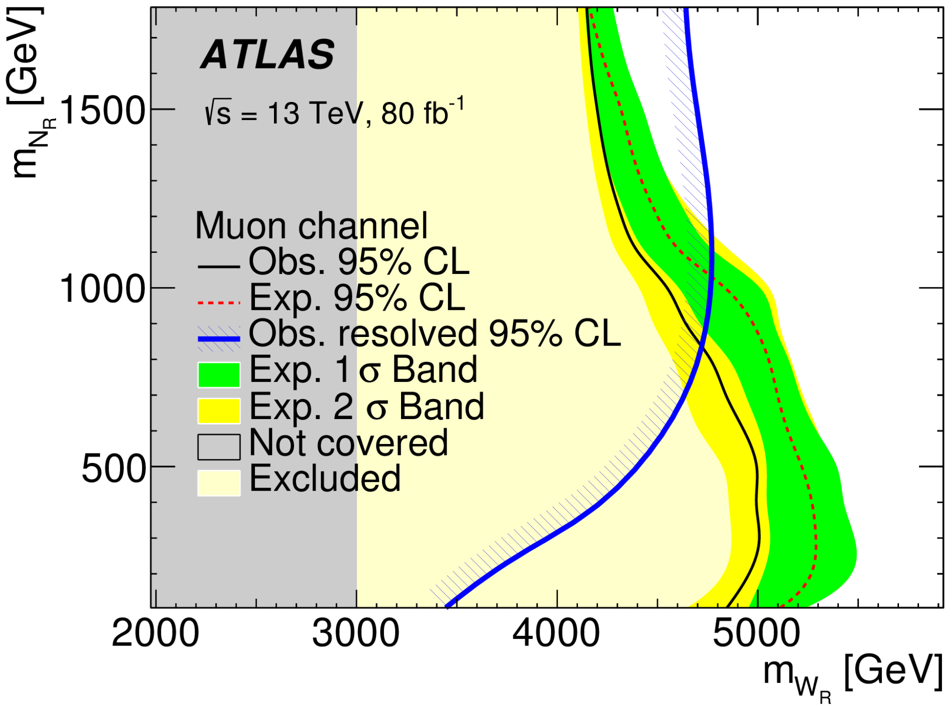

ATLAS-CONF-2019-014

Searches for electroweak production of SUSY particles with compressed mass spectra at ATLAS

$139\ \text{fb}^{-1}$

- SM extensions that include new states with nearly-degenerate masses, these mass spectra are referred to as "***compressed***".
- Testing 3 simplified models of R-parity-conserving SUSY with lightest partner a ***neutralino*** with mass similar to a *chargino*, heavier *neutralino*, or *slepton*. If stable - LSP is a **dark matter candidate**.
    - pair production of SUSY particles via EW interactions (***electroweakinos***) with cascade decays to neutralinos and SM particles
    - mass eigenstates are a mixture of wino, bino, and Higgsino fields, parametrised as M_1, M_2 and μ
    - extension of LEP results
- Looking at events with $E_{T,miss}$, two same-flavour opposite-charge low p_T leptons (e/μ) and hadronic activity from ISR.

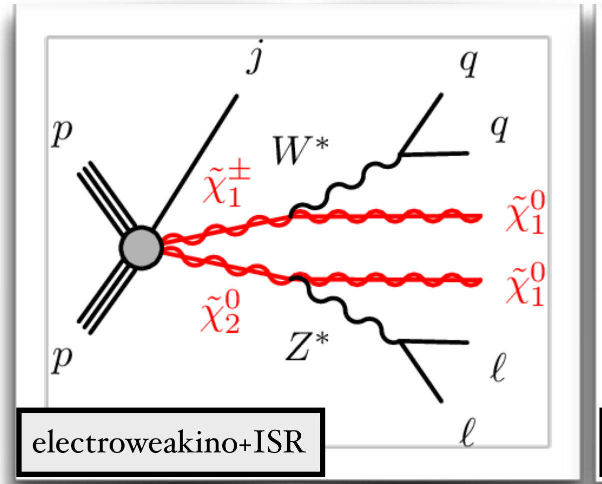

electroweakino+ISR

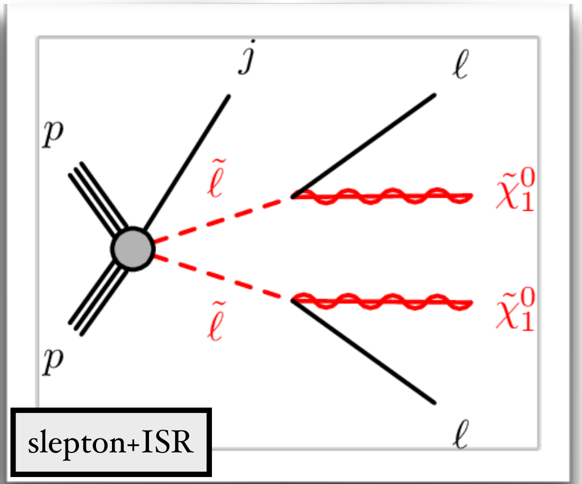

slepton+ISR

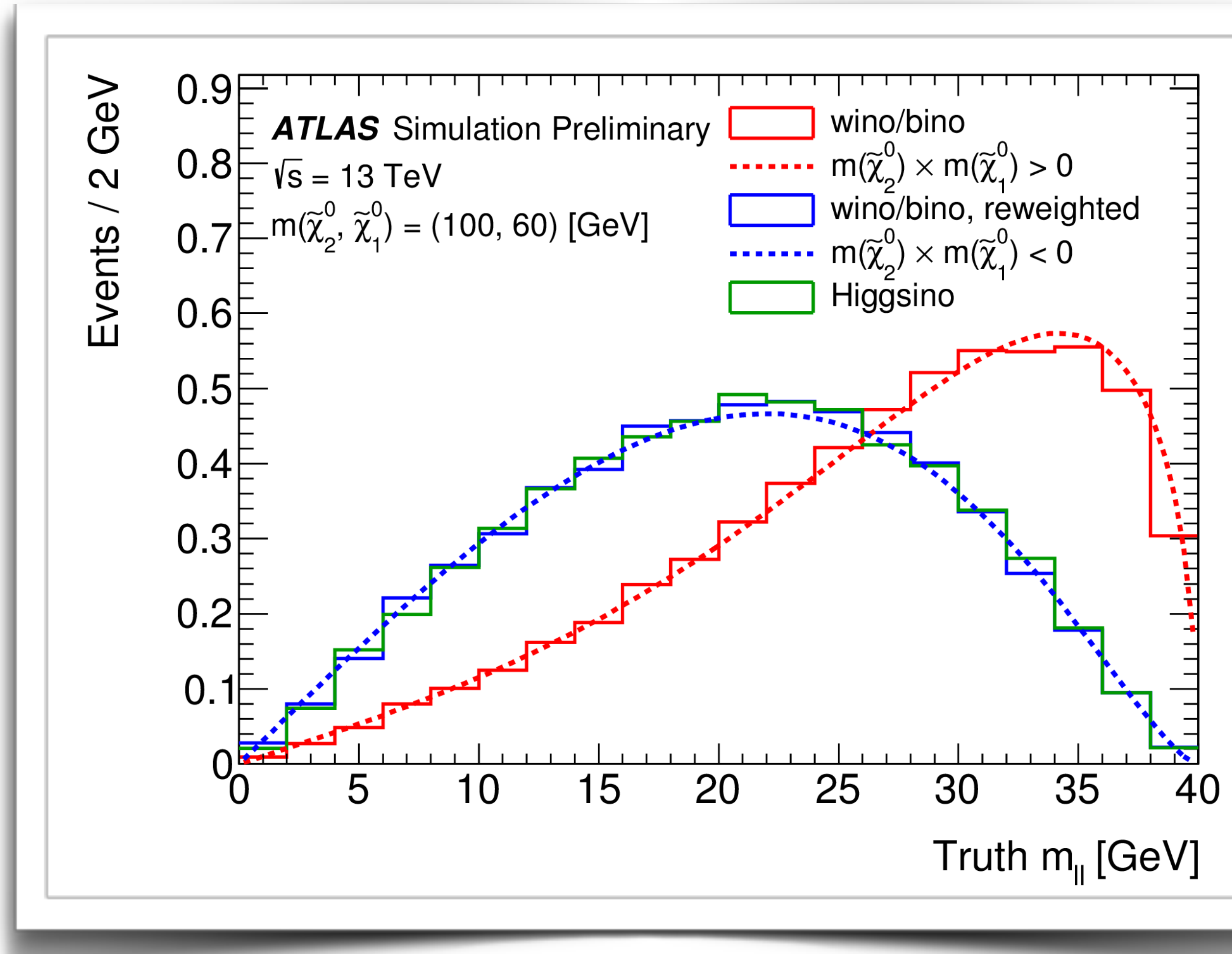

Searches for electroweak production of SUSY particles with compressed mass spectra at ATLAS

- Signal regions are defined to enhance the signal and reduce the BG: $E_{T,miss} > 200$ GeV, the transverse mass is used $m_{\mathrm{T}}^{\ell_1} = \sqrt{2(E_{\mathrm{T}}^{\ell_1} E_{\mathrm{T}}^{\mathrm{miss}} - \mathbf{p}_{\mathrm{T}}^{\ell_1} \cdot \mathbf{p}_{\mathrm{T}}^{\mathrm{miss}})}$
- No excess, lower limits set on the chargino mass range from 162 GeV - 205 GeV for moderate mass splittings, and extend down to mass splittings of 2 GeV - 2.6 GeV at the LEP chargino bounds.
- Similar lower limits on degenerate light-flavour sleptons reach up to masses of 256 GeV and down to mass splittings of 590 MeV. Assuming Higgsino production masses below 162 GeV are excluded for mass splittings of 10 GeV.
- High-mass limit expected to match CMS one once updated to full Run 2 luminosity.

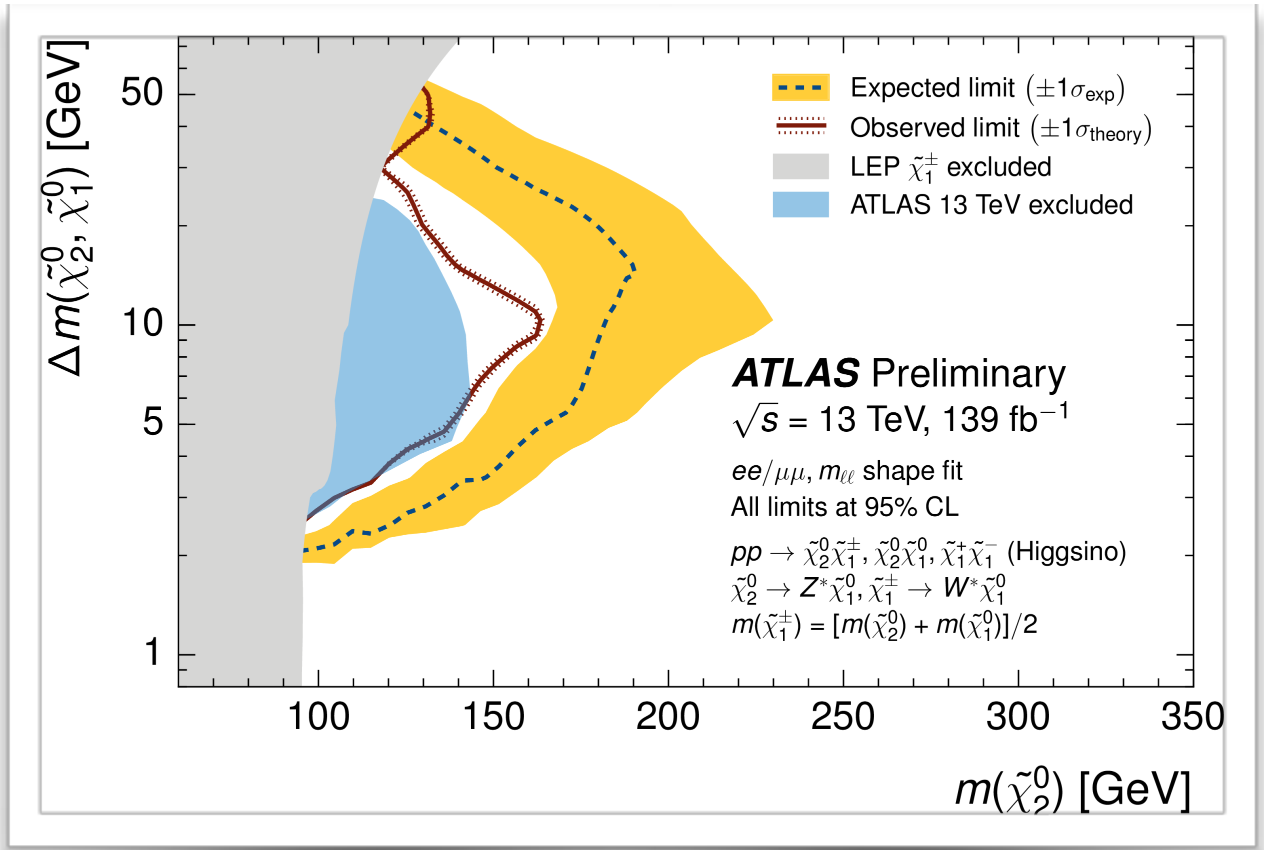

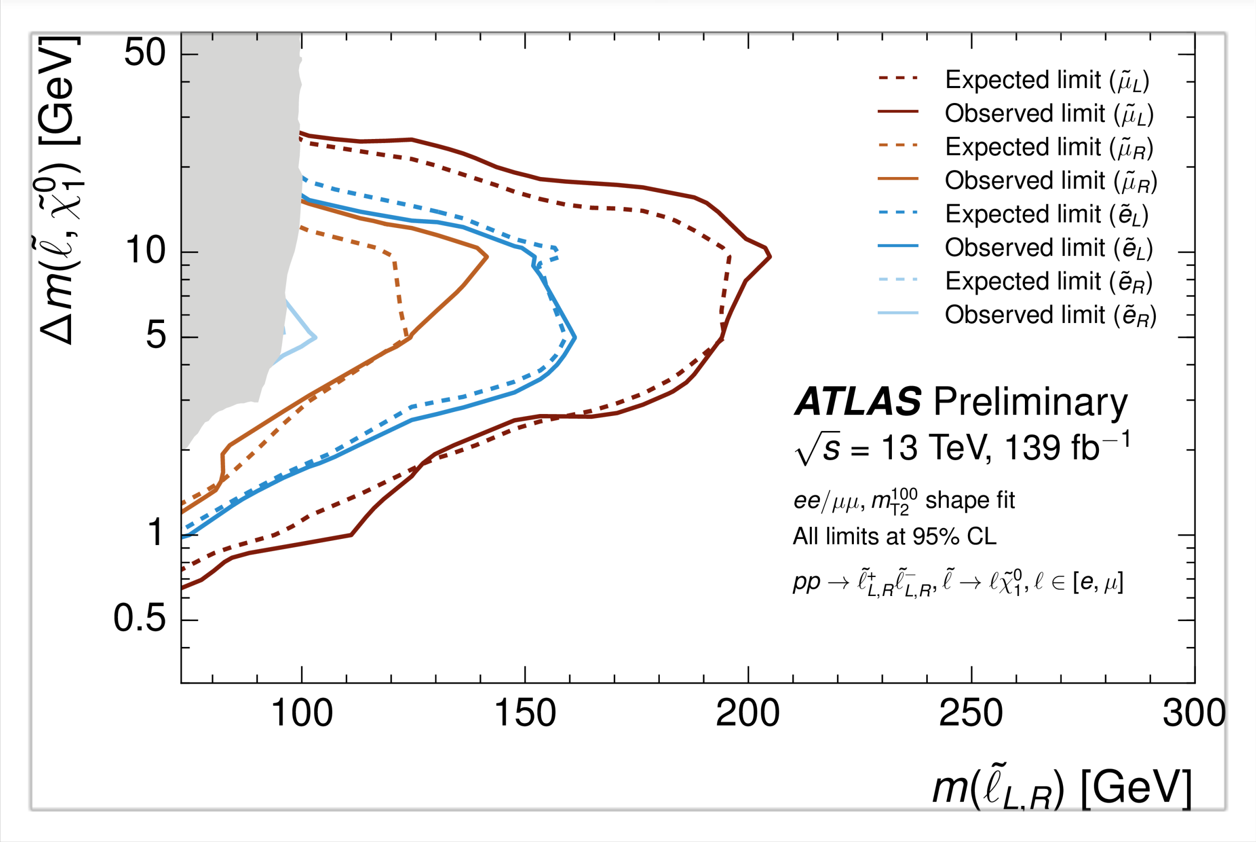

ATLAS-CONF-2019-018

Search for direct staus decaying to hadronic taus at ATLAS

139 fb^{-1}

- Investigate models that conserve R-parity where ***sparticles*** are produced in pairs, and the LSP is stable and is a ***dark-matter candidate***.
- First ATLAS sensitivity study to direct stau pair production.
- Look at final states with *two hadronically decaying taus* and $E_{T,miss}$
  - tag-and-probe method used for hadronically decaying taus corrections; ABDC method for multi-jet; for other BG MC simulation.
- Searches performed in two separate signal regions targeting low and high masses, no excess found, but broad exclusions obtained - stau masses from 120-390 GeV are excluded at 95% CL for a massless LSP

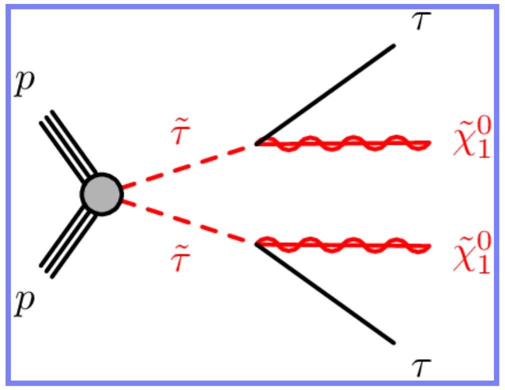

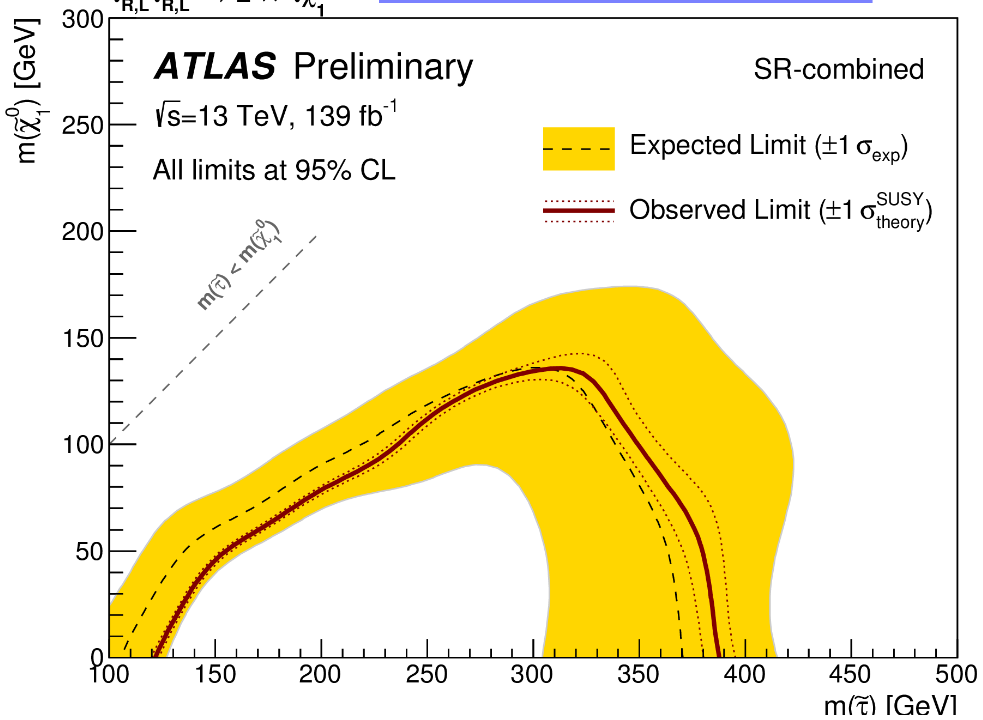

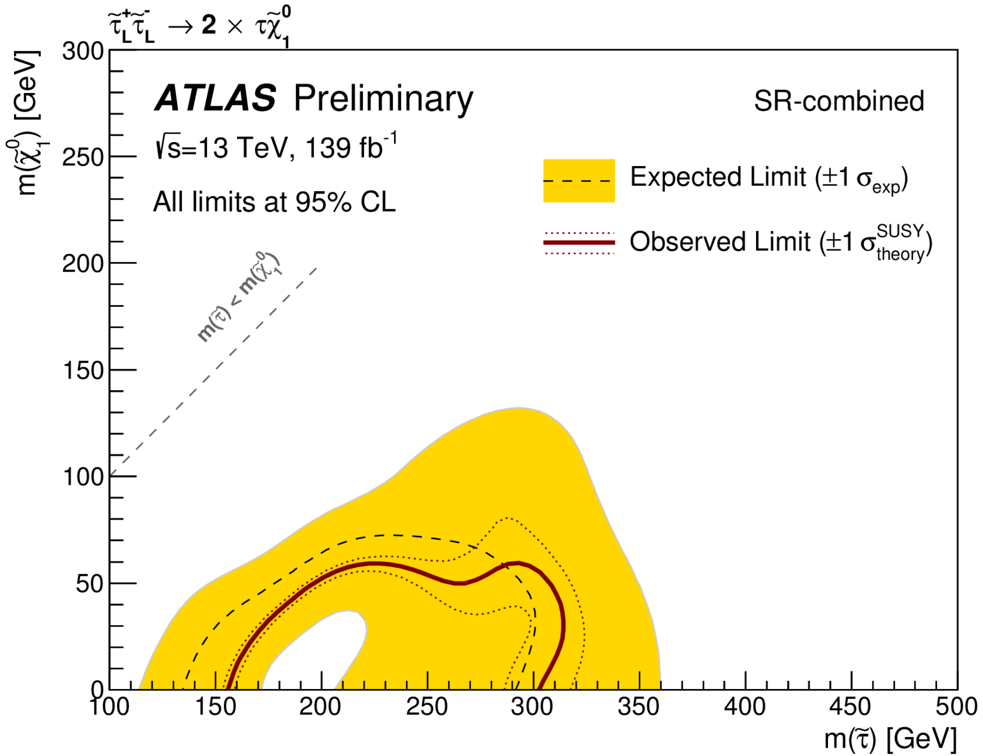

$137\ \mathrm{fb}^{-1}$

CMS-PAS-SUS-19-005

Searches for new phenomena including disappearing tracks at CMS

- Two searches: (a) events with at least two jets, p_T imbalance is inferred through the variable:

$$M_{\mathrm{T2}} = \min_{\vec{p}_{\mathrm{T}}^{\,\mathrm{miss}\,X(1)}+\vec{p}_{\mathrm{T}}^{\,\mathrm{miss}\,X(2)}=\vec{p}_{\mathrm{T}}^{\,\mathrm{miss}}} \left[\max\left(M_{\mathrm{T}}^{(1)}, M_{\mathrm{T}}^{(2)}\right)\right]$$

- (b) ***disappearing tracks*** (ST) produced by new long-lived charged particles
  - A disappearing track is identified as a well reconstructed isolated track, disappearing within the volume of the CMS tracking detector.

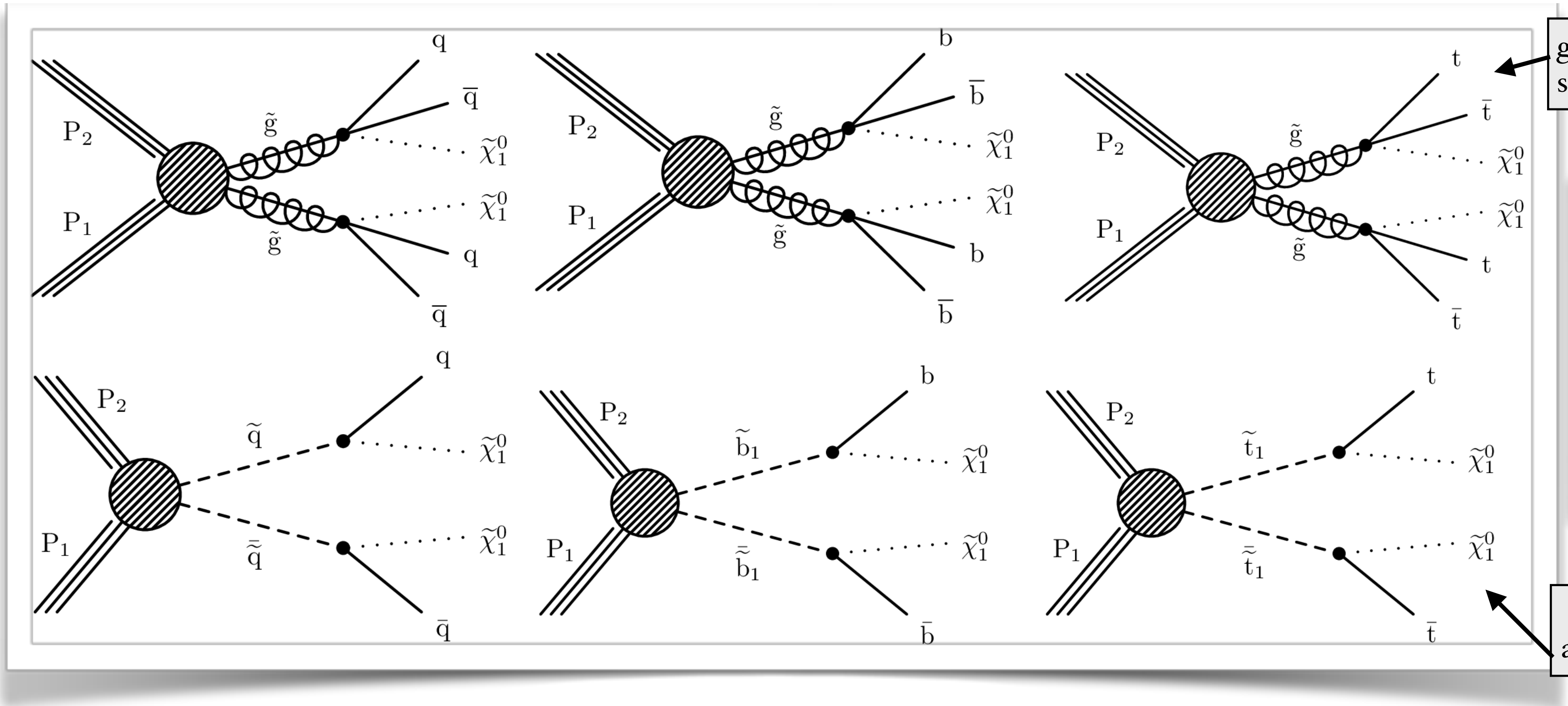

gluino mediated light-flavor squark, bottom squark and top squark production

direct production of light-flavor, bottom and top squark pairs

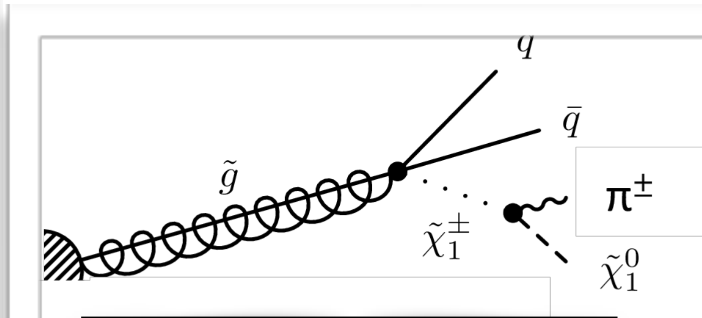

gluino decay via a long-lived $\chi^{\pm}_1$

Searches for new phenomena including disappearing tracks at CMS

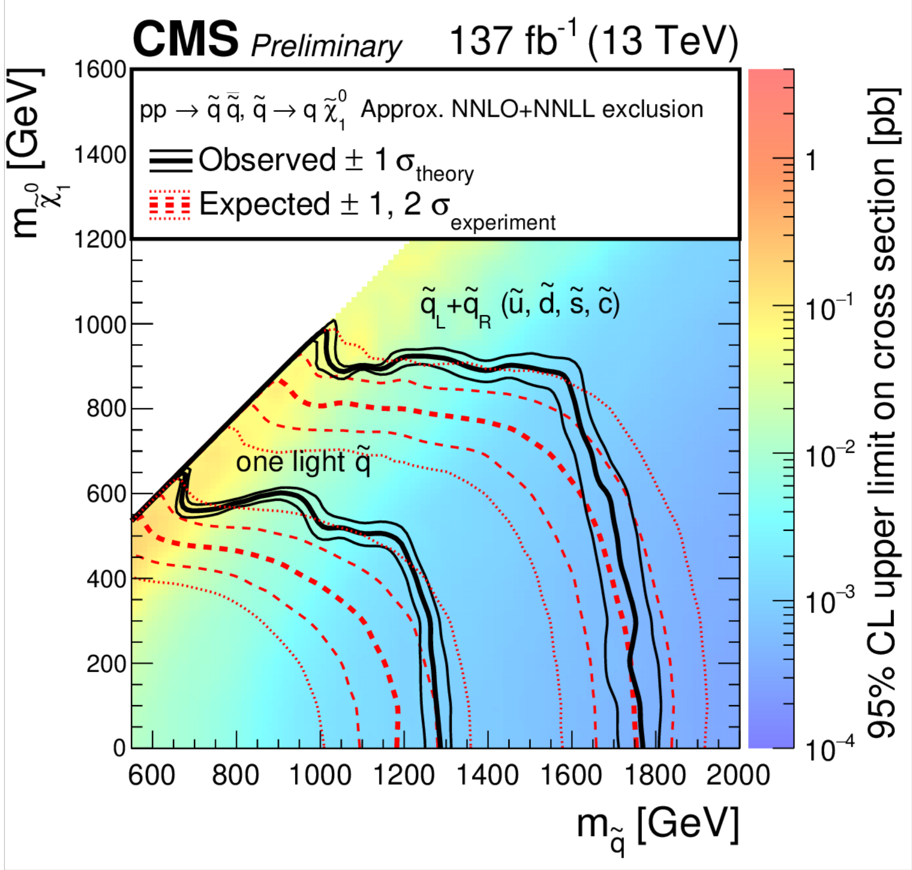

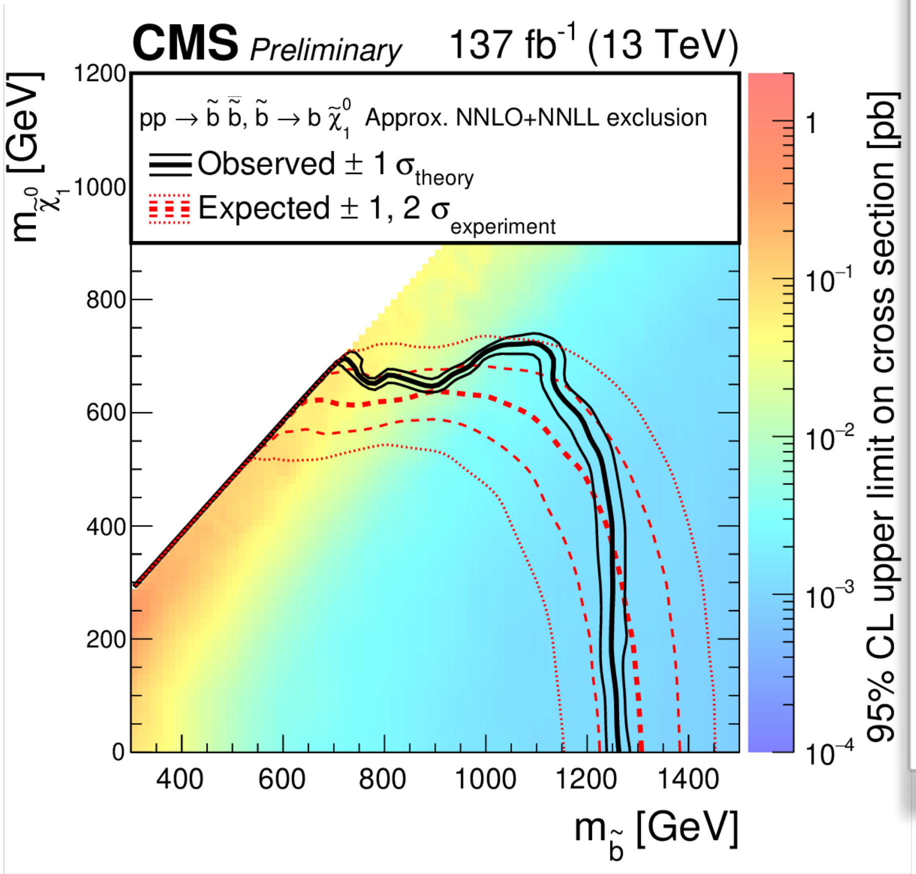

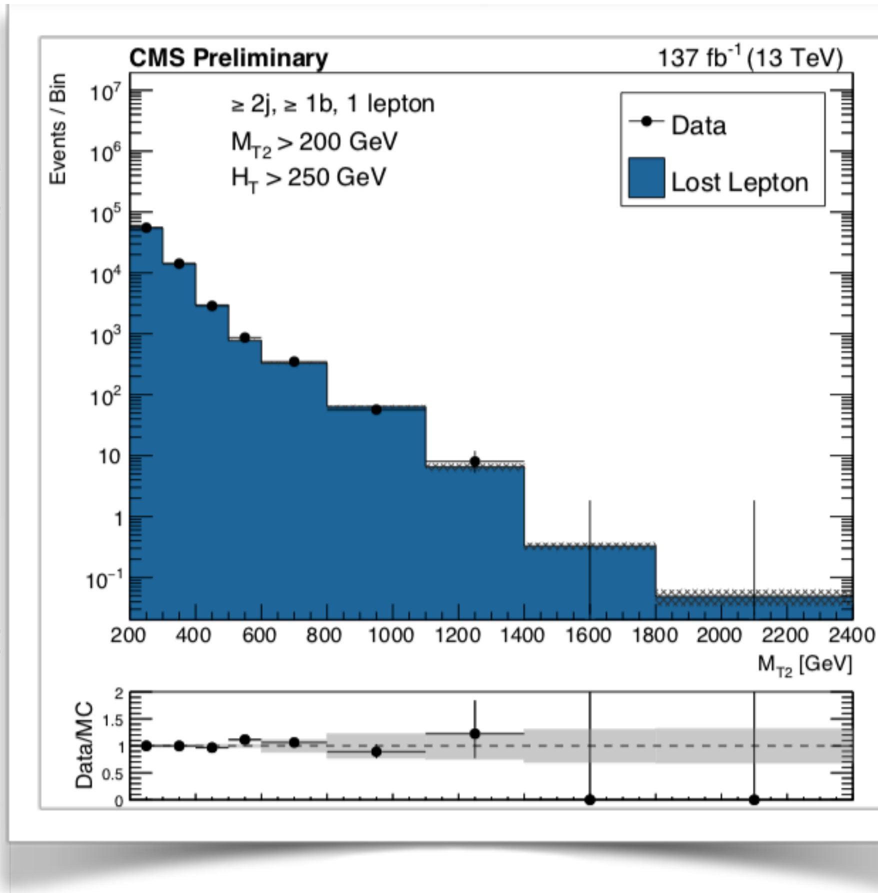

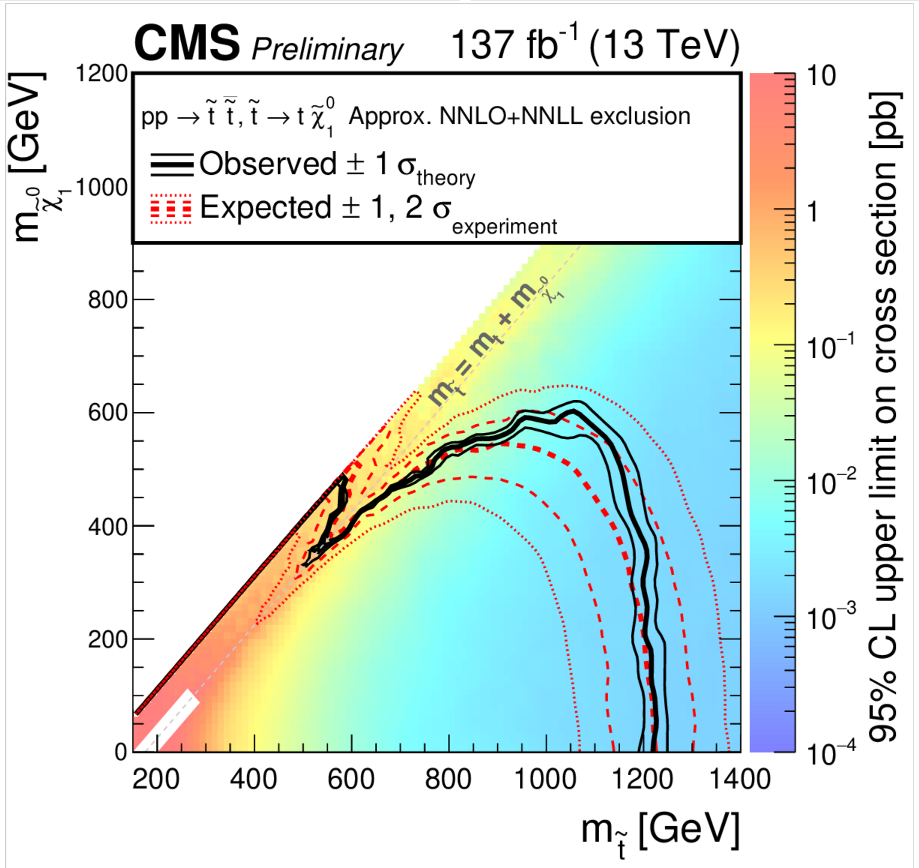

- No excess found, limits set at 95% CL, 2.25 TeV, 1.77 TeV, 1.26 TeV and 1.225 TeV are obtained from the inclusive M_{T2} search for gluinos, light-flavor squarks, bottom squarks and top squarks

- The search for ***disappearing tracks*** extends the gluino mass limit to 2.46 TeV.

36 fb^{-1}

arXiv:1905.04246

Anomalous quartic gauge couplings search at CMS

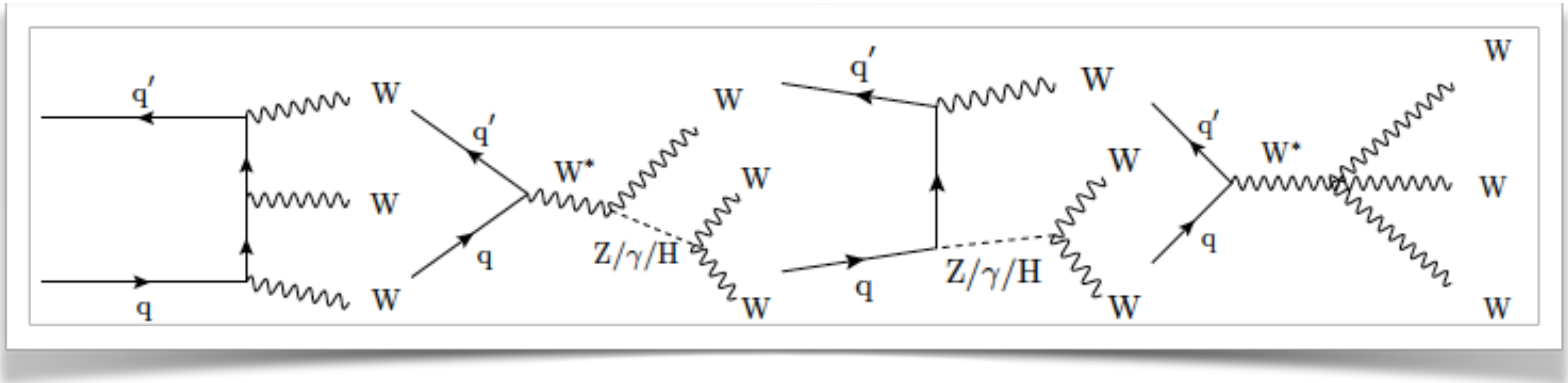

- Search for the production of events containing three W bosons in final states with three leptons (e/μ), or with two same-charge leptons + two jets
- 9 signal regions investigated

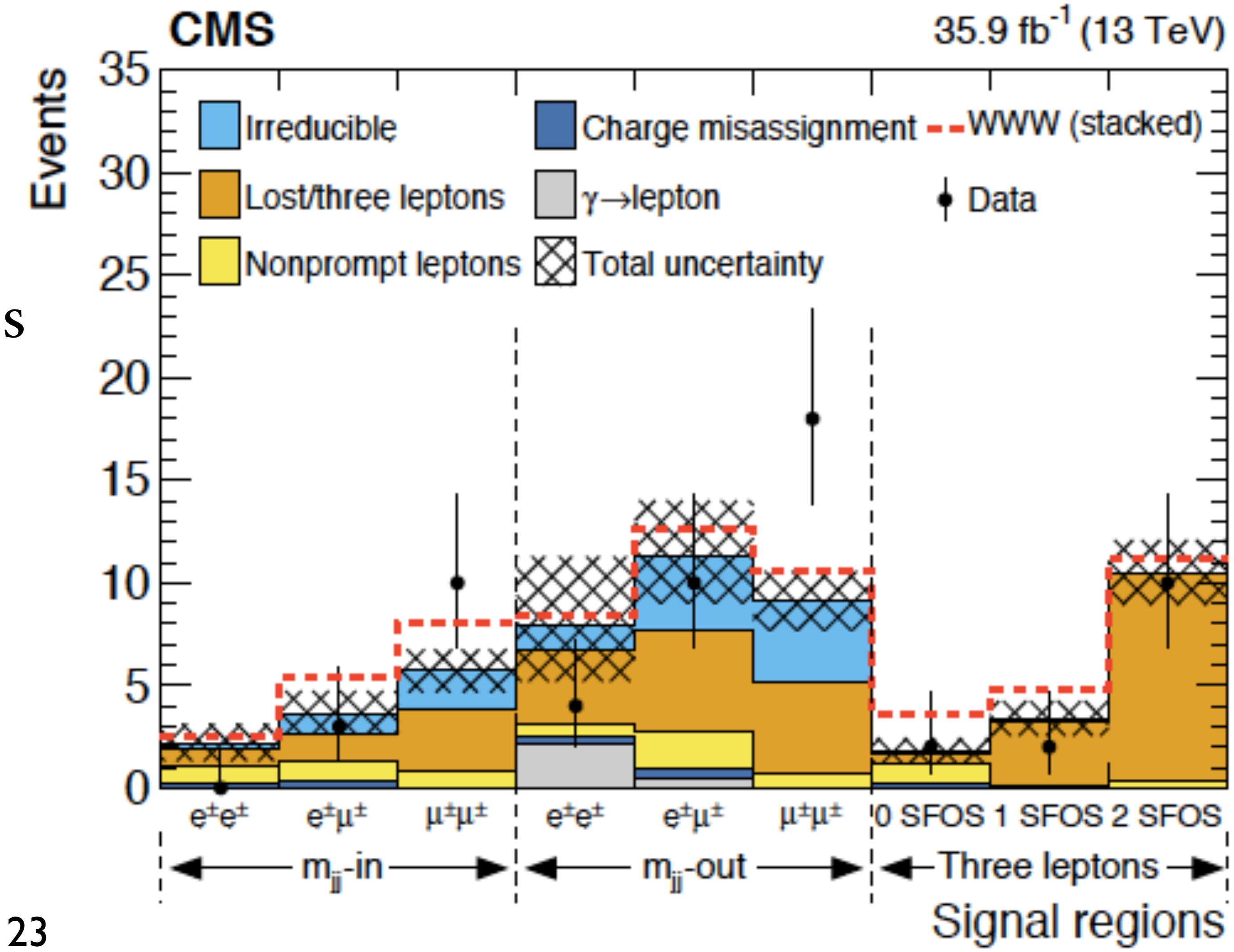

Anomalous quartic gauge couplings search at CMS

- Limits on anomalous quartic gauge couplings are set, e.g.
  - $\boxed{-1.2 < f_{T,0}/\Lambda^4 < 1.2\,\text{TeV}^{-4}}$ at 95% CL.
- Limits are also set on the production of ***axion-like particles*** in association with a W boson and mass points between m_a = 200-480 GeV are excluded

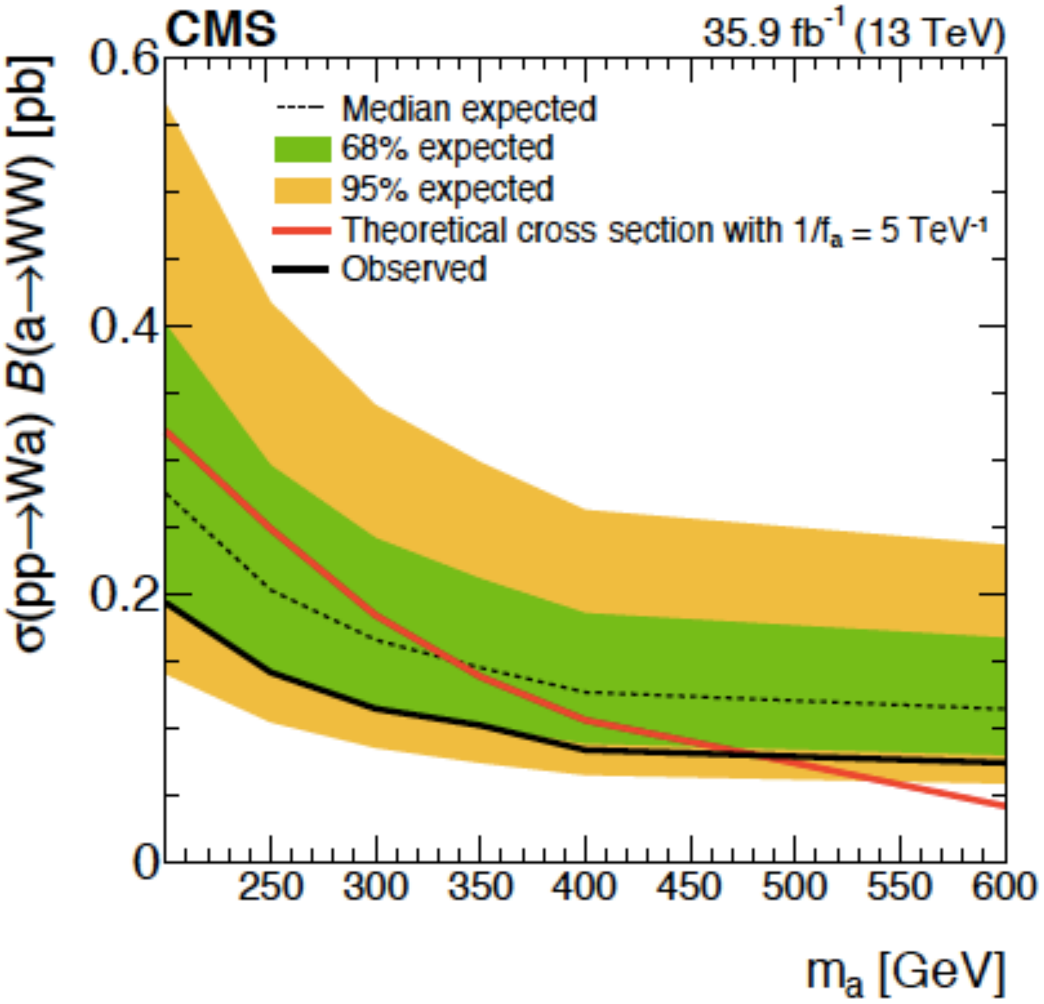

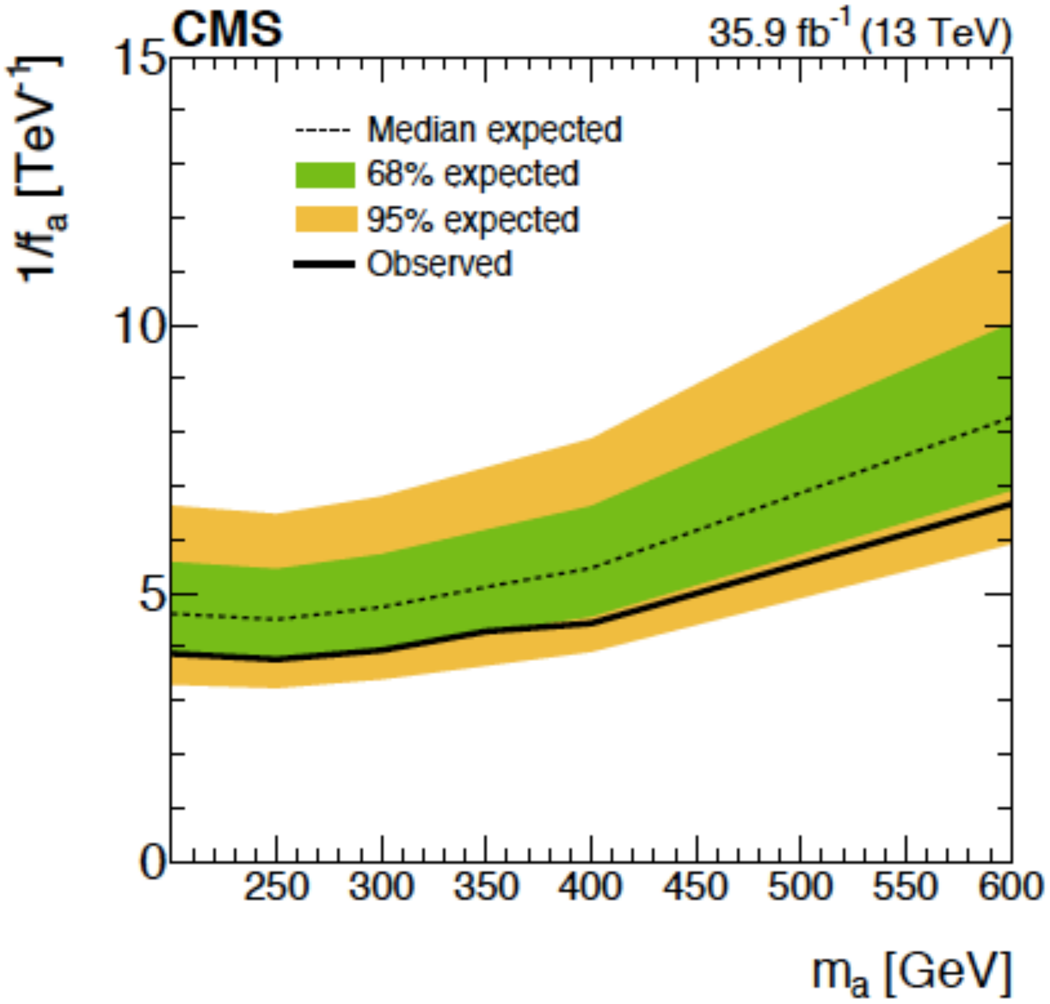

Summary and Outlook

- Presented latest search results in ATLAS and CMS
  - no evidence for BSM physics observed yet
- **Many new analyses of the complete Run 2**
  - **ATLAS Exotic Results** , **ATLAS SUSY Results**
  - **CMS Exotic Results** , **CMS SUSY Results**
- **Large effort to improve analyses beyond luminosity**:
  - physics objects ***reconstruction*** and identification
  - ***background estimation methods***
  - ***generalisation*** and ***unexplored phase space***
- ATLAS & CMS are currently in shut-down upgrading their subdetectors for Run 3

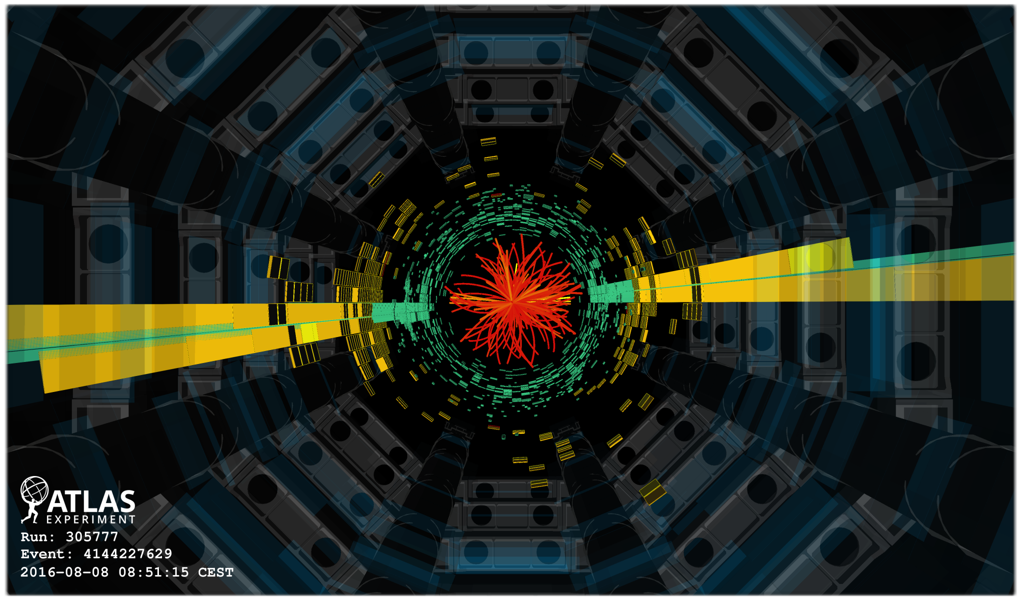

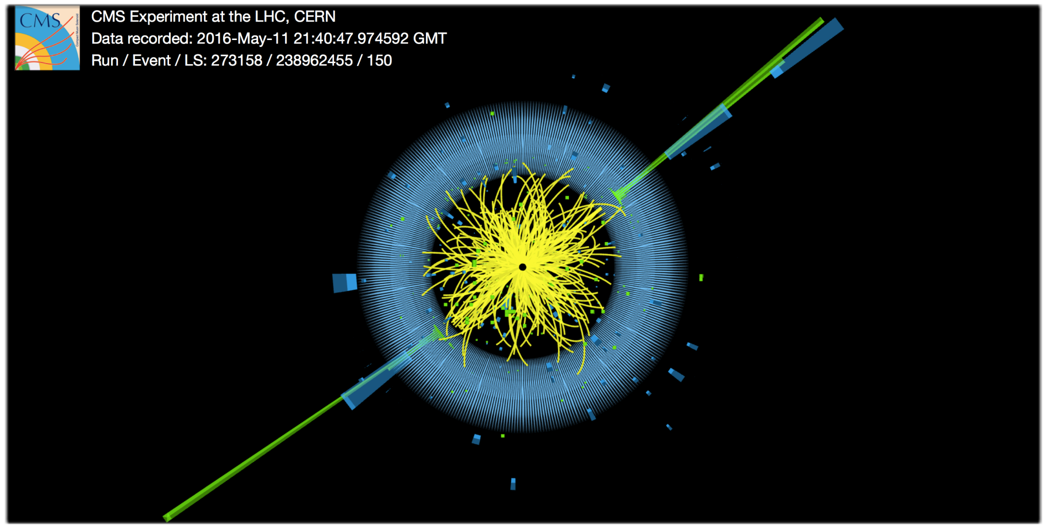

Expecting major results improvements in Run 3!

Backup Slides

High-mass di-lepton uncertainties

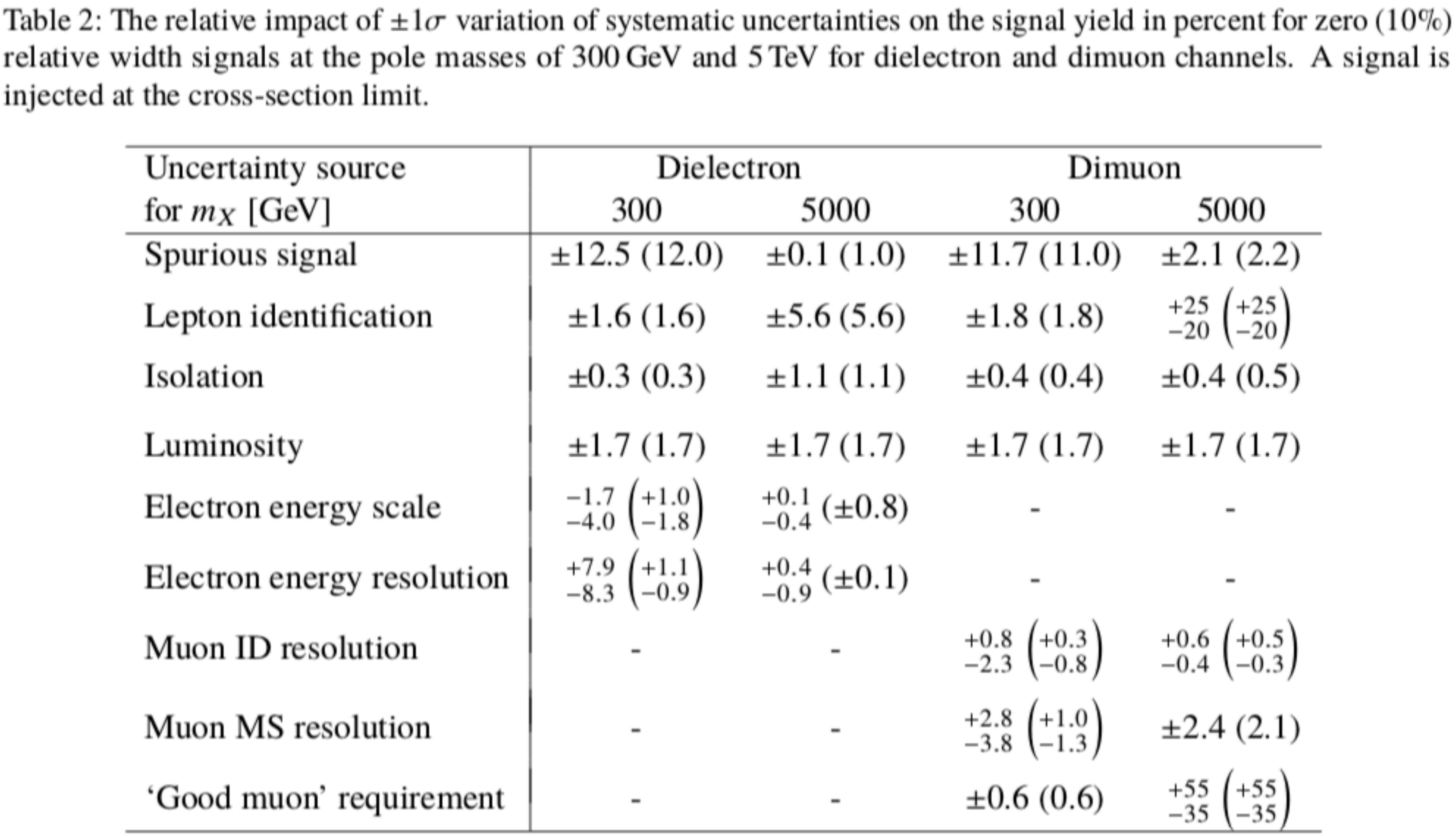

Table 2: The relative impact of ±1σ variation of systematic uncertainties on the signal yield in percent for zero (10%) relative width signals at the pole masses of 300 GeV and 5 TeV for dielectron and dimuon channels. A signal is injected at the cross-section limit.

Uncertainty source	Dielectron		Dimuon	
for m_X [GeV]	300	5000	300	5000
Spurious signal	±12.5 (12.0)	±0.1 (1.0)	±11.7 (11.0)	±2.1 (2.2)
Lepton identification	±1.6 (1.6)	±5.6 (5.6)	±1.8 (1.8)	$^{+25}_{-20}\left(^{+25}_{-20}\right)$
Isolation	±0.3 (0.3)	±1.1 (1.1)	±0.4 (0.4)	±0.4 (0.5)
Luminosity	±1.7 (1.7)	±1.7 (1.7)	±1.7 (1.7)	±1.7 (1.7)
Electron energy scale	$^{-1.7}_{-4.0}\left(^{+1.0}_{-1.8}\right)$	$^{+0.1}_{-0.4}$ (±0.8)	-	-
Electron energy resolution	$^{+7.9}_{-8.3}\left(^{+1.1}_{-0.9}\right)$	$^{+0.4}_{-0.9}$ (±0.1)	-	-
Muon ID resolution	-	-	$^{+0.8}_{-2.3}\left(^{+0.3}_{-0.8}\right)$	$^{+0.6}_{-0.4}\left(^{+0.5}_{-0.3}\right)$
Muon MS resolution	-	-	$^{+2.8}_{-3.8}\left(^{+1.0}_{-1.3}\right)$	±2.4 (2.1)
'Good muon' requirement	-	-	±0.6 (0.6)	$^{+55}_{-35}\left(^{+55}_{-35}\right)$

High-mass di-lepton exclusion contours

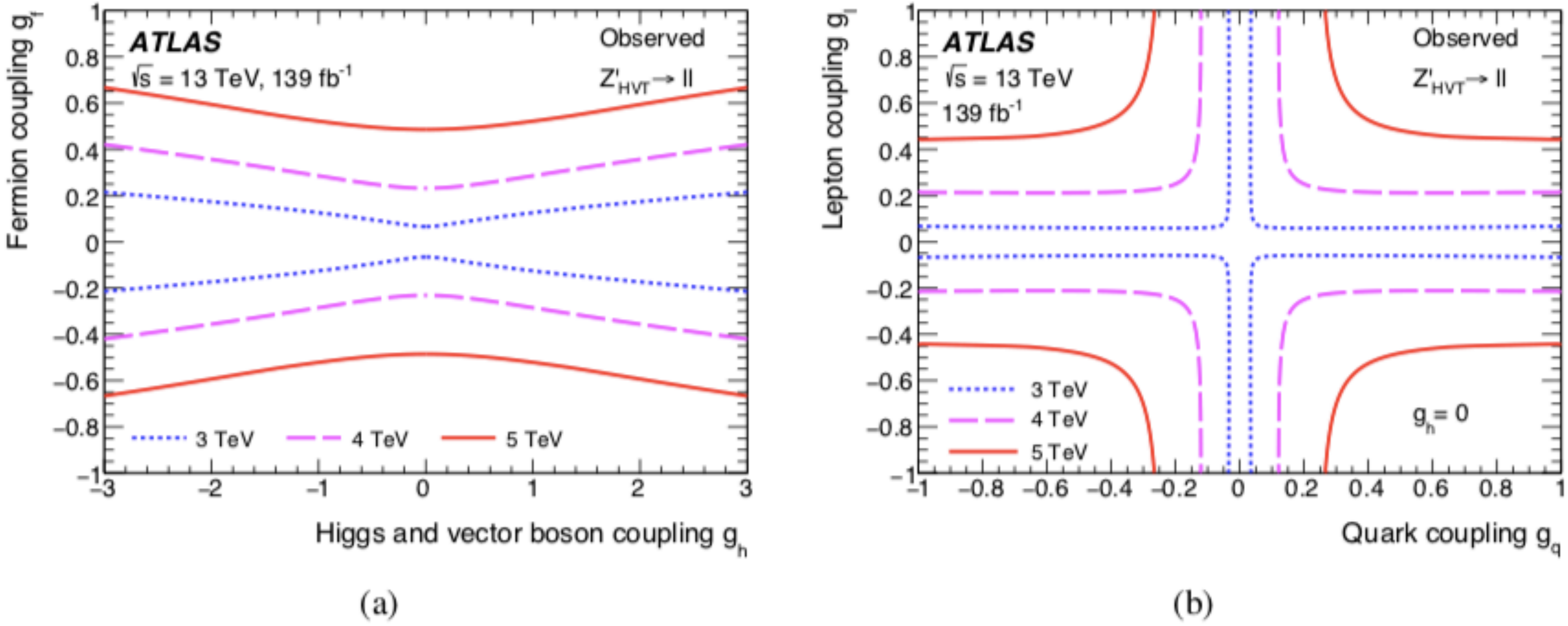

Figure 4: Observed 95% exclusion contours in the HVT parameter space (a) $\{g_h, g_f\}$ with $g_f \equiv g_\ell = g_q$ and (b) $\{g_q, g_\ell\}$ with g_h set to zero, for resonance masses of 3, 4, and 5 TeV for the dilepton channel. The area outside the curves is excluded.

W_R analysis uncertainties & signal vs BG comparison

Table 4: Relative systematic uncertainties of the signal yield in the signal region, in percentage for each source. The ranges indicate the different signal samples. The systematic uncertainties with sub-percent contributions are not shown.

Component	Electron channel [%]	Muon channel [%]
Lepton identification	4–20	4–8
Lepton isolation	4–5	1.0–1.5
Lepton reconstruction	4–5	1–4
Lepton trigger	4–5	0.5
Pile-up	< 0.5	2–3
Luminosity	2	2
Theory	10	10

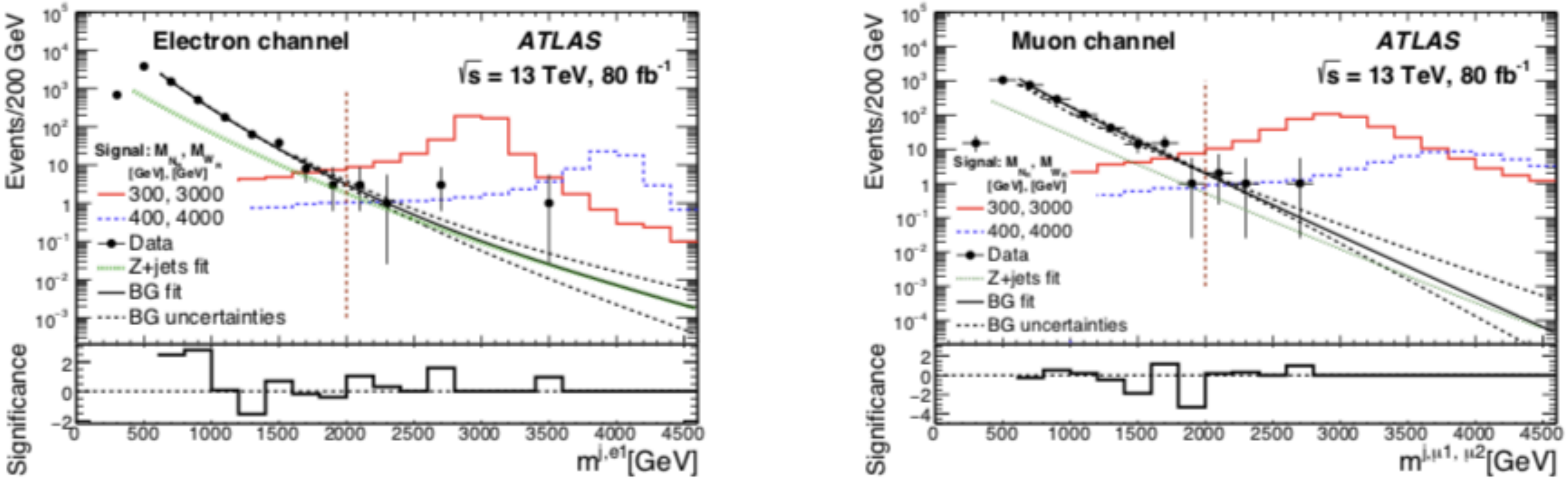

Figure 6: Comparison of the $m_{W_R}^{\text{reco}}$ distribution between data and the fitted background prediction for the electron (left) and muon (right) channels. Two signal scenarios considered in this search are overlayed. The dashed brown lines at 2 TeV show the boundary between the CR and SR. The significance, which indicates the deviation of data in each bin from the background fit, is computed as the difference between the observed data and fit values, divided by the square root of the observed data value.

Search for high-mass di-lepton resonances at CMS

36 fb^{-1}

- Searching for resonances → two high p_T isolated e/μ
- $m_{ll} > 120$ GeV
- Main backgrounds: DY, real leptons from tt, single top quark, di-boson and DY+$\tau\tau$ processes

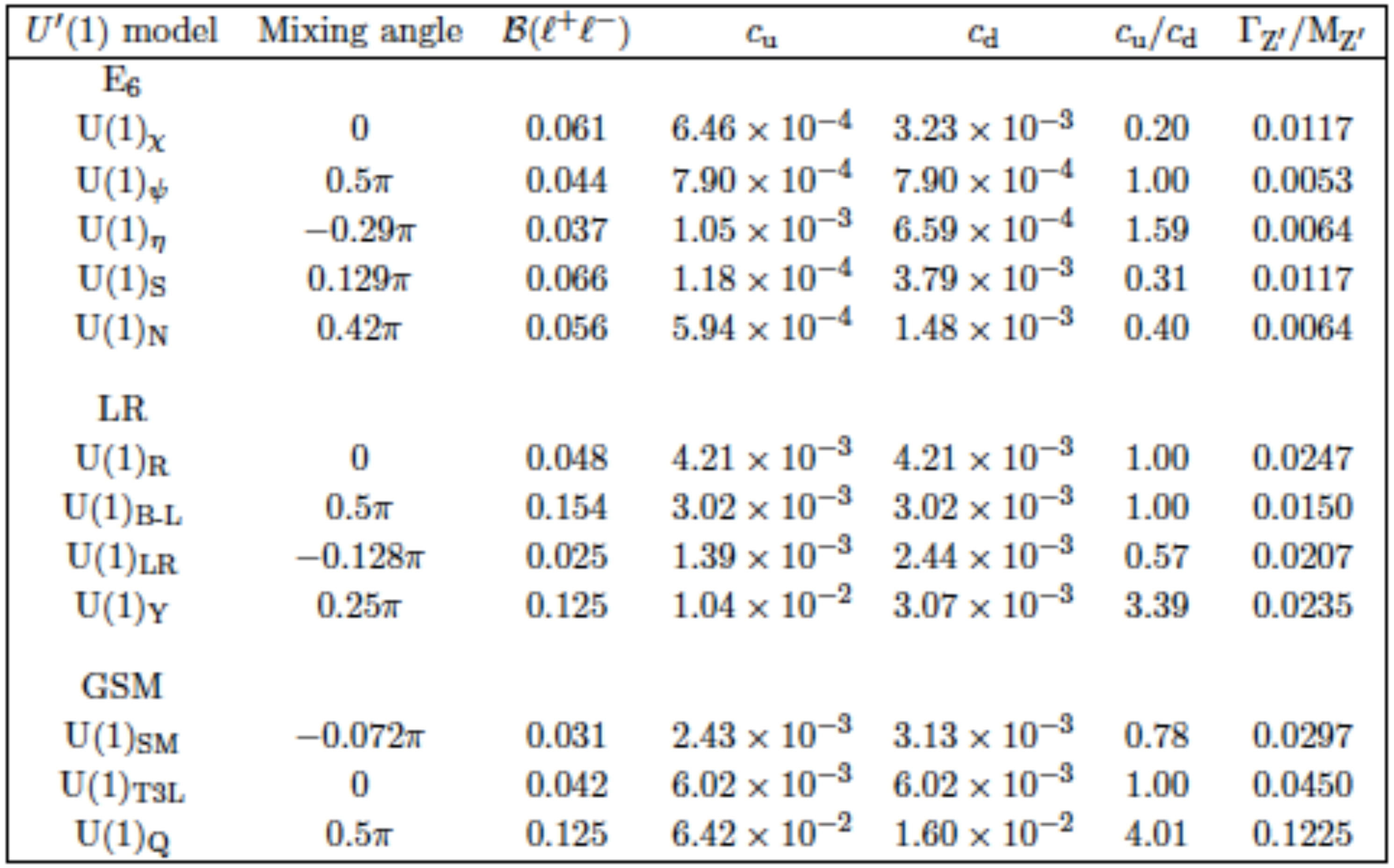

$U'(1)$ model	Mixing angle	$\mathcal{B}(\ell^+\ell^-)$	c_u	c_d	c_u/c_d	$\Gamma_{Z'}/M_{Z'}$
E_6						
$U(1)_\chi$	0	0.061	6.46×10^{-4}	3.23×10^{-3}	0.20	0.0117
$U(1)_\psi$	0.5π	0.044	7.90×10^{-4}	7.90×10^{-4}	1.00	0.0053
$U(1)_\eta$	-0.29π	0.037	1.05×10^{-3}	6.59×10^{-4}	1.59	0.0064
$U(1)_S$	0.129π	0.066	1.18×10^{-4}	3.79×10^{-3}	0.31	0.0117
$U(1)_N$	0.42π	0.056	5.94×10^{-4}	1.48×10^{-3}	0.40	0.0064
LR						
$U(1)_R$	0	0.048	4.21×10^{-3}	4.21×10^{-3}	1.00	0.0247
$U(1)_{B-L}$	0.5π	0.154	3.02×10^{-3}	3.02×10^{-3}	1.00	0.0150
$U(1)_{LR}$	-0.128π	0.025	1.39×10^{-3}	2.44×10^{-3}	0.57	0.0207
$U(1)_Y$	0.25π	0.125	1.04×10^{-2}	3.07×10^{-3}	3.39	0.0235
GSM						
$U(1)_{SM}$	-0.072π	0.031	2.43×10^{-3}	3.13×10^{-3}	0.78	0.0297
$U(1)_{T3L}$	0	0.042	6.02×10^{-3}	6.02×10^{-3}	1.00	0.0450
$U(1)_Q$	0.5π	0.125	6.42×10^{-2}	1.60×10^{-2}	4.01	0.1225

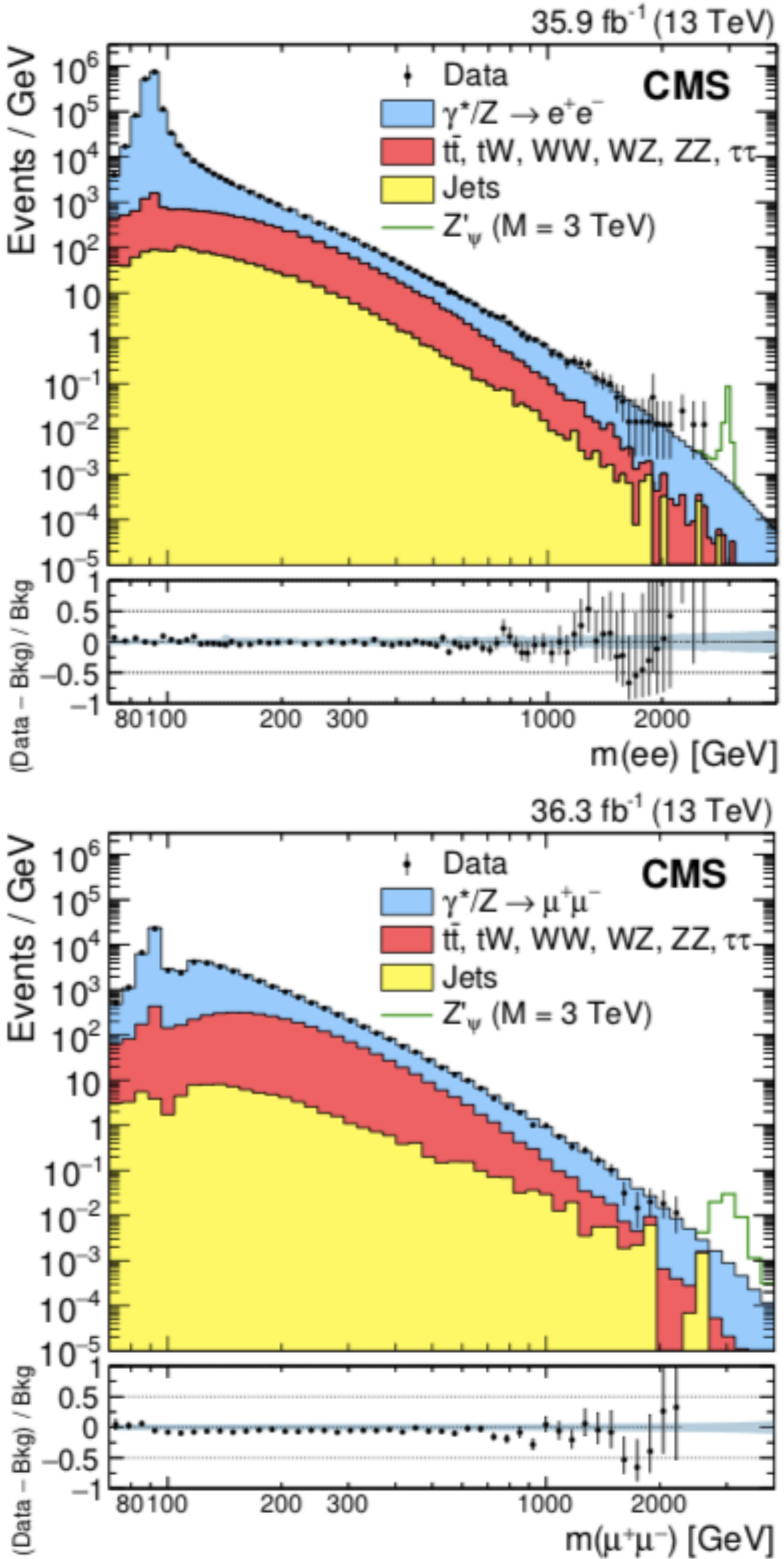

JHEP 06 (2018) 120

Search for high-mass di-lepton resonances at CMS

- Limits set on the masses of various hypothetical particles:
  - Z’$_{\text{SSM}}$ (Z’$_{\psi}$) a lower mass limit of 4.50 (3.90) TeV is set at 95% CL
  - The lightest Kaluza-Klein graviton arising in the Randall-Sundrum model of extra dimensions: is excluded at 95% CL below 2.10, 3.65, and 4.25TeV for different coupling parameters

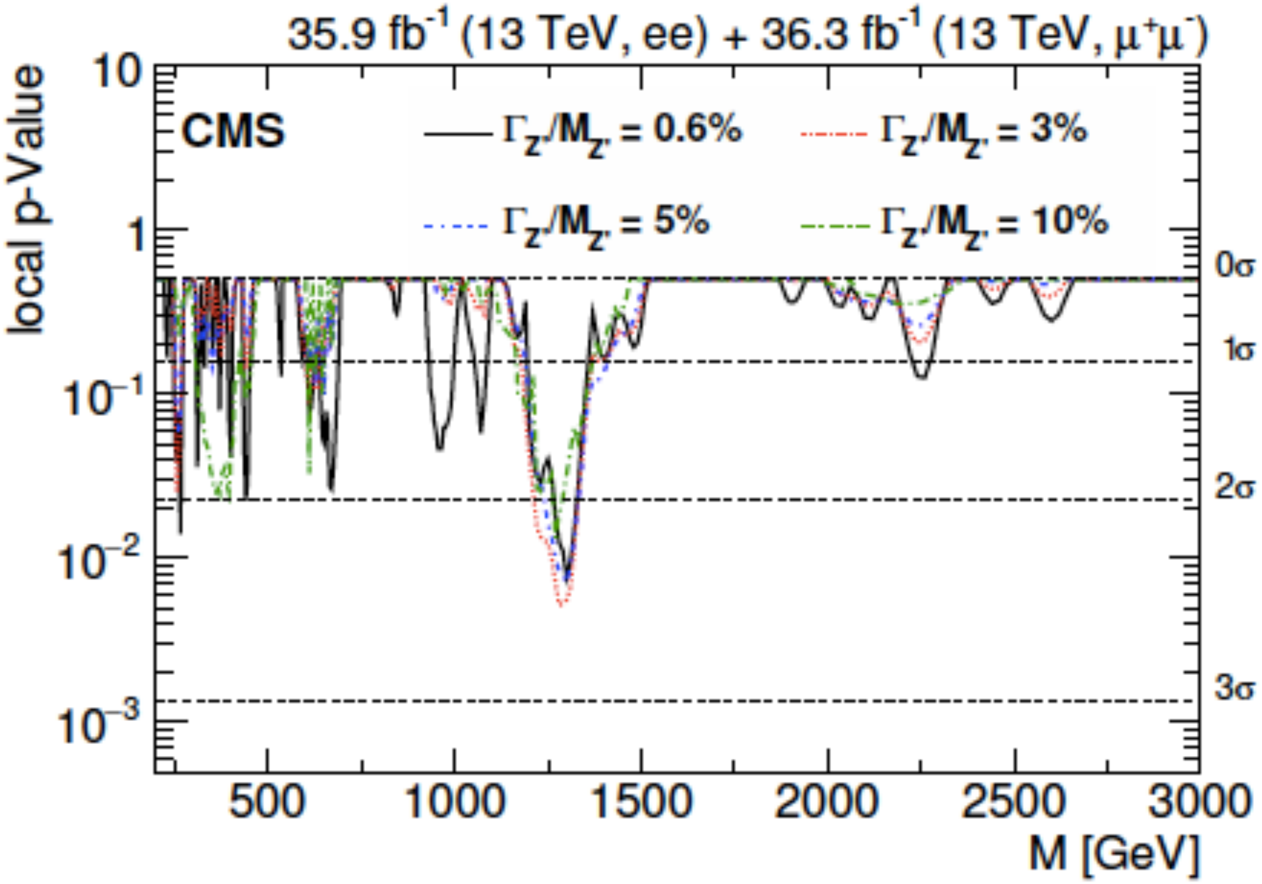

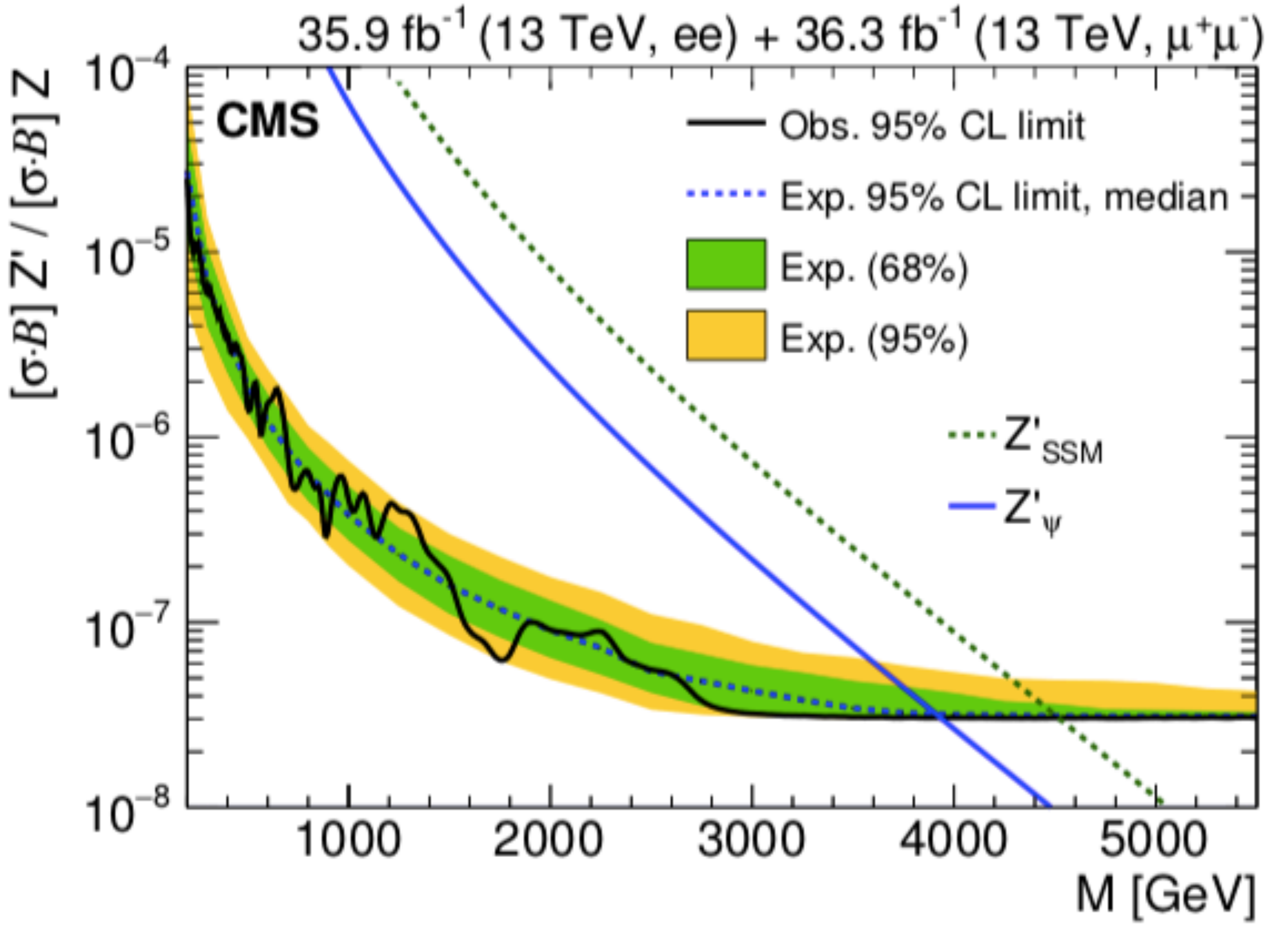

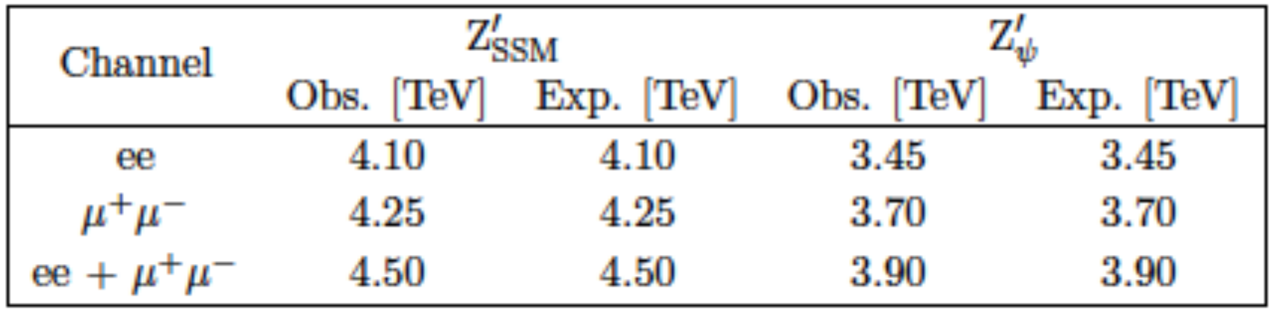

Channel	Z'_{SSM}		Z'_{ψ}	
	Obs. [TeV]	Exp. [TeV]	Obs. [TeV]	Exp. [TeV]
ee	4.10	4.10	3.45	3.45
$\mu^+\mu^-$	4.25	4.25	3.70	3.70
ee + $\mu^+\mu^-$	4.50	4.50	3.90	3.90

CMS PAS EXO-17-026

Search for high-mass di-jet resonances at CMS

78 fb^{-1}

- Trigger on high p_T jets
- Form jets from particle flow candidates (anti-k_T algorithm, R = 0:4).
  - Choose 2 with highest p_T, combine subleading jets within ΔR <1.1
- A high-mass search:
  - m_{jj}>1.8 TeV using particle-flow di-jets reconstructed offline
- Main QCD background estimated both by:
  - fitting the data with an empirical functional form and
  - with a new data-driven method via a $\Delta\eta$ sideband

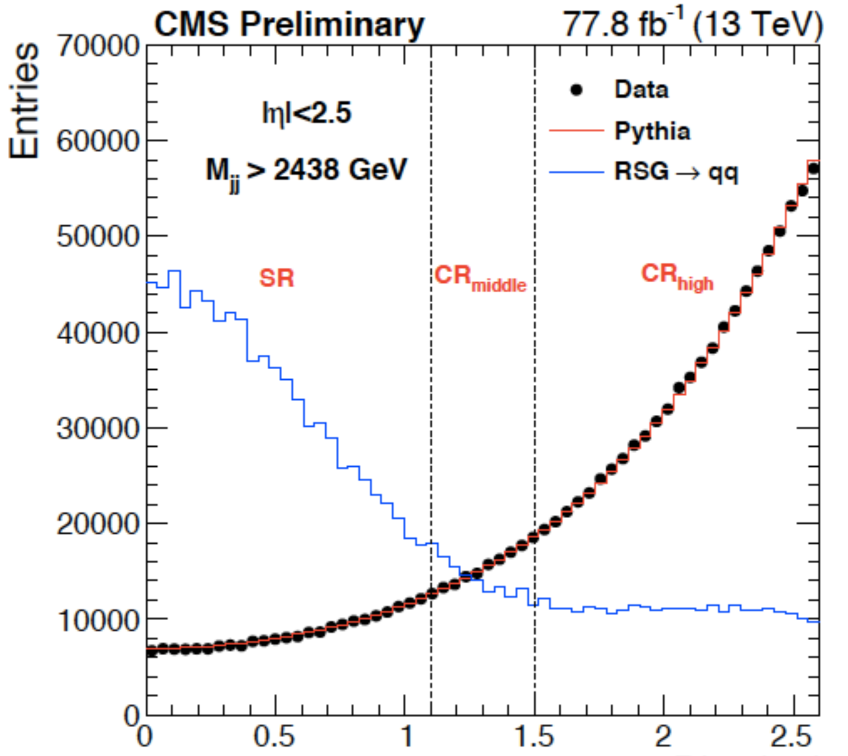

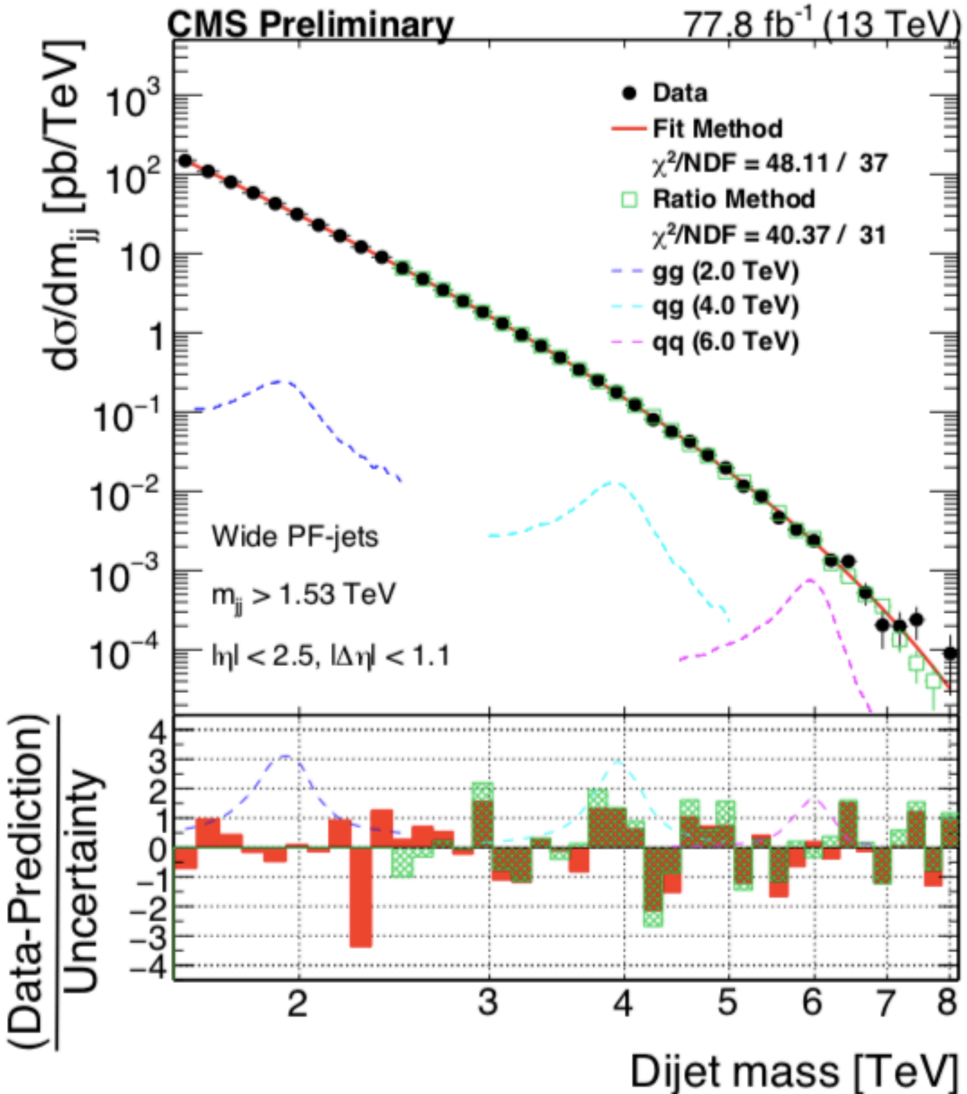

Search for high-mass di-jet resonances at CMS

- No evidence for resonant particle production.
- Generic upper limits are presented on the product of the cross section, the branching fraction, and the acceptance for narrow q-q, q-g, and g-g resonances that are applicable to any model of narrow di-jet resonance production.

Model	Final State	Observed (expected) mass limit [TeV] 36 fb^{-1} 13 TeV	 77.8 fb^{-1} 13 TeV
String	qg	7.7 (7.7)	7.6 (7.9)
Scalar diquark	qq	7.2 (7.4)	7.3 (7.5)
Axigluon/coloron	$q\bar{q}$	6.1 (6.0)	6.2 (6.3)
Excited quark	qg	6.0 (5.8)	6.0 (6.0)
Color-octet scalar ($k_s^2 = 1/2$)	gg	3.4 (3.6)	3.7 (3.8)
W′	$q\bar{q}$	3.3 (3.6)	3.6 (3.8)
Z′	$q\bar{q}$	2.7 (2.9)	2.9 (3.1)
RS graviton ($k/M_{\rm PL} = 0.1$)	$q\bar{q}$, gg	1.8 (2.3)	2.4 (2.4)
DM mediator ($m_{\rm DM} = 1$ GeV)	$q\bar{q}$	2.6 (2.5)	2.5 (2.8)

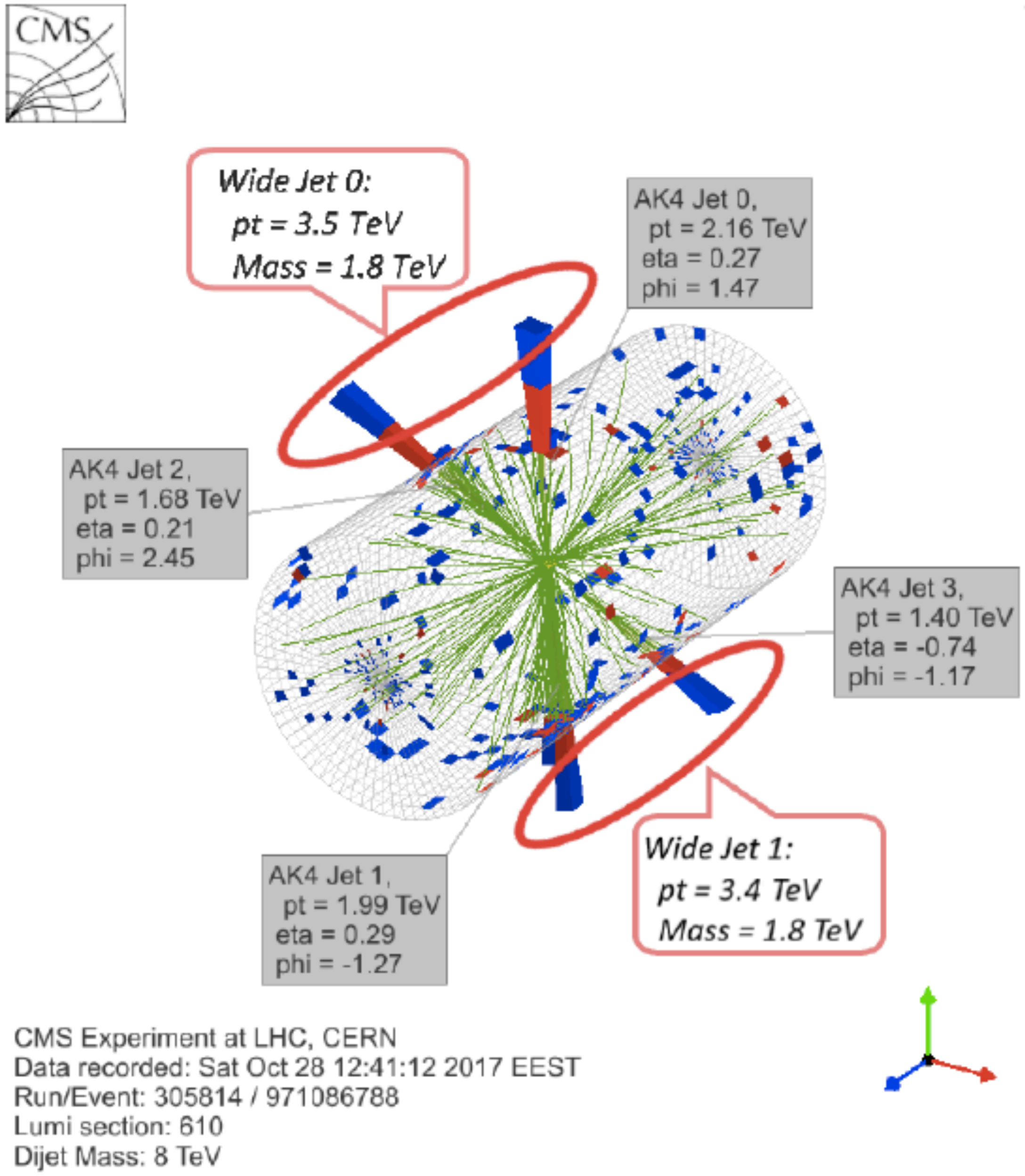

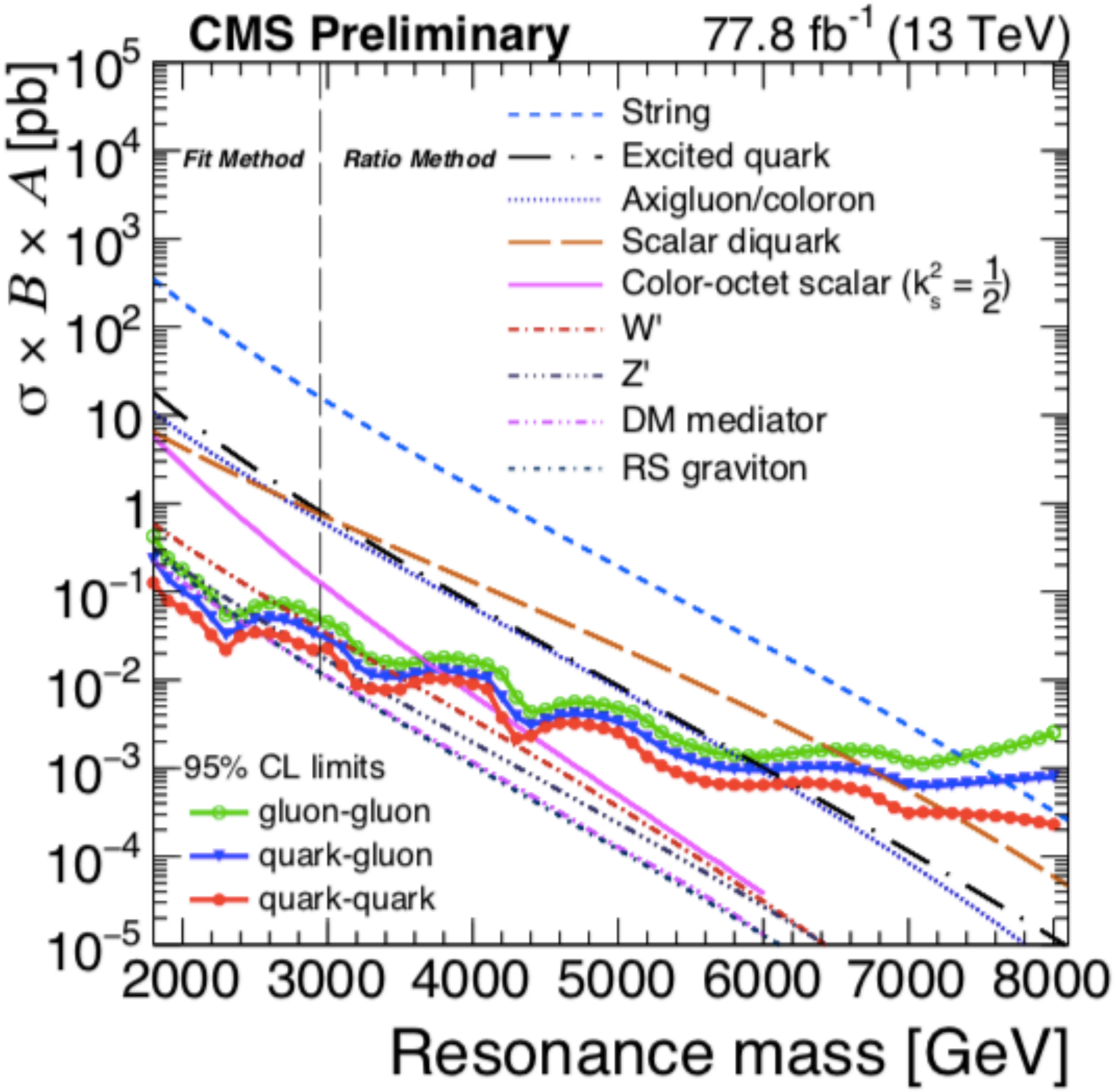

Multilepton search at CMS

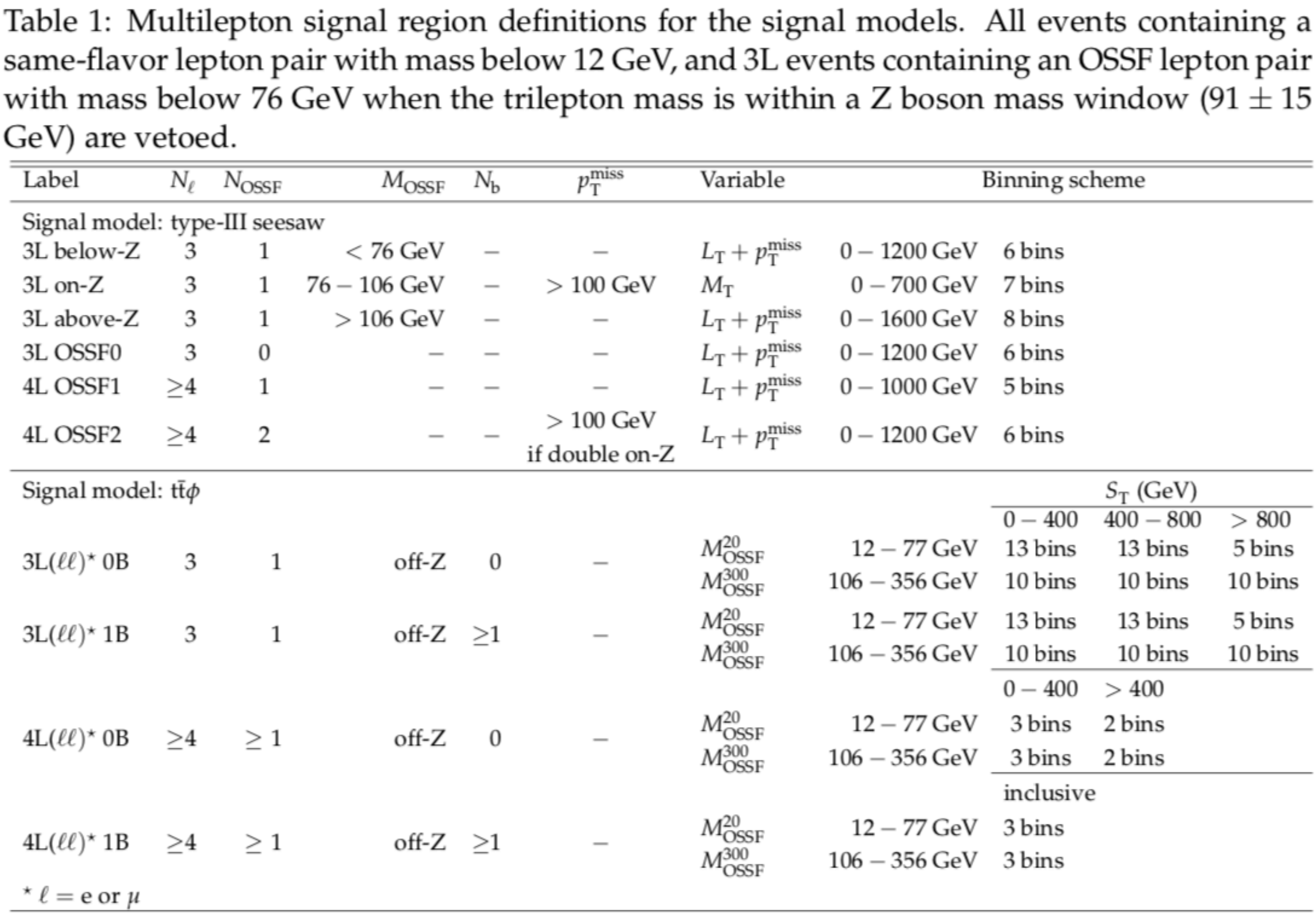

Table 1: Multilepton signal region definitions for the signal models. All events containing a same-flavor lepton pair with mass below 12 GeV, and 3L events containing an OSSF lepton pair with mass below 76 GeV when the trilepton mass is within a Z boson mass window (91 ± 15 GeV) are vetoed.

Label	N_ℓ	N_{OSSF}	M_{OSSF}	N_{b}	$p_{\mathrm{T}}^{\mathrm{miss}}$	Variable	Binning scheme			
Signal model: type-III seesaw										
3L below-Z	3	1	< 76 GeV	–	–	$L_{\mathrm{T}} + p_{\mathrm{T}}^{\mathrm{miss}}$	$0 - 1200$ GeV	6 bins		
3L on-Z	3	1	$76 - 106$ GeV	–	> 100 GeV	M_{T}	$0 - 700$ GeV	7 bins		
3L above-Z	3	1	> 106 GeV	–	–	$L_{\mathrm{T}} + p_{\mathrm{T}}^{\mathrm{miss}}$	$0 - 1600$ GeV	8 bins		
3L OSSF0	3	0	–	–	–	$L_{\mathrm{T}} + p_{\mathrm{T}}^{\mathrm{miss}}$	$0 - 1200$ GeV	6 bins		
4L OSSF1	≥4	1	–	–	–	$L_{\mathrm{T}} + p_{\mathrm{T}}^{\mathrm{miss}}$	$0 - 1000$ GeV	5 bins		
4L OSSF2	≥4	2	–	–	> 100 GeV if double on-Z	$L_{\mathrm{T}} + p_{\mathrm{T}}^{\mathrm{miss}}$	$0 - 1200$ GeV	6 bins		
Signal model: $\mathrm{t\bar{t}}\phi$								S_{T} (GeV)		
								$0 - 400$	$400 - 800$	> 800
$3\mathrm{L}(\ell\ell)^\star$ 0B	3	1	off-Z	0	–	M_{OSSF}^{20}	$12 - 77$ GeV	13 bins	13 bins	5 bins
						M_{OSSF}^{300}	$106 - 356$ GeV	10 bins	10 bins	10 bins
$3\mathrm{L}(\ell\ell)^\star$ 1B	3	1	off-Z	≥1	–	M_{OSSF}^{20}	$12 - 77$ GeV	13 bins	13 bins	5 bins
						M_{OSSF}^{300}	$106 - 356$ GeV	10 bins	10 bins	10 bins
								$0 - 400$	> 400	
$4\mathrm{L}(\ell\ell)^\star$ 0B	≥4	≥ 1	off-Z	0	–	M_{OSSF}^{20}	$12 - 77$ GeV	3 bins	2 bins	
						M_{OSSF}^{300}	$106 - 356$ GeV	3 bins	2 bins	
								inclusive		
$4\mathrm{L}(\ell\ell)^\star$ 1B	≥4	≥ 1	off-Z	≥1	–	M_{OSSF}^{20}	$12 - 77$ GeV	3 bins		
						M_{OSSF}^{300}	$106 - 356$ GeV	3 bins		

* $\ell = \mathrm{e}$ or μ

Multilepton search at CMS

The M_T distribution in the WZ enriched control selection (upper left), the L_T distribution in the misidentified lepton enriched control selection (upper right), the L_T distribution in the ttZ enriched control selection (lower left), and the S_T distribution in the ZZ enriched control selection (lower right). The lower panels show the ratio of observed to expected events. The hatched grey band in the upper panels and the light gray bands in the lower panels represent the total (systematic and statistical) uncertainty in each bin, whereas the dark grey bands in the lower panels represent the statistical uncertainty only. The last bins contain the overflow events in each distribution.

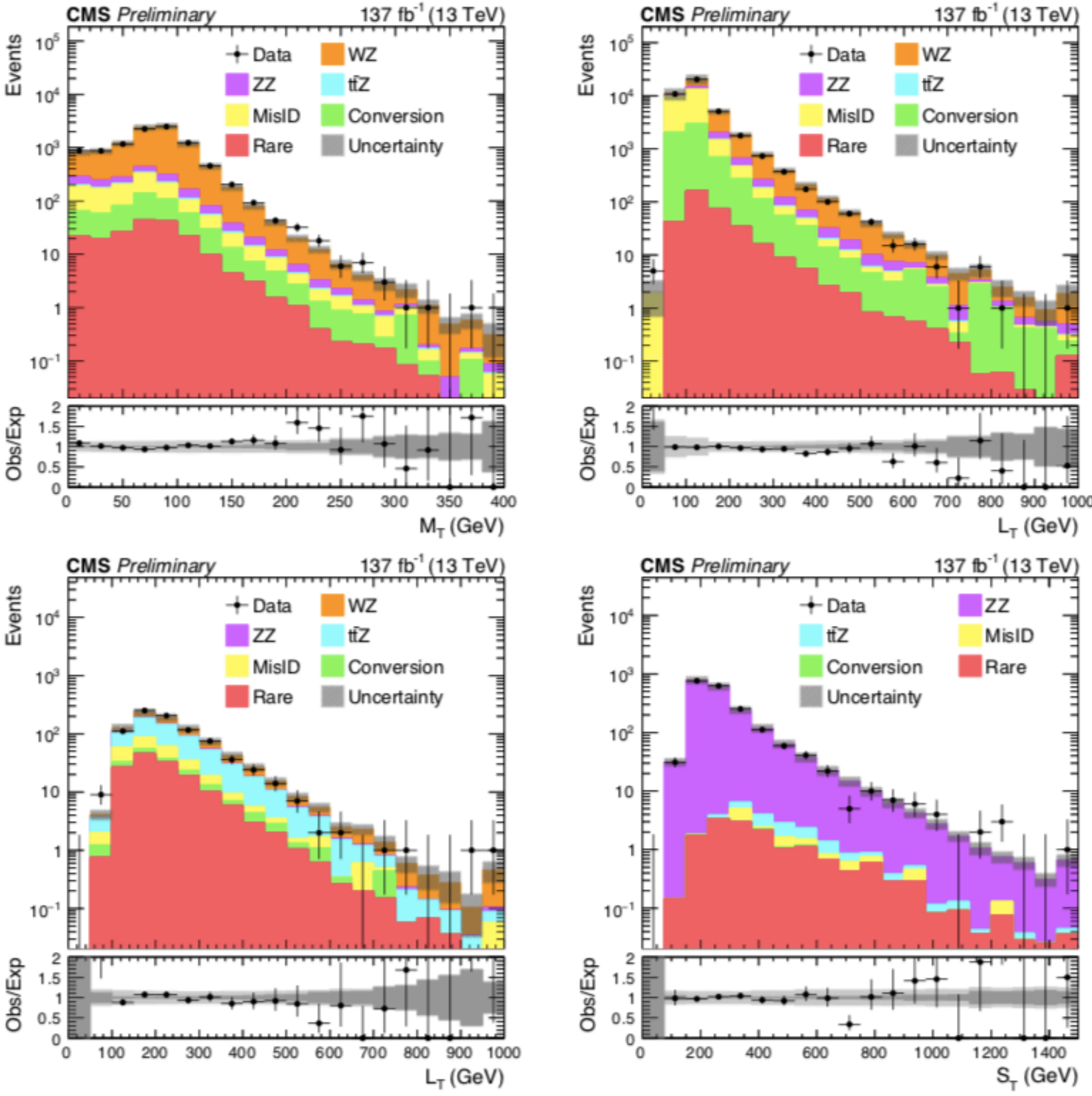

- The ATLAS results can be found here

Search for magnetic monopoles at ATLAS

arXiv:1905.10130

$34.4\ \mathrm{fb}^{-1}$

- Search for high-electric-charge objects
  - Dirac magnetic monopoles
  - Can explain charge quantisation
- Look for events with a single highly ionising particle in TRT and pencil-shape deposit in ECal
- Trigger used in the selection:
  - HW: RoI in ECAL ($E_T > 22$ GeV)
  - SW: high ionisation in corresponding TRT region
- Background: overlapping charged particles and noise in TRT straws (high f_{HT} values); high-energy electrons and noise in EM calorimeter cells (high w values)
- The estimated and observed event yields are consistent with the BG

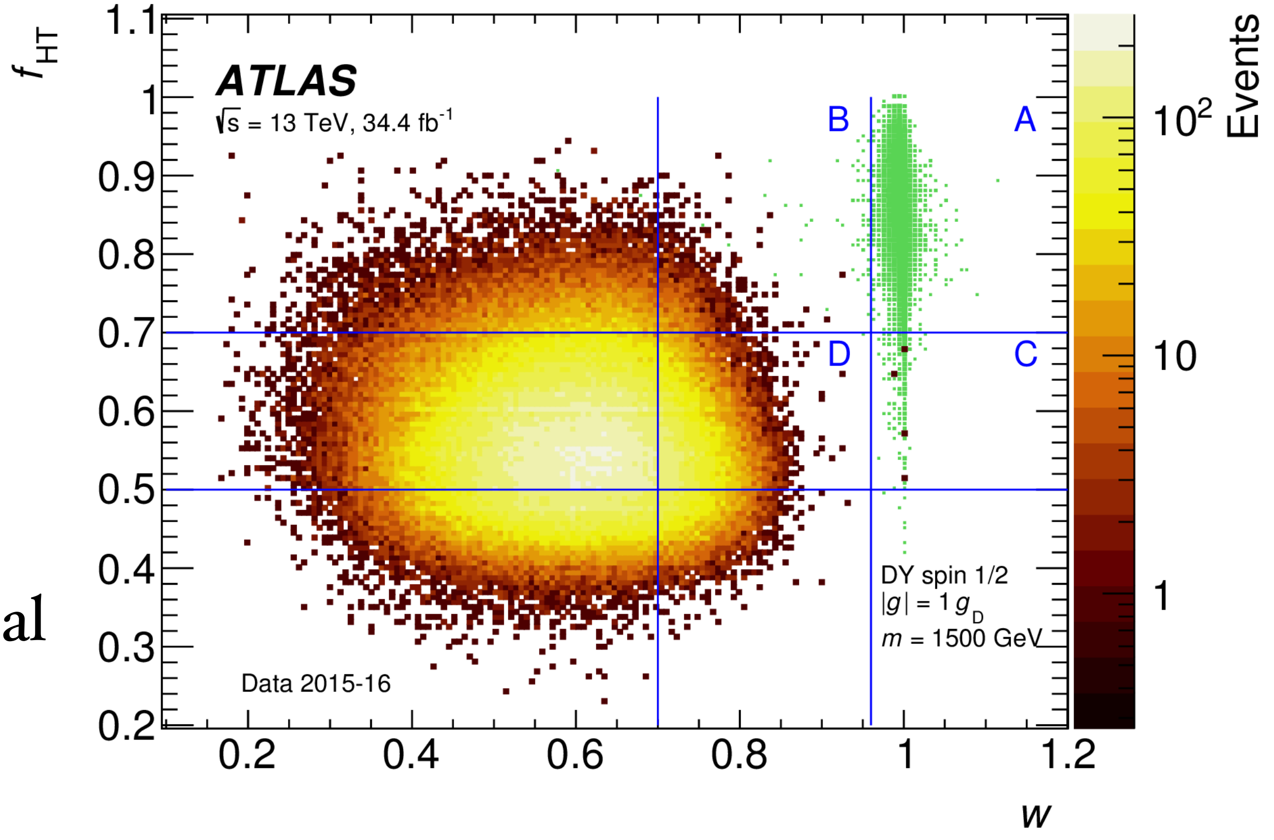

- Exclude monopoles with m > 1.8 TeV

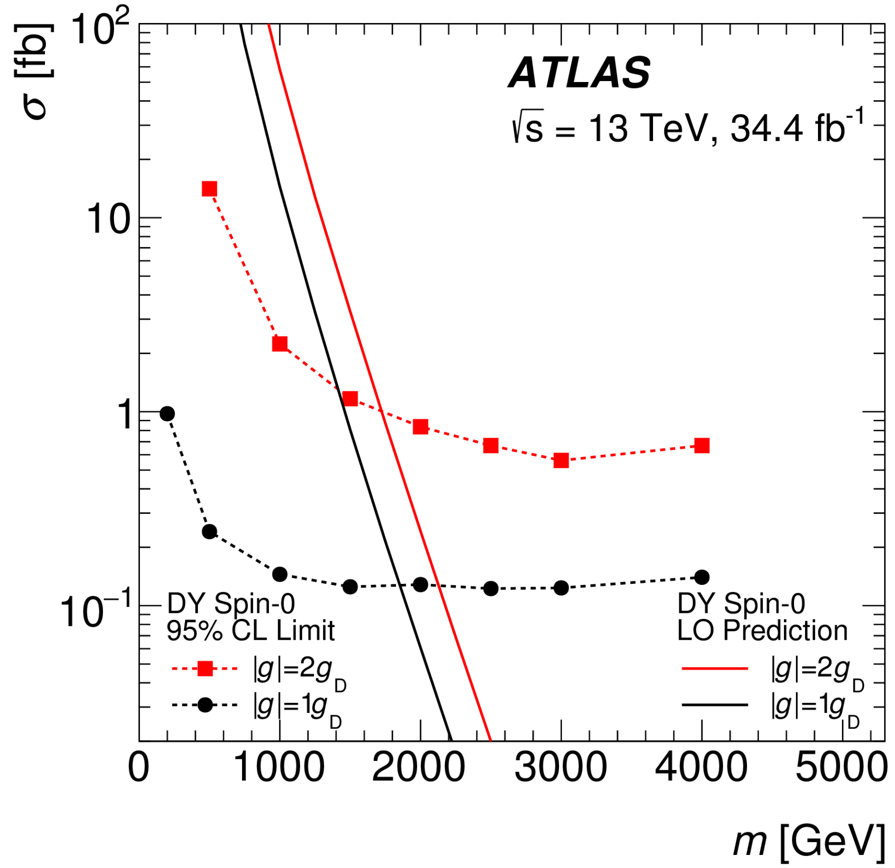

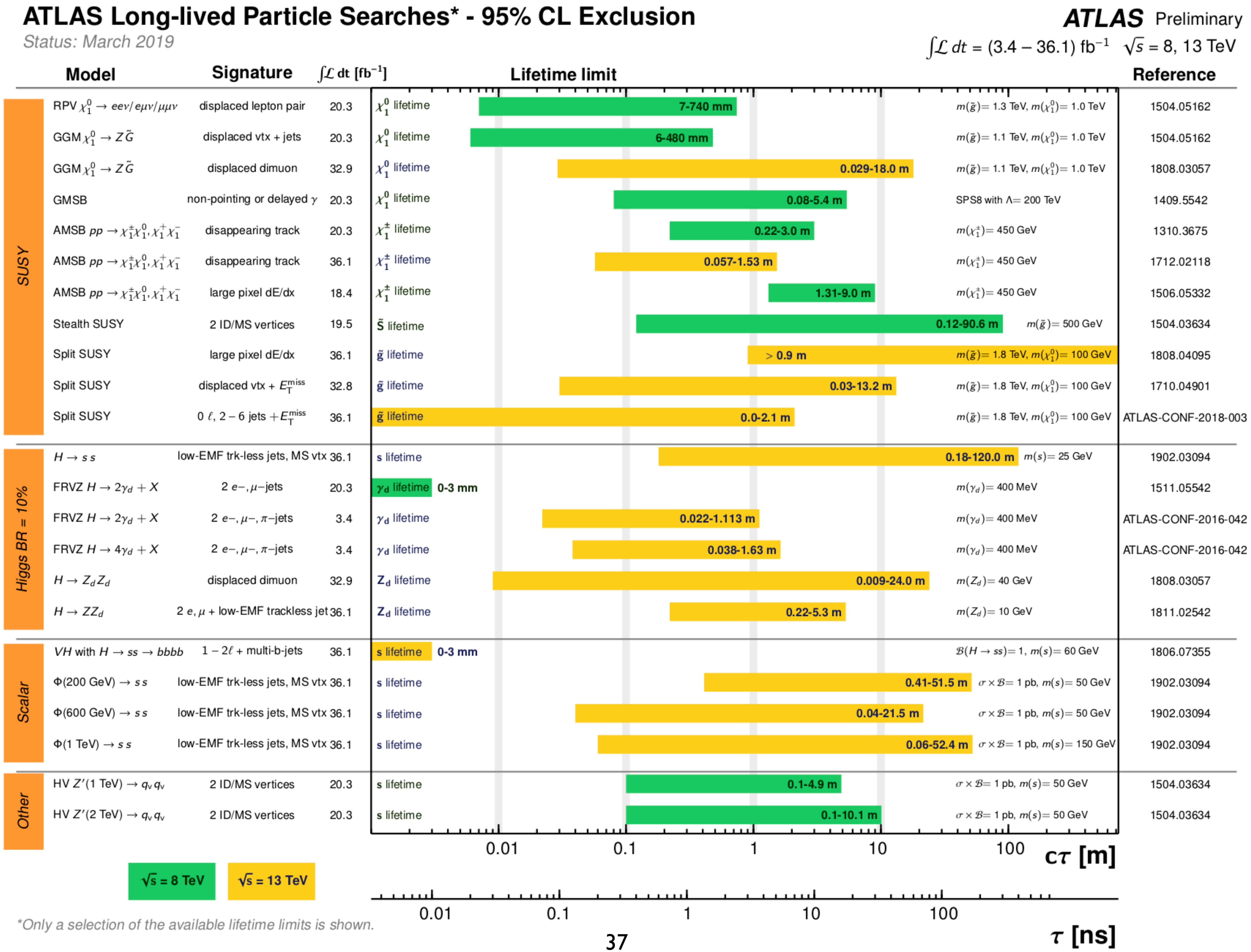
ATLAS Long-lived Particle Searches* - 95% CL Exclusion
Status: March 2019
ATLAS Preliminary
$\int \mathcal{L}\,dt = (3.4 - 36.1)\ \mathrm{fb}^{-1}$ $\sqrt{s} = 8, 13$ TeV
Model
Signature
$\int \mathcal{L}\,dt\ [\mathrm{fb}^{-1}]$
Lifetime limit
Reference
SUSY
RPV $\chi_1^0 \to ee\nu/e\mu\nu/\mu\mu\nu$ | displaced lepton pair | 20.3 | χ_1^0 lifetime | 7-740 mm | $m(\tilde{g})$= 1.3 TeV, $m(\chi_1^0)$= 1.0 TeV | 1504.05162
GGM $\chi_1^0 \to Z\tilde{G}$ | displaced vtx + jets | 20.3 | χ_1^0 lifetime | 6-480 mm | $m(\tilde{g})$= 1.1 TeV, $m(\chi_1^0)$= 1.0 TeV | 1504.05162
GGM $\chi_1^0 \to Z\tilde{G}$ | displaced dimuon | 32.9 | χ_1^0 lifetime | 0.029-18.0 m | $m(\tilde{g})$= 1.1 TeV, $m(\chi_1^0)$= 1.0 TeV | 1808.03057
GMSB | non-pointing or delayed γ | 20.3 | χ_1^0 lifetime | 0.08-5.4 m | SPS8 with Λ= 200 TeV | 1409.5542
AMSB $pp \to \chi_1^\pm\chi_1^0, \chi_1^+\chi_1^-$ | disappearing track | 20.3 | $\chi_1^\pm$ lifetime | 0.22-3.0 m | $m(\chi_1^\pm)$= 450 GeV | 1310.3675
AMSB $pp \to \chi_1^\pm\chi_1^0, \chi_1^+\chi_1^-$ | disappearing track | 36.1 | $\chi_1^\pm$ lifetime | 0.057-1.53 m | $m(\chi_1^\pm)$= 450 GeV | 1712.02118
AMSB $pp \to \chi_1^\pm\chi_1^0, \chi_1^+\chi_1^-$ | large pixel dE/dx | 18.4 | $\chi_1^\pm$ lifetime | 1.31-9.0 m | $m(\chi_1^\pm)$= 450 GeV | 1506.05332
Stealth SUSY | 2 ID/MS vertices | 19.5 | $\tilde{S}$ lifetime | 0.12-90.6 m | $m(\tilde{g})$= 500 GeV | 1504.03634
Split SUSY | large pixel dE/dx | 36.1 | $\tilde{g}$ lifetime | > 0.9 m | $m(\tilde{g})$= 1.8 TeV, $m(\chi_1^0)$= 100 GeV | 1808.04095
Split SUSY | displaced vtx + E_T^{miss} | 32.8 | $\tilde{g}$ lifetime | 0.03-13.2 m | $m(\tilde{g})$= 1.8 TeV, $m(\chi_1^0)$= 100 GeV | 1710.04901
Split SUSY | 0 ℓ, 2 – 6 jets + E_T^{miss} | 36.1 | $\tilde{g}$ lifetime | 0.0-2.1 m | $m(\tilde{g})$= 1.8 TeV, $m(\chi_1^0)$= 100 GeV | ATLAS-CONF-2018-003
Higgs BR = 10%
$H \to s\,s$ | low-EMF trk-less jets, MS vtx | 36.1 | s lifetime | 0.18-120.0 m | $m(s)$= 25 GeV | 1902.03094
FRVZ $H \to 2\gamma_d + X$ | 2 $e-,\mu-$jets | 20.3 | γ_d lifetime | 0-3 mm | $m(\gamma_d)$= 400 MeV | 1511.05542
FRVZ $H \to 2\gamma_d + X$ | 2 $e-,\mu-,\pi-$jets | 3.4 | γ_d lifetime | 0.022-1.113 m | $m(\gamma_d)$= 400 MeV | ATLAS-CONF-2016-042
FRVZ $H \to 4\gamma_d + X$ | 2 $e-,\mu-,\pi-$jets | 3.4 | γ_d lifetime | 0.038-1.63 m | $m(\gamma_d)$= 400 MeV | ATLAS-CONF-2016-042
$H \to Z_d Z_d$ | displaced dimuon | 32.9 | Z_d lifetime | 0.009-24.0 m | $m(Z_d)$= 40 GeV | 1808.03057
$H \to ZZ_d$ | 2 e, μ + low-EMF trackless jet | 36.1 | Z_d lifetime | 0.22-5.3 m | $m(Z_d)$= 10 GeV | 1811.02542
Scalar
VH with $H \to ss \to bbbb$ | $1 - 2\ell$ + multi-b-jets | 36.1 | s lifetime | 0-3 mm | $\mathcal{B}(H \to ss)$= 1, $m(s)$= 60 GeV | 1806.07355
Φ(200 GeV) $\to s\,s$ | low-EMF trk-less jets, MS vtx | 36.1 | s lifetime | 0.41-51.5 m | $\sigma \times \mathcal{B}$= 1 pb, $m(s)$= 50 GeV | 1902.03094
Φ(600 GeV) $\to s\,s$ | low-EMF trk-less jets, MS vtx | 36.1 | s lifetime | 0.04-21.5 m | $\sigma \times \mathcal{B}$= 1 pb, $m(s)$= 50 GeV | 1902.03094
Φ(1 TeV) $\to s\,s$ | low-EMF trk-less jets, MS vtx | 36.1 | s lifetime | 0.06-52.4 m | $\sigma \times \mathcal{B}$= 1 pb, $m(s)$= 150 GeV | 1902.03094
Other
HV Z'(1 TeV) $\to q_v q_v$ | 2 ID/MS vertices | 20.3 | s lifetime | 0.1-4.9 m | $\sigma \times \mathcal{B}$= 1 pb, $m(s)$= 50 GeV | 1504.03634
HV Z'(2 TeV) $\to q_v q_v$ | 2 ID/MS vertices | 20.3 | s lifetime | 0.1-10.1 m | $\sigma \times \mathcal{B}$= 1 pb, $m(s)$= 50 GeV | 1504.03634
0.01
0.1
1
10
100
$c\tau$ [m]
0.01
0.1
1
10
100
τ [ns]
🟩 $\sqrt{s}$ = 8 TeV
🟨 $\sqrt{s}$ = 13 TeV
*Only a selection of the available lifetime limits is shown.

Overview of CMS EXO results

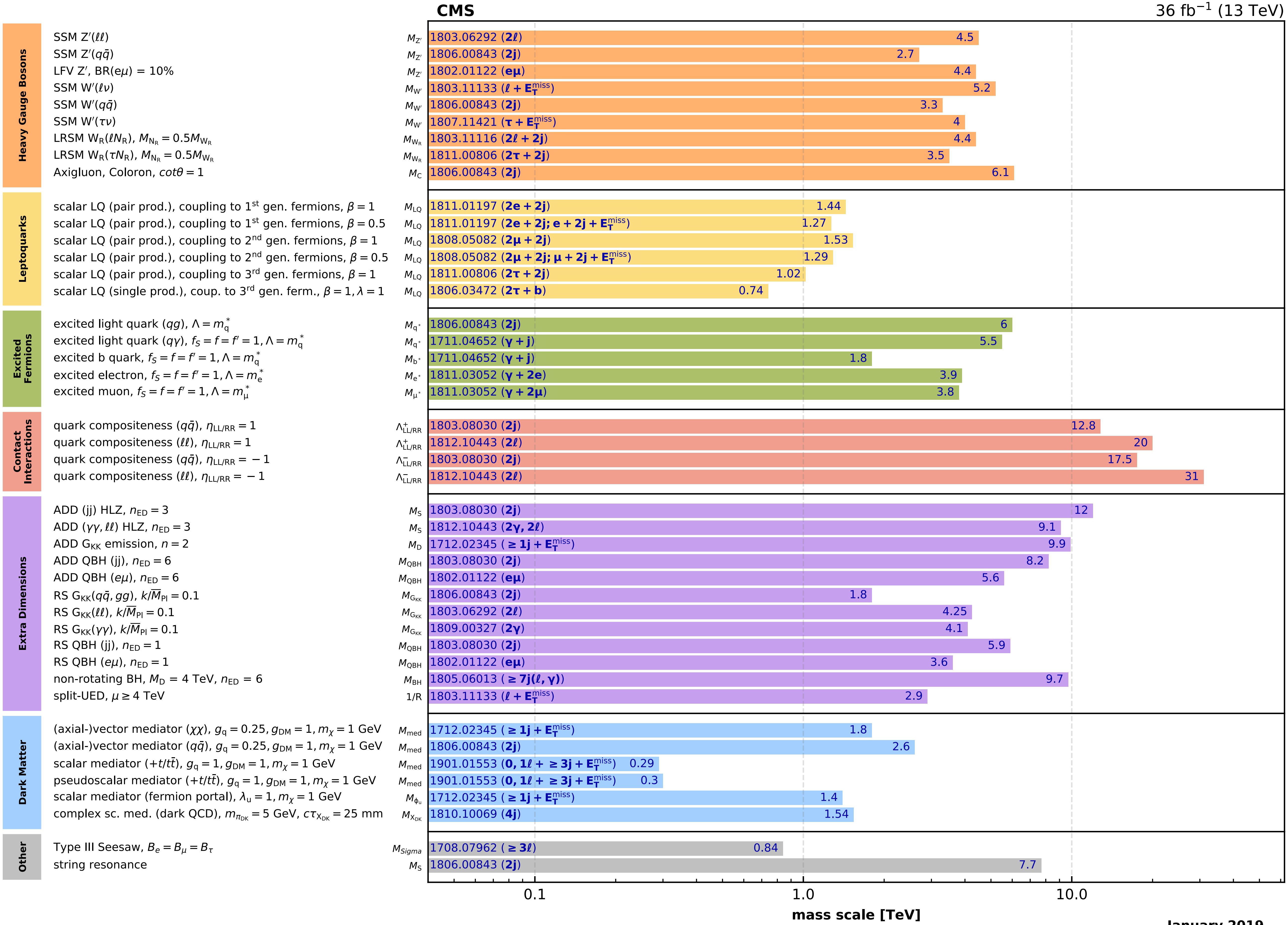

Selection of observed exclusion limits at 95% C.L. (theory uncertainties are not included).

January 2019

ATLAS Run 2 Detector Status

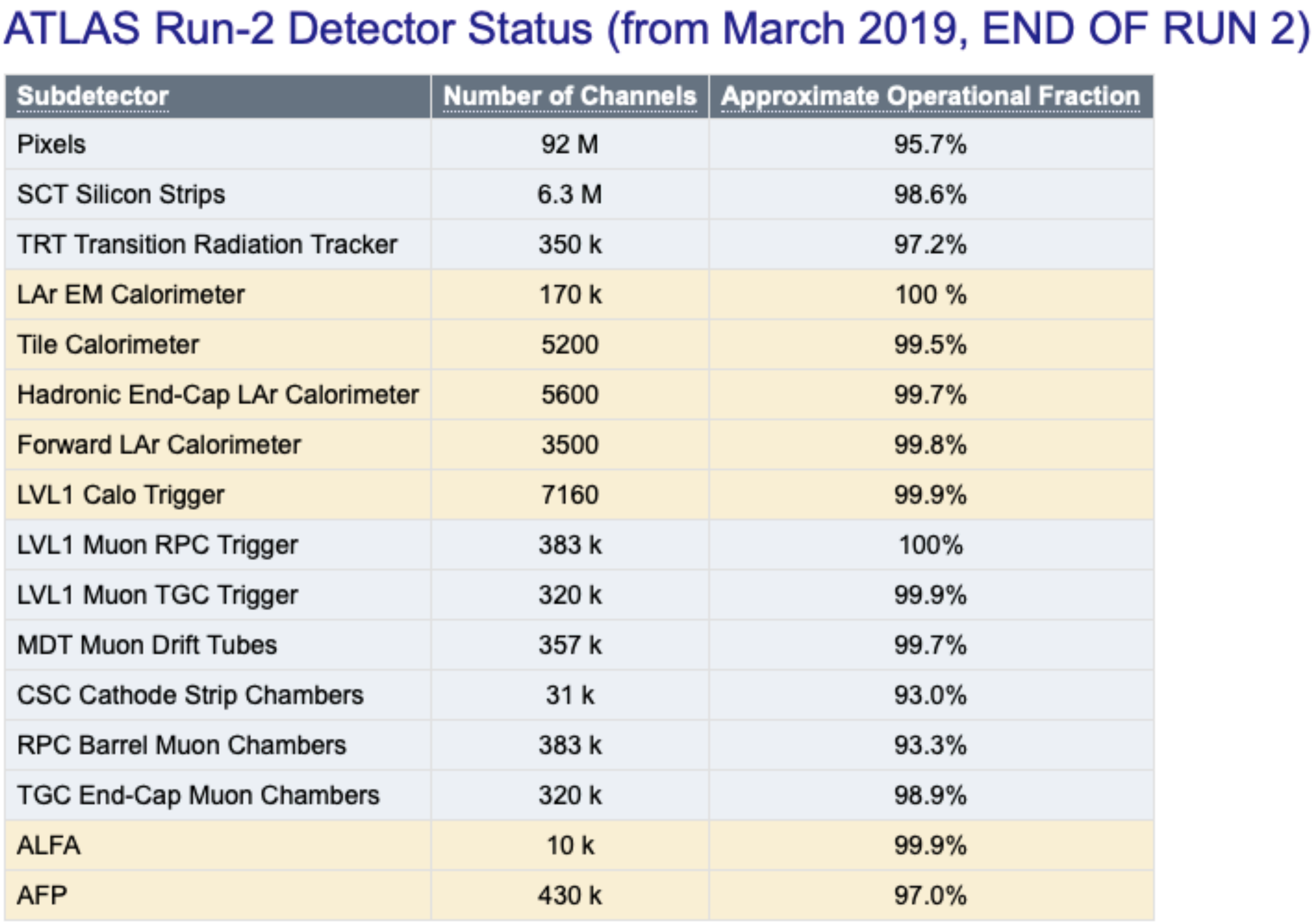

ATLAS Run-2 Detector Status (from March 2019, END OF RUN 2)

Subdetector	Number of Channels	Approximate Operational Fraction
Pixels	92 M	95.7%
SCT Silicon Strips	6.3 M	98.6%
TRT Transition Radiation Tracker	350 k	97.2%
LAr EM Calorimeter	170 k	100 %
Tile Calorimeter	5200	99.5%
Hadronic End-Cap LAr Calorimeter	5600	99.7%
Forward LAr Calorimeter	3500	99.8%
LVL1 Calo Trigger	7160	99.9%
LVL1 Muon RPC Trigger	383 k	100%
LVL1 Muon TGC Trigger	320 k	99.9%
MDT Muon Drift Tubes	357 k	99.7%
CSC Cathode Strip Chambers	31 k	93.0%
RPC Barrel Muon Chambers	383 k	93.3%
TGC End-Cap Muon Chambers	320 k	98.9%
ALFA	10 k	99.9%
AFP	430 k	97.0%

Standard Model Production Cross Section Measurements

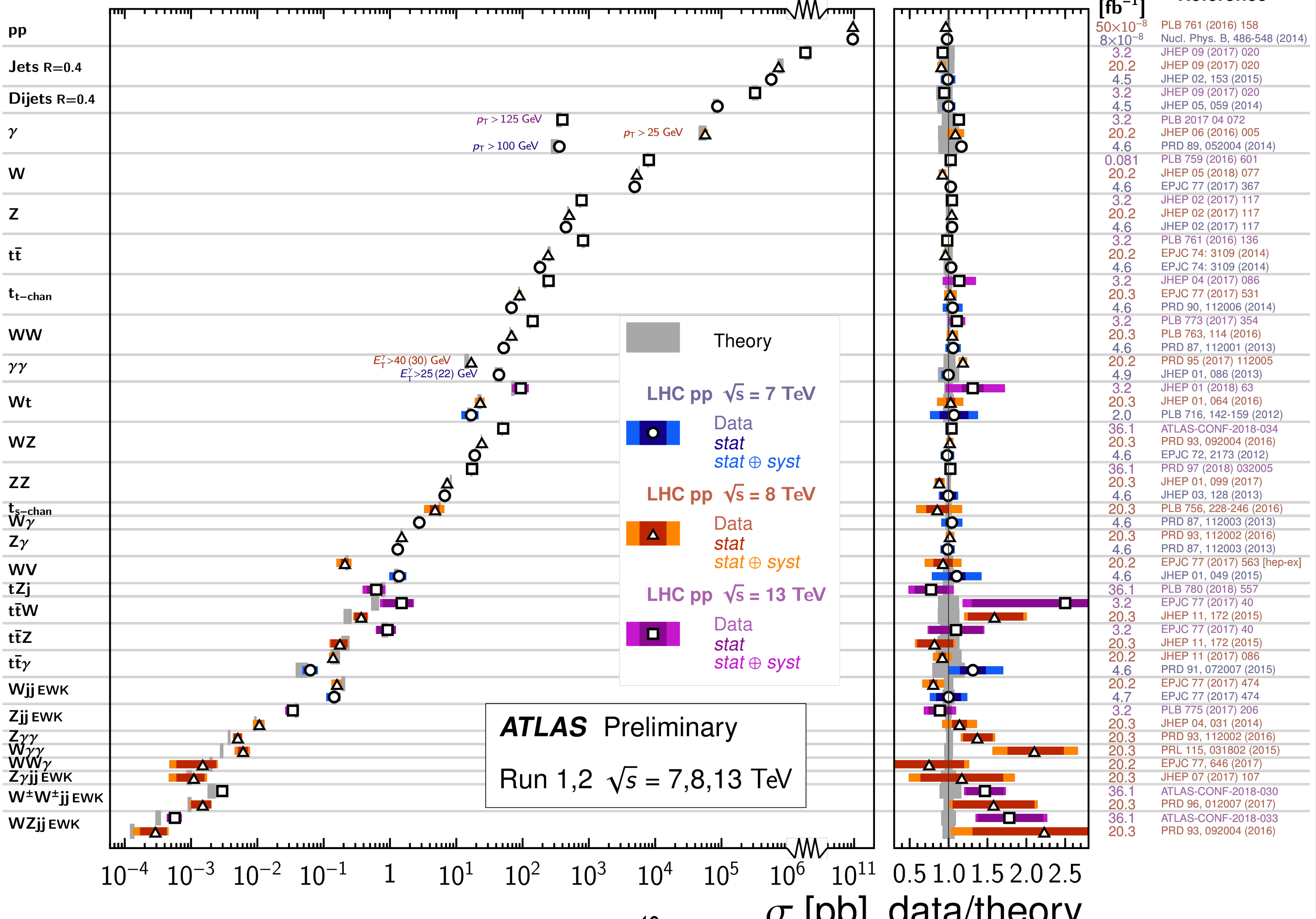

$\int \mathcal{L}\, dt$ [fb^{-1}]	Reference
50×10^{-8}	PLB 761 (2016) 158
8×10^{-8}	Nucl. Phys. B, 486-548 (2014)
3.2	JHEP 09 (2017) 020
20.2	JHEP 09 (2017) 020
4.5	JHEP 02, 153 (2015)
3.2	JHEP 09 (2017) 020
4.5	JHEP 05, 059 (2014)
3.2	PLB 2017 04 072
20.2	JHEP 06 (2016) 005
4.6	PRD 89, 052004 (2014)
0.081	PLB 759 (2016) 601
20.2	JHEP 05 (2018) 077
4.6	EPJC 77 (2017) 367
3.2	JHEP 02 (2017) 117
20.2	JHEP 02 (2017) 117
4.6	JHEP 02 (2017) 117
3.2	PLB 761 (2016) 136
20.2	EPJC 74: 3109 (2014)
4.6	EPJC 74: 3109 (2014)
3.2	JHEP 04 (2017) 086
20.3	EPJC 77 (2017) 531
4.6	PRD 90, 112006 (2014)
3.2	PLB 773 (2017) 354
20.3	PLB 763, 114 (2016)
4.6	PRD 87, 112001 (2013)
20.2	PRD 95 (2017) 112005
4.9	JHEP 01, 086 (2013)
3.2	JHEP 01 (2018) 63
20.3	JHEP 01, 064 (2016)
2.0	PLB 716, 142-159 (2012)
36.1	ATLAS-CONF-2018-034
20.3	PRD 93, 092004 (2016)
4.6	EPJC 72, 2173 (2012)
36.1	PRD 97 (2018) 032005
20.3	JHEP 01, 099 (2017)
4.6	JHEP 03, 128 (2013)
20.3	PLB 756, 228-246 (2016)
4.6	PRD 87, 112003 (2013)
20.3	PRD 93, 112002 (2016)
4.6	PRD 87, 112003 (2013)
20.2	EPJC 77 (2017) 563 [hep-ex]
4.6	JHEP 01, 049 (2015)
36.1	PLB 780 (2018) 557
3.2	EPJC 77 (2017) 40
20.3	JHEP 11, 172 (2015)
3.2	EPJC 77 (2017) 40
20.3	JHEP 11, 172 (2015)
20.2	JHEP 11 (2017) 086
4.6	PRD 91, 072007 (2015)
20.2	EPJC 77 (2017) 474
4.7	EPJC 77 (2017) 474
3.2	PLB 775 (2017) 206
20.3	JHEP 04, 031 (2014)
20.3	PRD 93, 112002 (2016)
20.3	PRL 115, 031802 (2015)
20.2	EPJC 77, 646 (2017)
20.3	JHEP 07 (2017) 107
36.1	ATLAS-CONF-2018-030
20.3	PRD 96, 012007 (2017)
36.1	ATLAS-CONF-2018-033
20.3	PRD 93, 092004 (2016)

SM particles interaction with the CMS detector

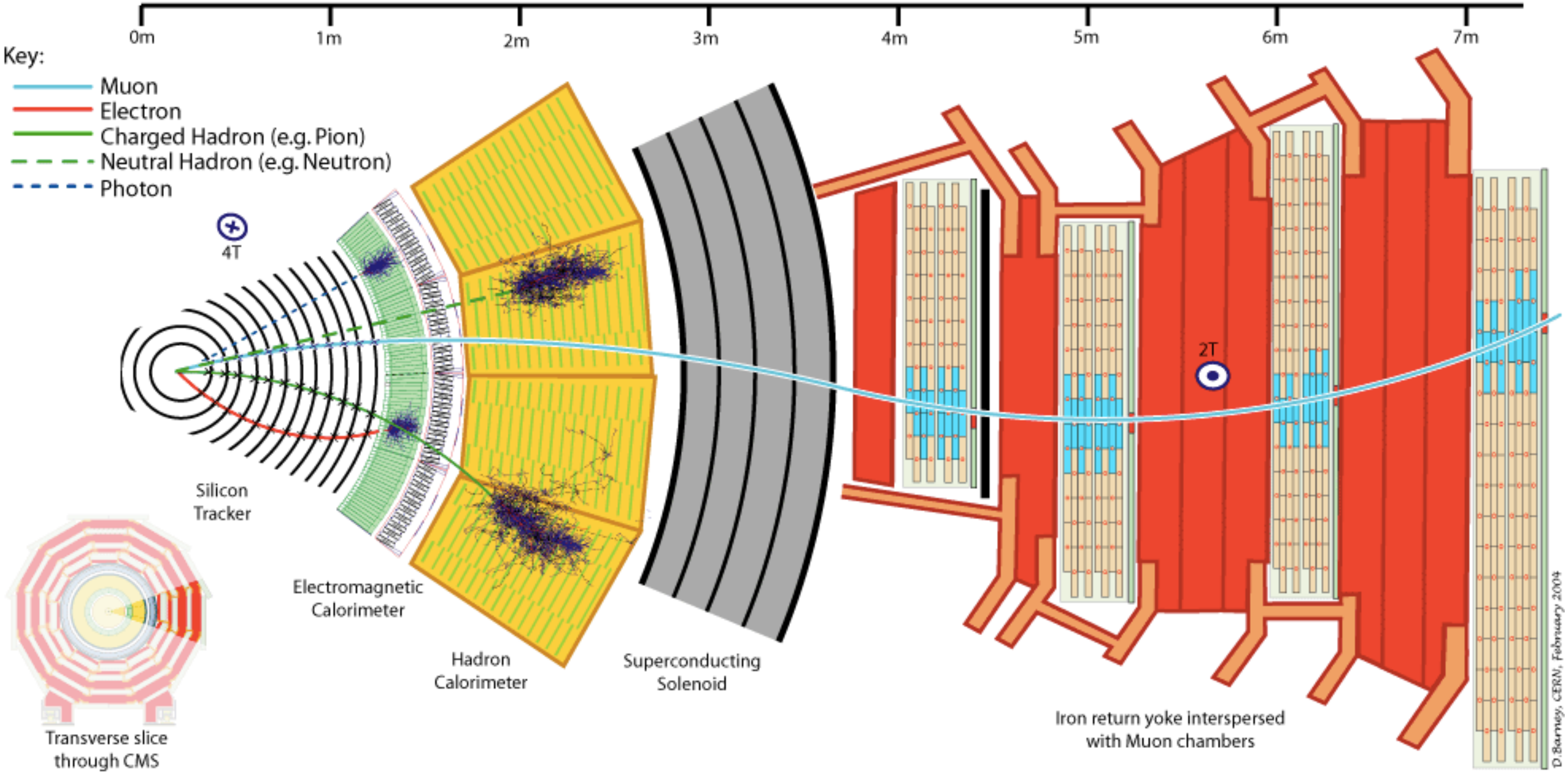

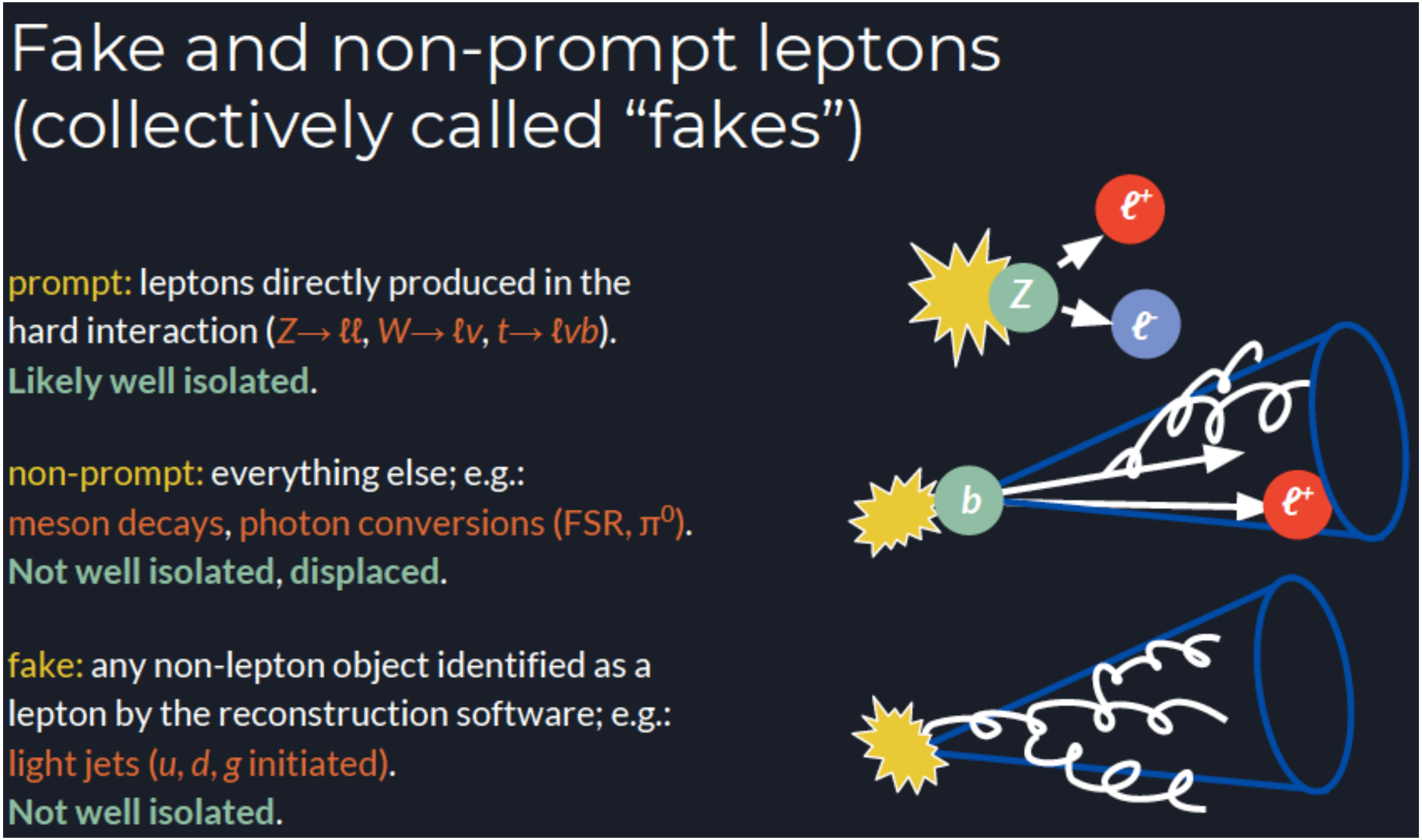

Fake and non-prompt leptons (collectively called “fakes”)

prompt: leptons directly produced in the hard interaction ($Z\to\ell\ell$, $W\to\ell\nu$, $t\to\ell\nu b$).
Likely well isolated.

non-prompt: everything else; e.g.:
meson decays, photon conversions (FSR, π^0).
Not well isolated, displaced.

fake: any non-lepton object identified as a lepton by the reconstruction software; e.g.:
light jets (*u*, *d*, *g* initiated).
Not well isolated.

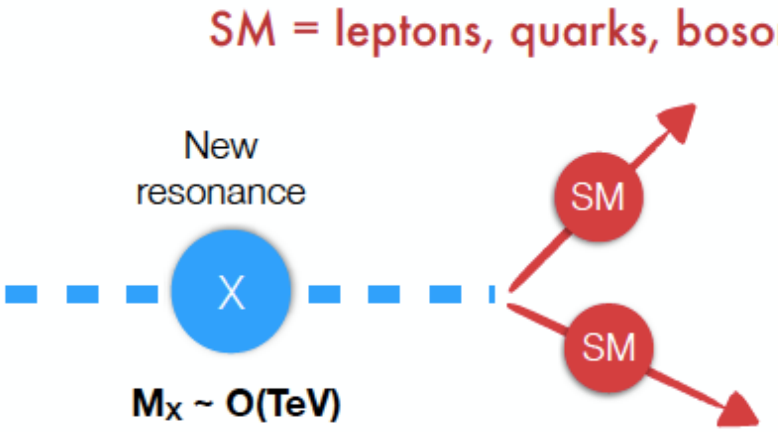

Rapidity definition:

$$\boxed{y = \frac{1}{2}\ln\left[(E+p_z)/(E-p_z)\right]}$$

Some statistical methods used in analyses explained here.

Tag and probe tool described here.

Sliding Window Fit (SWiFt) tries to obtain the background estimate in each bin by fitting a constrained region which is referred to as a ‘window’, instead of fitting the full spectrum.

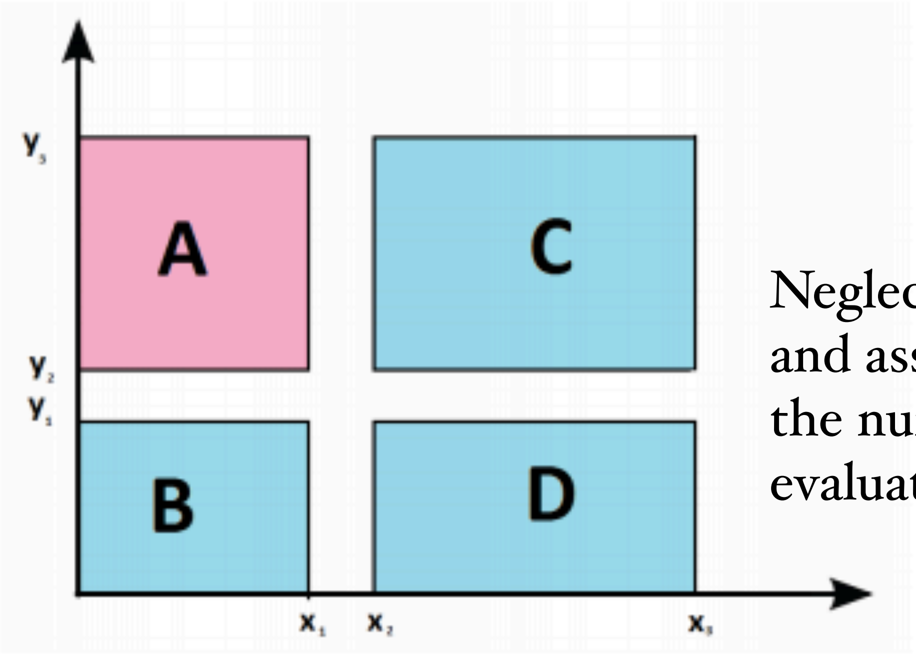

Fig. 1. – The ABCD method. The x and y axis are two uncorrelated variables. The region A is dominated by the signal (for instance, large E_T^{miss} and low isolation or small impact parameter (d_0) significance), while all other regions are dominated by backgrounds, which are characterized e.g. by non-isolated leptons or leptons with large d_0 significance, or events with small E_T^{miss}).

Neglecting the signal contribution in regions B and D, and assuming that variables x and y are uncorrelated, the number of QCD events in the signal region can be evaluated as $N_A = N_B \times N_C / N_D$.